Implementation of Phased Array Ultrasonic Testing (PAUT) For Bridge Welds

PUBLICATION NO. FHWA-HRT-24-010

FEBRUARY 2024

U.S. Department of Transportation
Federal Highway Administration

Research, Development, and Technology
Turner-Fairbank Highway Research Center
6300 Georgetown Pike
McLean, VA 22101-2296

FOREWORD

This study aims to elevate the quality control standards in steel bridge fabrication by expanding the available testing options beyond conventional ultrasonic and radiographic inspection. The research evaluates the feasibility and effectiveness of phased array ultrasonic testing, an innovative technology, for its potential integration into bridge weld nondestructive inspection processes as an efficient alternative to radiographic testing.[1]

This report is tailored for professionals involved in or overseeing steel bridge fabrication shop inspection, encompassing bridge owners, their quality control representatives, and third-party inspection firms. The findings and recommendations of this study empower these stakeholders to make informed decisions and embrace advanced inspection methodologies to enhance the overall quality control of steel bridge fabrication projects.

Jean A. Nehme, Ph.D., P.E.
Director, Office of Infrastructure
Research and Development

TECHNICAL DOCUMENTATION PAGE

1. Report No. FHWA-HRT-24-010	2. Government Accession No.	3. Recipient's Catalog No.
4. Title and Subtitle Implementation of Phased Array Ultrasonic Testing (PAUT) For Bridge Welds		5. Report Date February 2024
		6. Performing Organization Code
7. Author(s) Nikesh Jose (ORCID: 0009-0002-0043-379X) and Hoda Azari (ORCID: 0000-0002-7340-0035)		8. Performing Organization Report No.
9. Performing Organization Name and Address: Highway Technology Partners, LLC 9220 Rumsey Road, Suite 100 Columbia, MD 21045		10. Work Unit No.
		11. Contract or Grant No.
12. Sponsoring Agency Name and Address Office of Infrastructure Research and Development Federal Highway Administration 6300 Georgetown Pike McLean, VA 22101-2296		13. Type of Report and Period Covered Final Report; October 2016–March 2023
		14. Sponsoring Agency Code HRDI-20

15. Supplementary Notes
The contracting officer's representative was Dr. Hoda Azari (HRDI-20; ORCID: 0000-0002-7340-0035).

16. Abstract
The objective of this study is to improve the quality control of steel bridge fabrication by expanding the available nondestructive testing options beyond conventional ultrasonic testing (UT) and radiographic inspection methods. The primary focus of this research is to assess the acceptability of phased array ultrasonic testing (PAUT) as an alternative to radiography when the governing American Welding Society (AWS) specification mandates the latter for fabrication inspection.[1,2] To achieve this goal, the research team created a series of representative heavy section steel welds containing fabricated discontinuities. Subsequently, the team inspected these welds using PAUT, conventional UT, and radiography.[3–5] The study successfully demonstrated the feasibility of employing PAUT on typical bridge complete joint penetration butt welds. Notably, the researchers observed a strong correlation among the results obtained from PAUT, conventional UT, and radiography within the limited sample set used for this study. Based on the research findings, this study offers two key recommendations. First, it suggests fabricating and inspecting a more comprehensive matrix of representative flaw types, joint configurations, and plate thicknesses. Second, the study proposes evaluating ultrasonic beam modeling techniques to reduce the number of additional specimens required for testing.

17. Key Words Nondestructive evaluation, phased array ultrasonic testing, PAUT, conventional ultrasonic testing, weld inspection, steel bridge	18. Distribution Statement No restrictions. This document is available to the public through the National Technical Information Service, Springfield, VA 22161. https://www.ntis.gov

19. Security Classif. (of this report) Unclassified	20. Security Classif. (of this page) Unclassified	21. No. of Pages 87	22. Price N/A

Form DOT F 1700.7 (8-72) Reproduction of completed page authorized.

SI* (MODERN METRIC) CONVERSION FACTORS

APPROXIMATE CONVERSIONS TO SI UNITS

Symbol	When You Know	Multiply By	To Find	Symbol
		LENGTH		
in	inches	25.4	millimeters	mm
ft	feet	0.305	meters	m
yd	yards	0.914	meters	m
mi	miles	1.61	kilometers	km
		AREA		
in^2	square inches	645.2	square millimeters	mm^2
ft^2	square feet	0.093	square meters	m^2
yd^2	square yard	0.836	square meters	m^2
ac	acres	0.405	hectares	ha
mi^2	square miles	2.59	square kilometers	km^2
		VOLUME		
fl oz	fluid ounces	29.57	milliliters	mL
gal	gallons	3.785	liters	L
ft^3	cubic feet	0.028	cubic meters	m^3
yd^3	cubic yards	0.765	cubic meters	m^3
	NOTE: volumes greater than 1,000 L shall be shown in m^3			
		MASS		
oz	ounces	28.35	grams	g
lb	pounds	0.454	kilograms	kg
T	short tons (2,000 lb)	0.907	megagrams (or "metric ton")	Mg (or "t")
		TEMPERATURE (exact degrees)		
°F	Fahrenheit	5 (F-32)/9 or (F-32)/1.8	Celsius	°C
		ILLUMINATION		
fc	foot-candles	10.76	lux	lx
fl	foot-Lamberts	3.426	candela/m^2	cd/m^2
		FORCE and PRESSURE or STRESS		
lbf	poundforce	4.45	newtons	N
lbf/in^2	poundforce per square inch	6.89	kilopascals	kPa

APPROXIMATE CONVERSIONS FROM SI UNITS

Symbol	When You Know	Multiply By	To Find	Symbol
		LENGTH		
mm	millimeters	0.039	inches	in
m	meters	3.28	feet	ft
m	meters	1.09	yards	yd
km	kilometers	0.621	miles	mi
		AREA		
mm^2	square millimeters	0.0016	square inches	in^2
m^2	square meters	10.764	square feet	ft^2
m^2	square meters	1.195	square yards	yd^2
ha	hectares	2.47	acres	ac
km^2	square kilometers	0.386	square miles	mi^2
		VOLUME		
mL	milliliters	0.034	fluid ounces	fl oz
L	liters	0.264	gallons	gal
m^3	cubic meters	35.314	cubic feet	ft^3
m^3	cubic meters	1.307	cubic yards	yd^3
		MASS		
g	grams	0.035	ounces	oz
kg	kilograms	2.202	pounds	lb
Mg (or "t")	megagrams (or "metric ton")	1.103	short tons (2,000 lb)	T
		TEMPERATURE (exact degrees)		
°C	Celsius	1.8C+32	Fahrenheit	°F
		ILLUMINATION		
lx	lux	0.0929	foot-candles	fc
cd/m^2	candela/m2	0.2919	foot-Lamberts	fl
		FORCE and PRESSURE or STRESS		
N	newtons	2.225	poundforce	lbf
kPa	kilopascals	0.145	poundforce per square inch	lbf/in^2

*SI is the symbol for International System of Units. Appropriate rounding should be made to comply with Section 4 of ASTM E380. (Revised March 2003)

TABLE OF CONTENTS

LIST OF FIGURES

LIST OF TABLES

LIST OF ABBREVIATIONS AND ACRONYMS

AASHTO	American Association of State Highway and Transportation Officials
ARL	automatic reject level
AWS	American Welding Society
CAD	computer-aided design
CJP	complete joint penetration
CP	complete penetration
DRL	disregard level
ESW	electroslag welding
ESW-NG	electroslag welding, narrow gap
FSH	full screen height
HAZ	heat-affected zone
HF	Hirschfeld
IIW	International Institute of Welding
IP	index position
NDE	nondestructive evaluation
PAUT	phased array ultrasonic testing
PE	pulse echo
RT	radiographic testing
SAW	submerged arc welding
SDH	side-drilled hole
SSL	standard sensitivity level
TCG	time-corrected gain
TOFD	time of flight diffraction
TP	test plate
UT	ultrasonic testing

CHAPTER 1. INTRODUCTION

This study assesses the acceptability of phased array ultrasonic testing (PAUT) as an alternative to radiography.[1] The quality of the welds in the bridges is inspected and assessed in compliance with the American Association of State Highway and Transportation Officials (AASHTO)/American Welding Society (AWS) D1.5M/D1.5 in *Bridge Welding Code*.[2] To inspect the full volume of the complete joint penetration (CJP) welds, nondestructive evaluation (NDE) methods, such as ultrasonic testing (UT) and radiographic testing (RT) are utilized.[3–6] Based on the joint type, welding process, and member design stress, the choice of the NDE method to inspect the welds changes. Currently, the code requires RT for CJP welds subjected to tensile or reversal stresses, as well as for the electroslag welding narrow gap process (ESW-NG) and electroslag welding (ESW). When CJP groove welds in butt joints subject only to compression or shear require testing, either RT or UT shall be used.[2] In recent years, the UT field has experienced remarkable innovation.[6] Notably, several manufacturers have introduced PAUT systems with real-time, fast data acquisition.[1] These PAUT systems feature a matrix of multiple transducers, with some capable of housing up to 128 elements within a single probe.

In the 2015 edition of AWS D1.5, the PAUT technique was acknowledged as a recognized inspection technology for use instead of conventional UT on CJP butt welds.[2] Weld inspection using the UT method comprise raster scanning using a single crystal transducer that produces sound beams at one of the angles—70°, 60°, and 45°—as stipulated by the code. In phased array inspection, the probe consists of multiple small transducers (elements) that can steer the ultrasonic beam electronically in the test medium at multiple angles, improving the inspection coverage of the weld's cross section, eliminating the need for manual raster of a single element transducer across the plate surface. Furthermore, using multiple beams facilitates the generation of extradimensional data, enabling visualization of discontinuity size, shape, and location with greater precision. Additionally, when coupled with encoded line scans, PAUT data can be digitally stored as permanent records, much like a radiograph, a feat not achievable with conventional UT.

While AWS D1.5 in *Bridge Welding Code* indicates some support for using PAUT, further investigation and validation are necessary to potentially replace the RT method for these other applications. This report presents the developmental efforts conducted at the NDE Laboratory, a part of the Federal Highway Administration's (FHWA) Turner-Fairbank Highway Research Center (TFHRC), to assess the state of PAUT technology and its potential application as an approved alternative to RT in the AASHTO/AWS D1.5M/D1.5 in *Bridge Welding Code*.[2]

The work reported herein involved comprehensively reviewing the current state of practice in inspecting welds using PAUT; developing a preliminary technical approach to inspect CJP butt welds, with and without transitions; fabricating suitable test specimens; developing detailed scan plans for sample test specimens with CJP butt welds; and comparing test results from PAUT, UT, and RT. Following the guidelines provided in AWS D1.5 2020 Annex J on advanced ultrasonic examination, the researchers inspected and analyzed 10 test specimens.[2] The indepth analysis of PAUT data obtained was utilized to determine location and sizing information related to the discontinuities. The report also compares PAUT results to those data obtained using conventional UT and RT with statistical correlations.

CHAPTER 2. TECHNICAL APPROACH

EQUIPMENT

PAUT

An ultrasonic phased array probe consists of multiple elements, usually ranging between 16 and 128, with each element functioning as an individual ultrasonic transducer. These elements can be arranged in various patterns, with the simplest being a linear array. The ultrasonic wavefronts can be excited by pulsing the elements individually or as a group, and their combination generates the beam profile. By varying the timing of the excitation for each element, the beam profile can be modified, and focal laws are used to control the amplitude and time delay for each element.

Three primary electronic scanning techniques are used for controlling the beam profile using a linear array pattern of the elements:[(1)]

1. Linear scanning: A subset or group of the array elements are pulsed to form the desired beam profile, and then the applicable focal law giving this beam profile is electronically multiplexed along the length of the array (figure 1). This electronic scanning technique is akin to mechanically scanning a conventional (single-crystal) probe along a distance equal to the length of the larger phased array probe. In the current market, most commercially available arrays have up to 128 elements, which are typically pulsed in groups of 8 to 16.

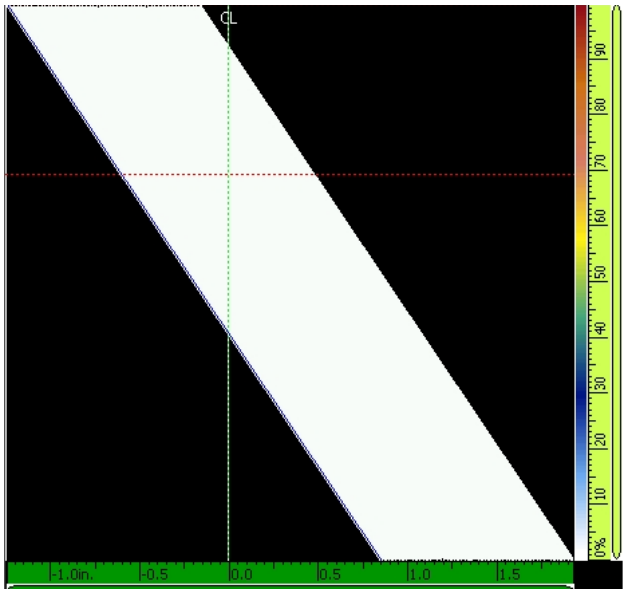

Source: FHWA.

Figure 1. Image. Linear scanning.

2. Dynamic depth focusing: The focal laws are varied to electronically move the focal point along the nominal beam axis.

3. Swept angular (sectorial or azimuthal) scanning: By selecting specific focal laws, the beam is electronically steered to a fixed angle of incidence or swept through a wide angular range (figure 2).

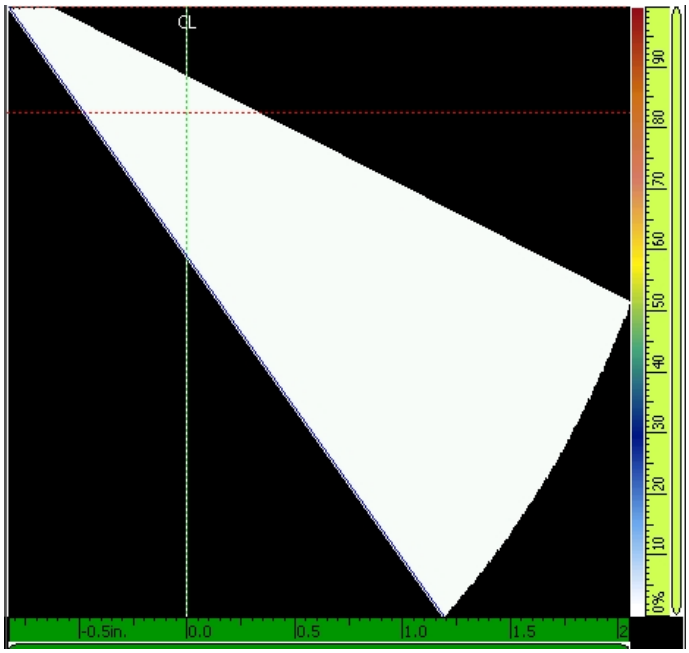

Source: FHWA.

Figure 2. Image. Sectorial scanning.

Pulse-Echo (PE) Technique

This process uses a transducer to both transmit and receive the ultrasonic pulse, as presented in figure 3. The received ultrasonic pulses are separated by the time the sound takes to reach the different surfaces from which the sound is reflected. The size (amplitude) of a reflection is related to the size of the reflecting surface.

Defect sizing approaches often used in standards and specifications are based on the amplitude of the returned signal and correlating it with an equivalent machined reflector, such as a notch or a side-drilled hole (SDH) (figure 4).

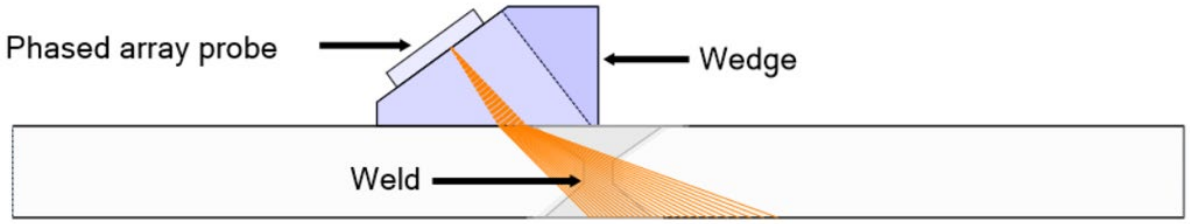

Source: FHWA.

Figure 3. Schematic. Phased array PE technique.

However, the correlation between defect size and amplitude is dependent on several variables, such as the material, equipment, and the defect itself. The equipment has potential amplitude variations due to the type of pulser, frequency band, cabling, and other inherent electrical parameters, but the disparities in the signal amplitude are minimized by the standardization. The purpose of standardization is to reduce variations in inspection outcomes by setting and maintaining a set of parameters that are calibrated to meet the required standards. Ultrasonics are highly sensitive to defect orientation, with roughness; curvature; type (slag, porosity, crack, or lack of fusion); and location also playing roles.

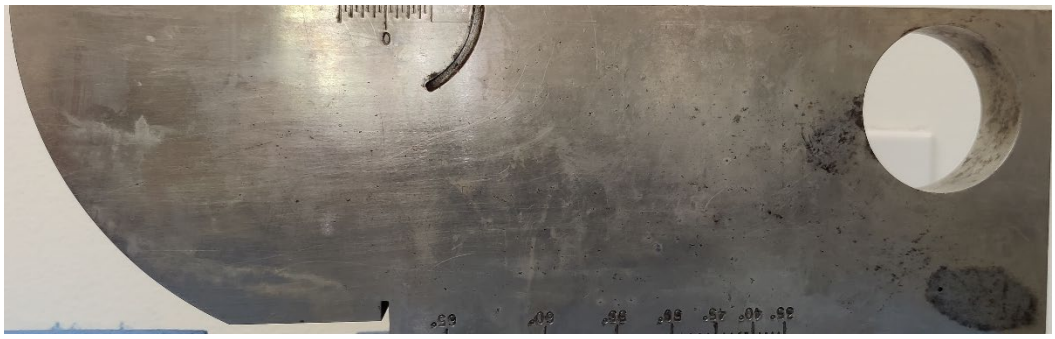

Source: FHWA.

Figure 4. Photo. International Institute of Welding (IIW) block.[(2).]

Two important factors influencing the PE technique are that large discontinuities are generally undersized and small discontinuities tend to be oversized. The oversizing of small discontinuities occurs mainly because small discontinuities act as omnidirectional emitters. Small discontinuities emit anywhere inside the beam and thus are influenced by the beam spread. The small discontinuity is essentially plotting the width of the sound beam. However, undersizing large discontinuities is more critical. In cases where the defect is irregularly shaped and inspection is conducted with a fixed-angle transducer beam, lower amplitude signals can result and nonconservative sizing measurement errors may occur.[(1)]

Standardization

The research team used a phased array probe with a center frequency of 5 MHz for testing. The phased array probes were a one-dimensional linear array type consisting of 64 elements. The team used a nominal shear wave refracted 55° from the wedge as the center sound beam angle, and they steered the beam electronically from 45° to 70°.[(2)] The following steps ensure good standardization:[(2)]

- Phased array element operability check.
- Sensitivity standardization.
- Time-corrected gain (TCG).
- Encoder standardization.

Calibration Blocks

In the ideal testing scenario, calibration blocks are made of the same material type and are heat treated in the same fashion as the test specimen. Different types of reflectors—such as SDHs, flat-bottomed holes, and notches—are used to calibrate phased array examinations for angle beam inspections. An SDH, which is known to be a well-defined and reproducible reflector, is widely used.[(1)]

The researchers used an IIW block for sensitivity standardization and range settings. The TCG phased array standardization block used was 1.25 inches wide, approximately 6.5 inches in height, and 26 inches in length. The block had 12 SDHs that were 0.06 inch in diameter. All SDHs were perpendicular to the sound beam and parallel to the scanning surface (figure 5).[(2)]

Source: FHWA.

Figure 5. Photo. TCG standardization block.[(2)]

CHAPTER 3. SPECIMEN FABRICATION

SUBMERGED ARC WELDING (SAW)

SAW is an arc welding process that fuses materials together by heating them with an electric arc or arcs between a bare electrode(s) and the specimen.[7] The arc is submerged under a blanket of granular flux. The filler metal is obtained from melting a solid electrode wire, sometimes with additional alloying elements in the flux. The SAW process joins all the weldable steels. The process provides high deposition rates, making it excellent for medium and thick sections of plates and pipes. Additionally, the process produces deep penetration. The process is typically limited to the flat and horizontal fillet positions because of the granular flux used to shield the weld puddle. However, with special flux dams, the process can be used in the horizontal groove weld position. Since the arc is hidden, only safety glasses are generally required by the welding operator. The process generally produces a smooth weld bead with no spatter. A layer of slag is left on the weld bead that is normally easy to remove. The deep penetration of the SAW process can lead to centerline cracking due to improper width-to-depth ratios in the bead cross sections.

ESW-NG

ESW-NG is a special automatic process normally used by larger fabricators to weld butt joints in plates.[7] Using a single-pass vertical process, ESW-NG offers good productivity and quality in heavy structural fabrications. The resistance of current through the slag pool covering the complete surface of the weld metal provides the heat for melting. A pool of molten slag is formed between the edges of the parts to be welded and the traveling shoes. The metal electrode is inserted into the molten slag. The current passes through the electrode, and the molten slag heats the slag pool. The electrode wire melts, and the molten metal settles at the bottom of the slag pool and solidifies to form the weld metal. Consumable guide tubes are used in narrow groove ESW-NG welds for bridge fabrications. Typically, discontinuities like slag, inclusions, porosity, undercuts, notches, etc., are not encountered in the ESW-NG process.

FABRICATION OF TEST SPECIMENS

Based on their interactions with other Federal agencies and experts in steel bridge fabrication, the researchers initially fabricated eight test specimens.[1] To ensure the welding would represent production bridge welding practices, the team manufactured specimens by using two steel bridge fabricators. They used the ESW-NG and SAW processes to fabricate the specimens. The objective of using two welding processes was to determine the microstructures' influence on the inspection technology. A brief overview of the two welding processes is provided in the following sections. The researchers instructed the fabricators to implant discontinuities in the specimens they typically encounter during fabrication. The typical discontinuities often found in welds are cracks, lack of fusion, lack of penetration, porosity, inclusions, and undercut. One approach used in this effort to implant a lack of fusion discontinuity was that a thick rectangular shim was used to simulate the lack of fusion discontinuity for an ESW-NG thickness transition CJP weld. The team attached a plate to the transition bevel with a fillet weld, and it was thick enough such that the molten ESW-NG weld pool would not penetrate through the thickness.

Later in the project, the researchers fabricated two additional transition butt-weld specimens using the ESW-NG process. They developed the fabrication plan in collaboration with the steel weld fabricator. The intent in fabricating these additional test specimens was to implant weld fusion line cracking using the ESW-NG process. The 10 butt-weld specimens fabricated are listed in table 1. The team request both fabricators to perform conventional UT and RT on each of the test specimens.

Table 1. Test specimens.

Sample Number	Sample Name	Weld Type	Length (Inches)	Width (Inches)	Height (Inches)	Transition
1	TP1	SAW	25.0	26.5	1–2	Yes
2	TP2	ESW-NG	28.0	24.5	1.5	No
3	TP3	ESW-NG	22.0	23.5	3.3	No
4	TP4	SAW	36.5	18.0	3.0	No
5	TP5	ESW-NG	30.0	24.5	1.5–2.7	Yes
6	ESW-2CP	ESW-NG	48.0	48.0	2.0	No
7	ESW-12-CP	ESW-NG	48.0	48.0	1.0–2.0	Yes
8	SAW-12CP	SAW	48.0	48.0	1.0–2.0	Yes
9	HF1	ESW-NG	36.0	49.0	2.0–2.5	Yes
10	HF2	ESW-NG	36.0	49.0	2.0–2.5	Yes

CP = complete penetration; HF = Hirschfeld[8]; TP = test plate.

CHAPTER 4. DATA ACQUISITION

SCAN PLAN DEVELOPMENT

The study team based the PAUT data acquisition throughout this research effort on the PE approach. They developed the scan plans for the butt-weld specimens listed in table 1. The strategy in developing these scan plans was to consider the detailed specific attributes of each specimen based on the thickness of the specimen, the weld centerline, the weld width, and the weld heat-affected zone (HAZ) size. The researchers developed the scan plans using a commercial ray tracing software.[9] The software enables input of the specimen specifics and the technical specifications of the phased array probe and the wedge used for inspections. The software provides a detailed sound beam center ray path analysis based on the position of the probe and the sequence in which the elements are pulsed. The teams used various combinations of the beam index points to determine the optimum location for the probe placement. The scan plans define the various refracted angles to be used during the examination. The complete coverage of the weld and the HAZ was an important aspect in developing the scan plans. The researchers developed the scan plans to optimize coverage to fully examine the weld and the HAZ. The index offset positions (distance of the wedge front face to the weld center) are configured to include the coverage as close to perpendicular to the weld fusion face as practicable. Table 2 provides the index offsets used to inspect the plates. Figure 6 to figure 15 present the scan plan for the plates. In the scan plans, index position (IP)1 represents the 90°-skew direction, and IP2 represents the 270°-skew direction.

Table 2. List of index offsets used in scan plan for the test specimens.

Plate ID	Index Offset (Inches)	
	90° Skews (IP1)	270° Skews (IP2)
TP1	0.8,0, −0.6, −1.65, −4.5, −6.2	0.5, 0, 2, 3.4, −0.8
TP2	0.4, 1, −0.1, −0.9, −3	0.1,0.9, 3, −0.4, −1
TP3	0.35, −0.15, −1.2, −3.3, −7.25	0.15, 1.2, 3.3, 7.25, −0.35
TP4	0.75, −0.5, −3, −5.7, −6.6	0.5, 3, 5.7, 6.6, −0.75
TP5	−9.5, 0, 1, −0.5, −1.75, −3.5	0.5, 0, 1.5, 3, 6.2
ESW-2CP	0.75, −1, −0.5, −3.5, −5, −7.5	0.5, 3.5, 5, 7.5, −1
ESW-12CP	0, 1, −0.6, −1.5, −3.25, −8	2,3, −0.1, −0.6, −1.4, 0.85
SAW-12CP	0.25,1, −1, −3, −5.5, −7.2	0.5, 0, 1.5, 2.5, 3.2, −1
HF1	0.9,0.25, −0.75, −2.5, −8	0.5, 2 ,4.5, 5.2, 6.2, 7.3, −0.5
HF2	0.7, −0.3, −1.7, −4.2, −6.6, −8.5	0.5, 2, 3.5, 4.7, 6.2, −1

ID = identification.

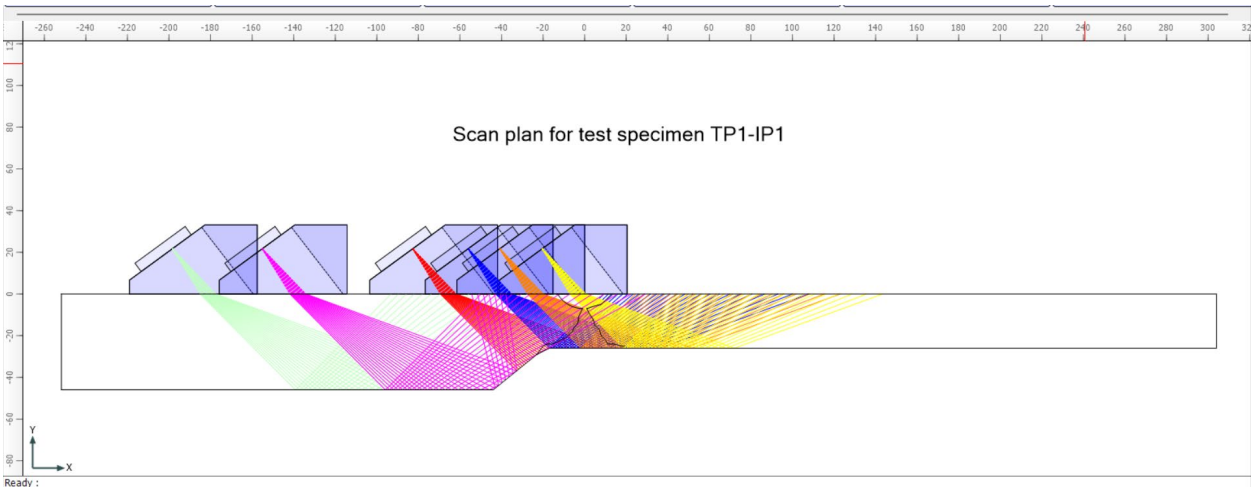

Source: FHWA.

A. Scan plan for test specimen test plate (TP)1-IP1.

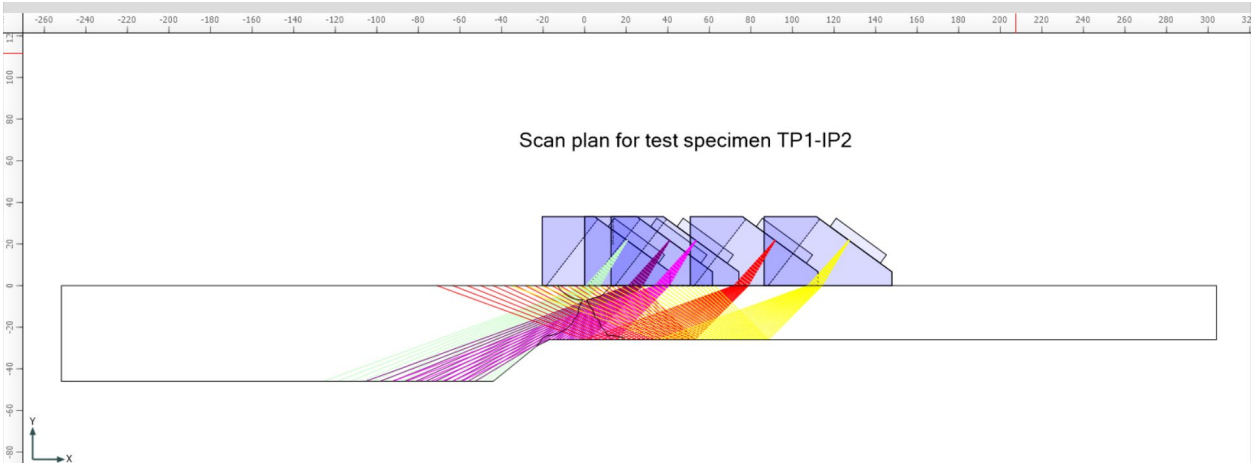

Source: FHWA.

B. Scan plan for test specimen TP1-IP2.

Figure 6. Schematics. TP1 scan plans for test specimens.

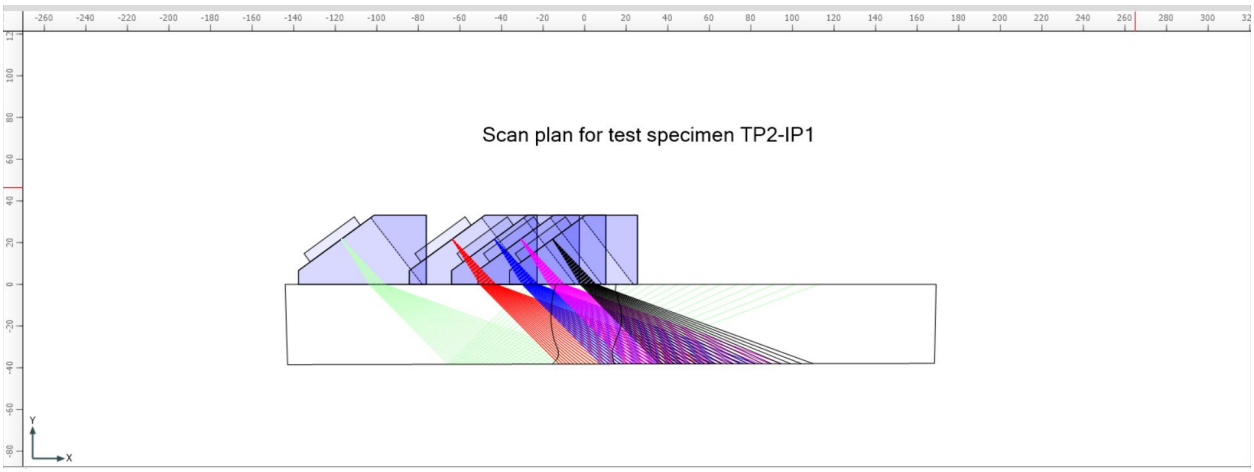

Source: FHWA.

A. Scan plan for test specimen TP2-IP1.

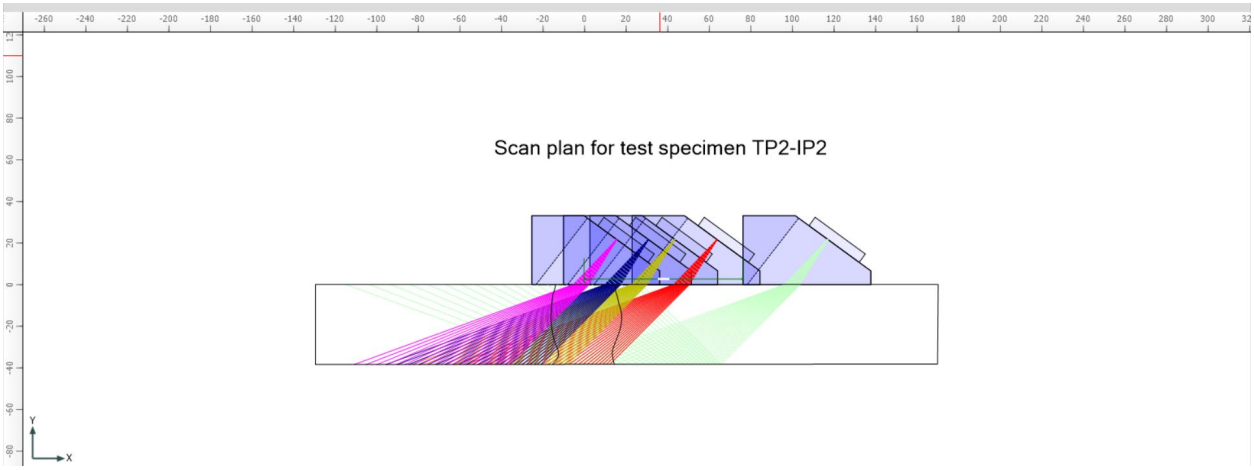

Source: FHWA.

B. Scan plan for test specimen TP2-IP2.

Figure 7. Schematics. TP2 scan plans for test specimens.

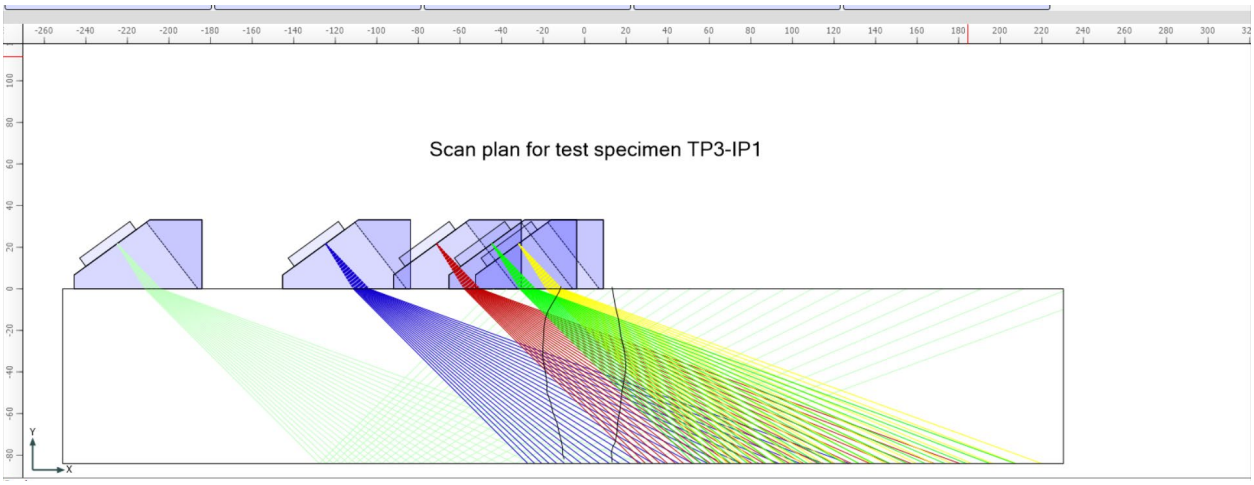

Source: FHWA.

A. Scan plan for test specimen TP3-IP1.

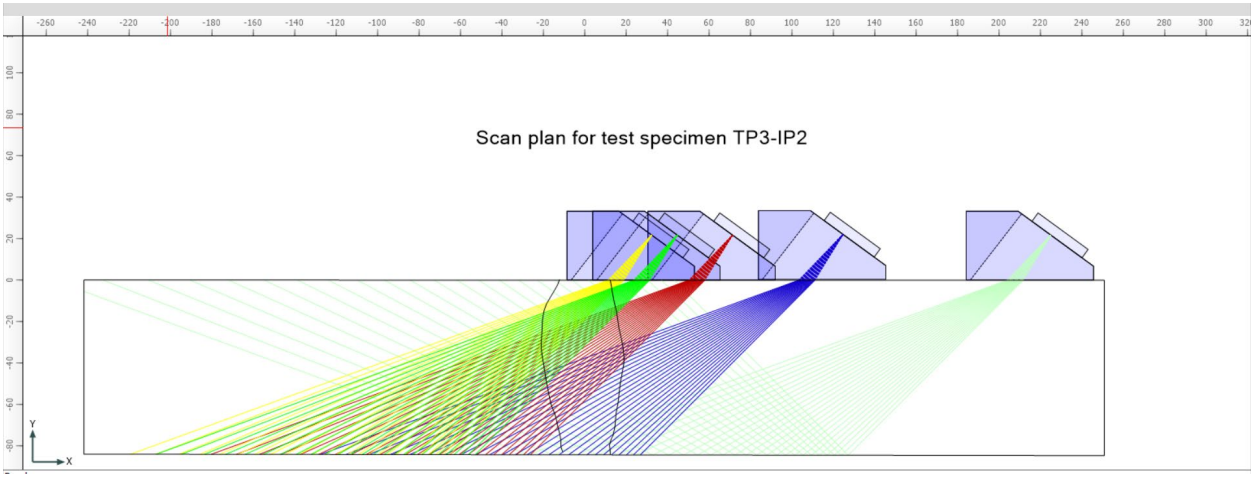

Source: FHWA.

B. Scan plan for test specimen TP3-IP2.

Figure 8. Schematics. TP3 scan plans for test specimens.

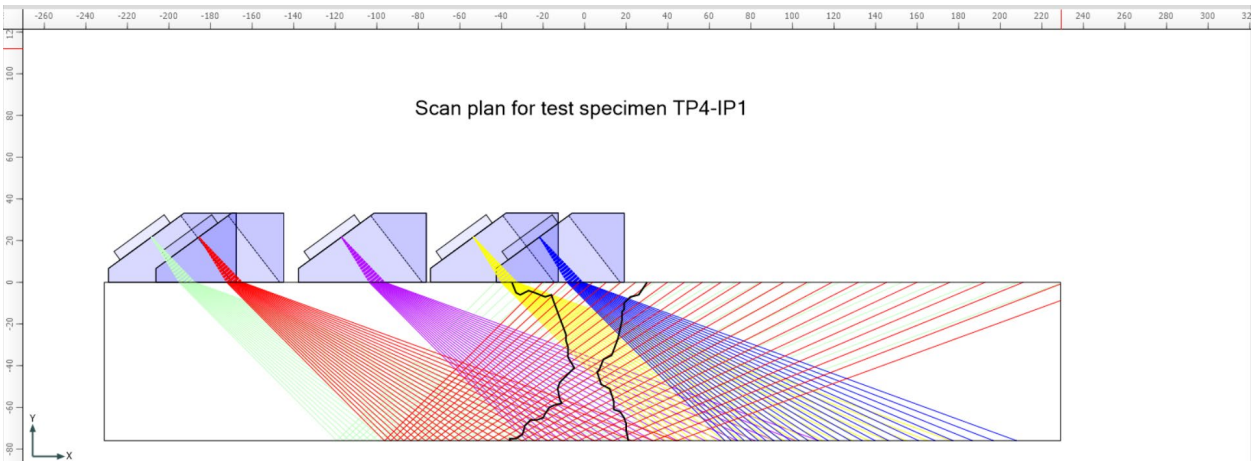

Source: FHWA.

A. Scan plan for test specimen TP4-IP1.

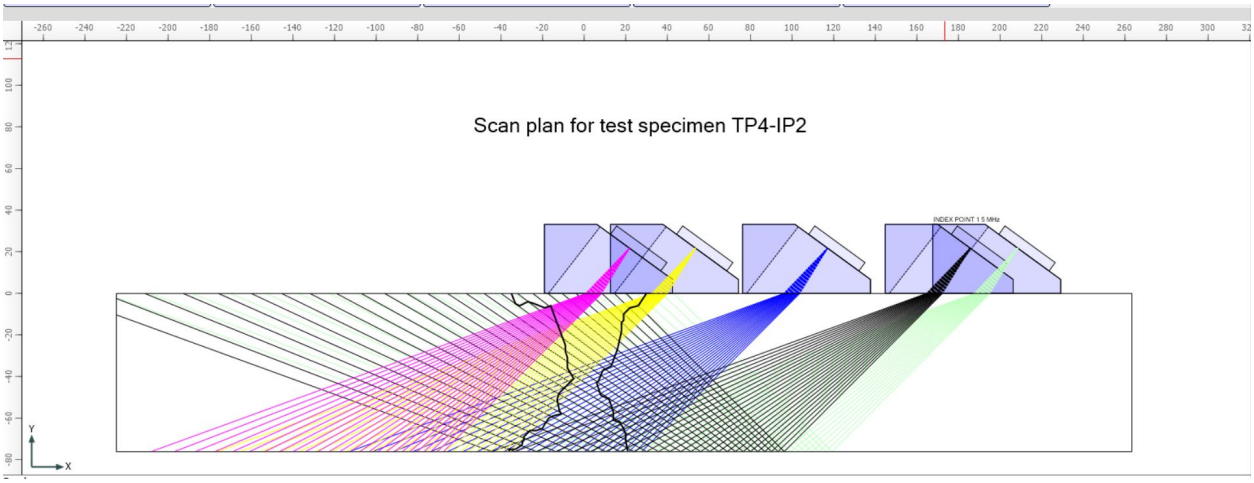

Source: FHWA.

B. Scan plan for test specimen TP4-IP2.

Figure 9. Schematics. TP4 scan plans for test specimens.

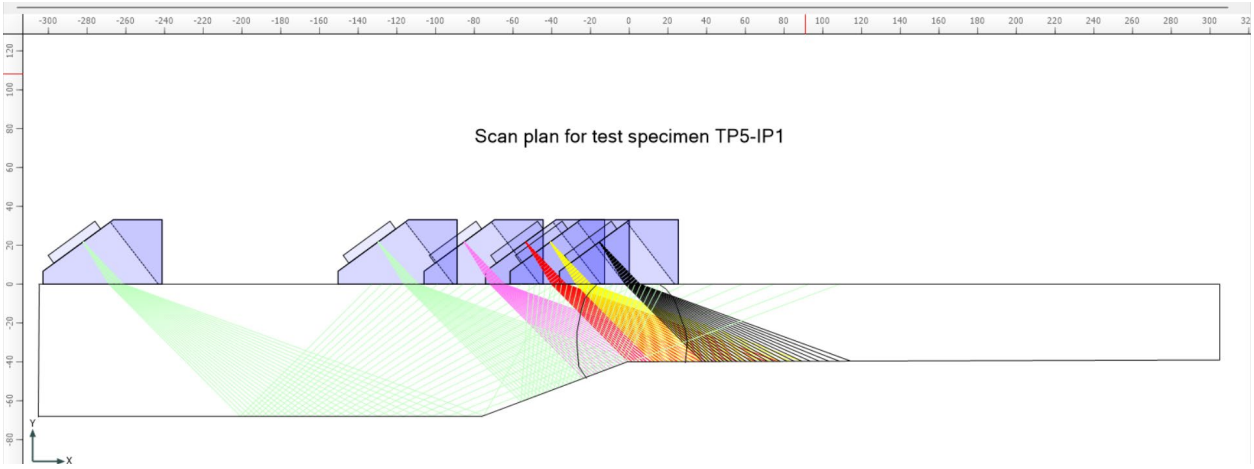

Source: FHWA.

A. Scan plan for test specimen TP5-IP1.

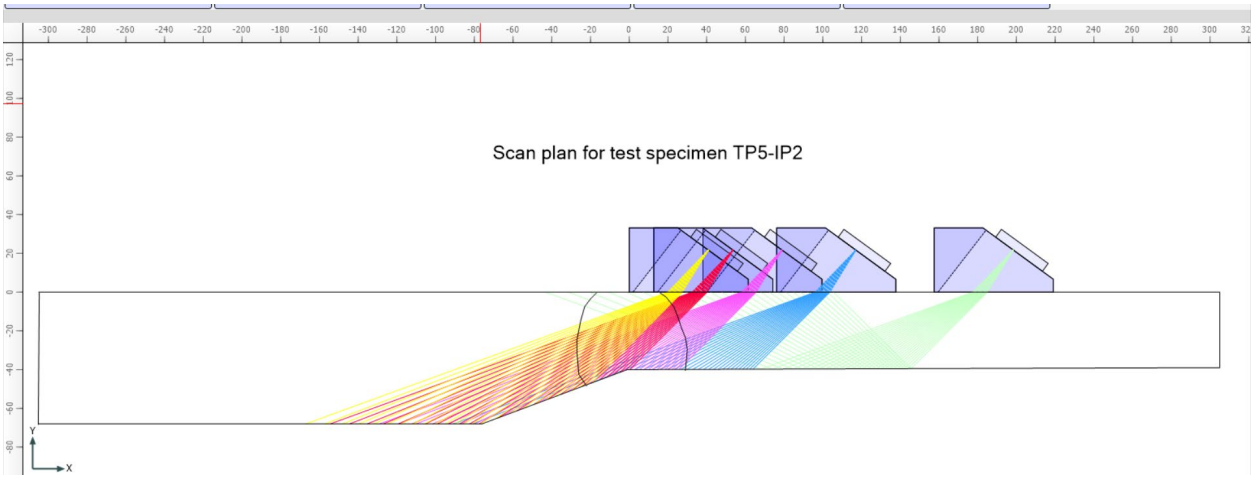

Source: FHWA.

B. Scan plan for test specimen TP5-IP2.

Figure 10. Schematics. TP5 scan plans for test specimens.

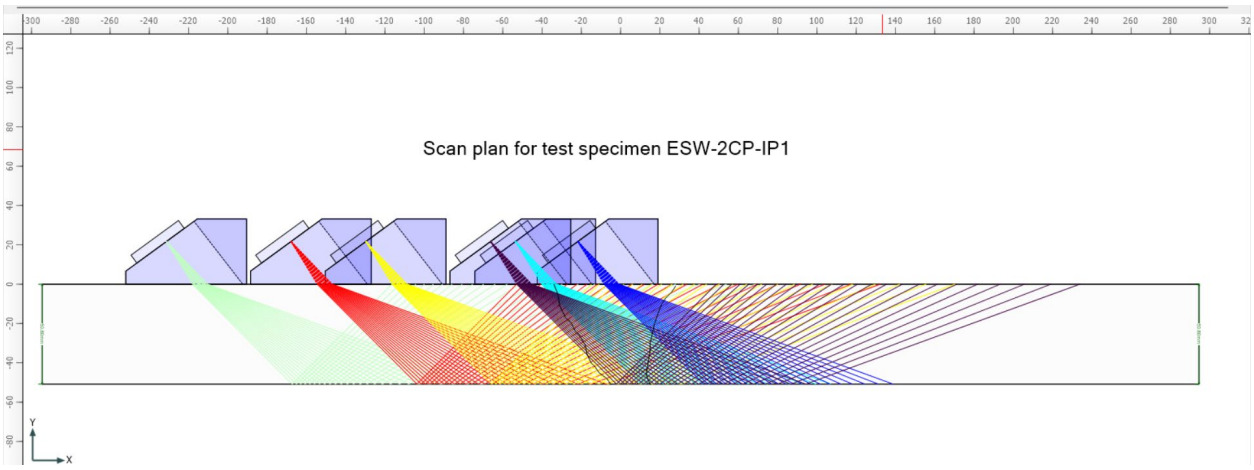

Source: FHWA.

A. Scan plan for test specimen ESW-2 complete penetration (CP)-IP1.

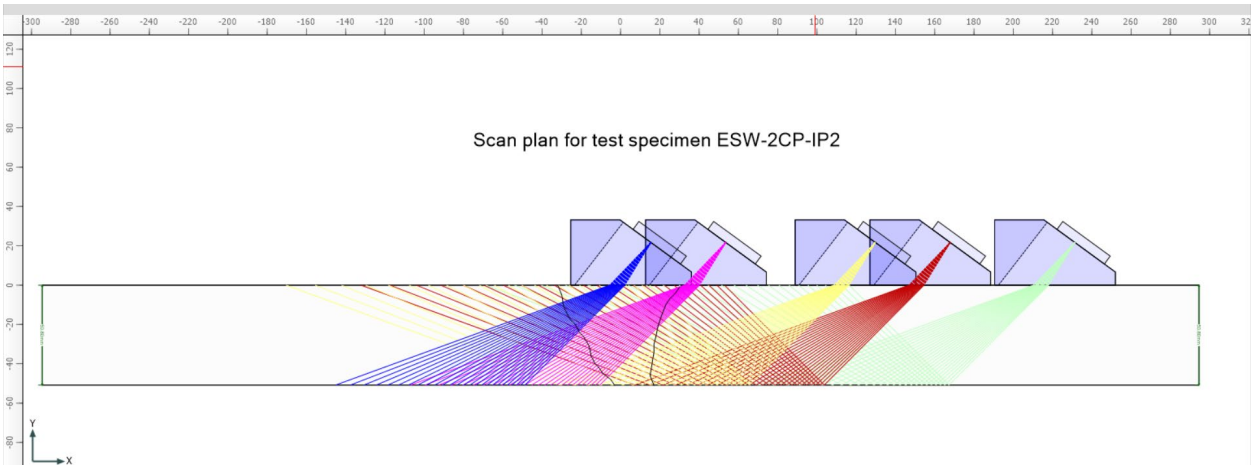

Source: FHWA.

B. Scan plan for test specimen ESW-2CP-IP2.

Figure 11. Schematics. ESW-2CP scan plans for test specimens.

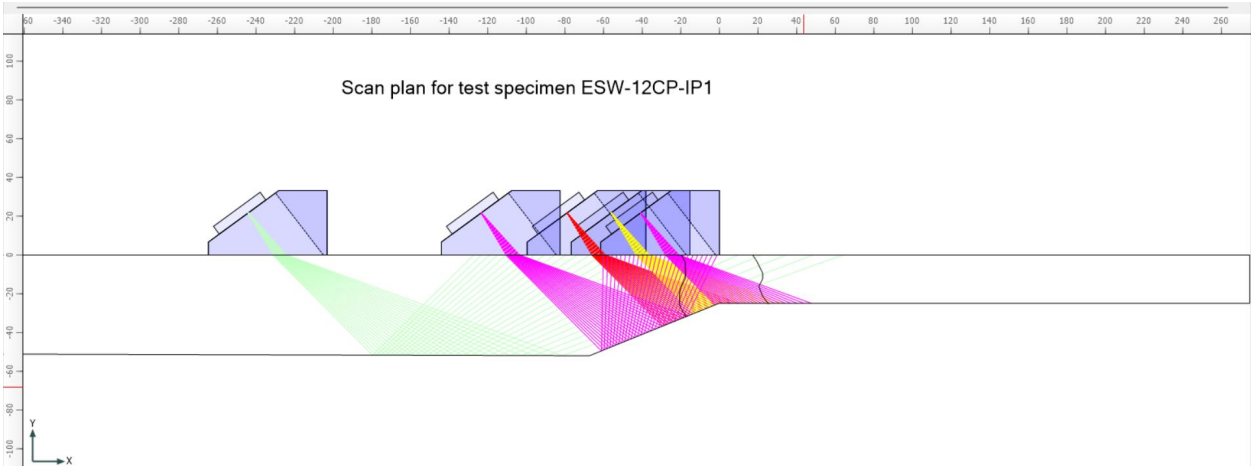

Source: FHWA.

A. Scan plan for test specimen ESW-12CP-IP1.

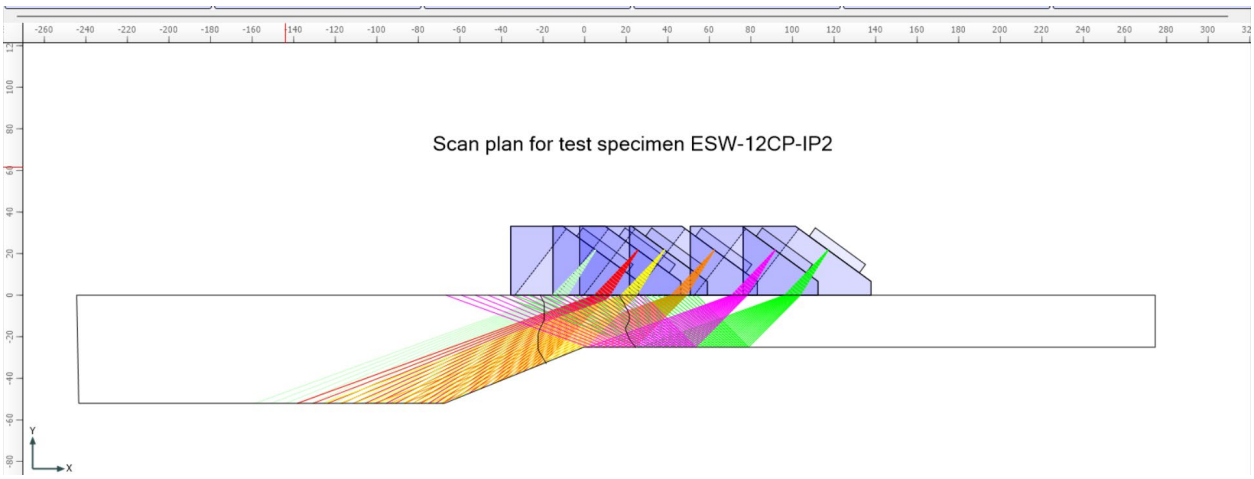

Source: FHWA.

B. Scan plan for test specimen ESW-12CP-IP2.

Figure 12. Schematics. ESW-12CP scan plans for test specimens.

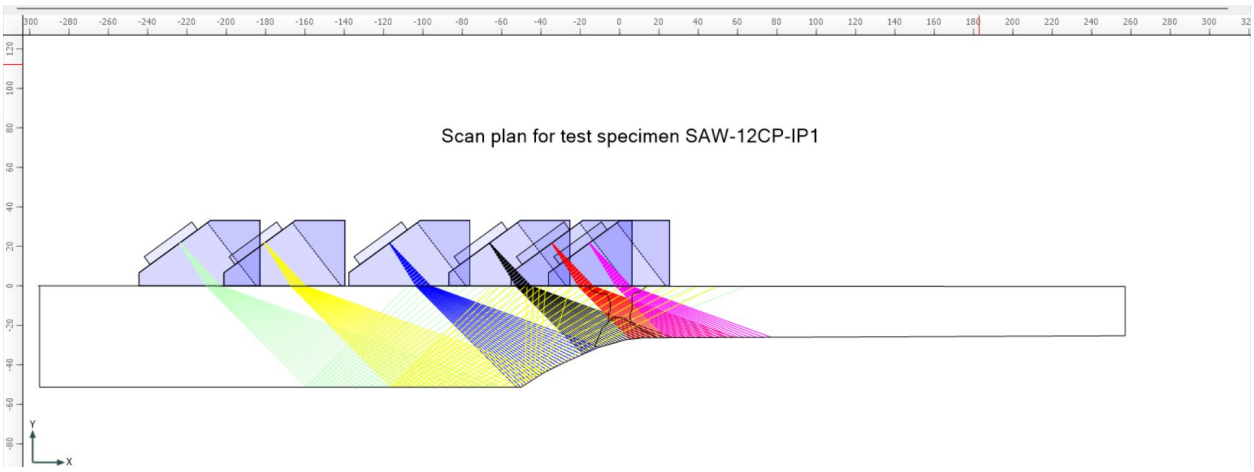

Source: FHWA.

A. Scan plan for test specimen SAW-12CP-IP1.

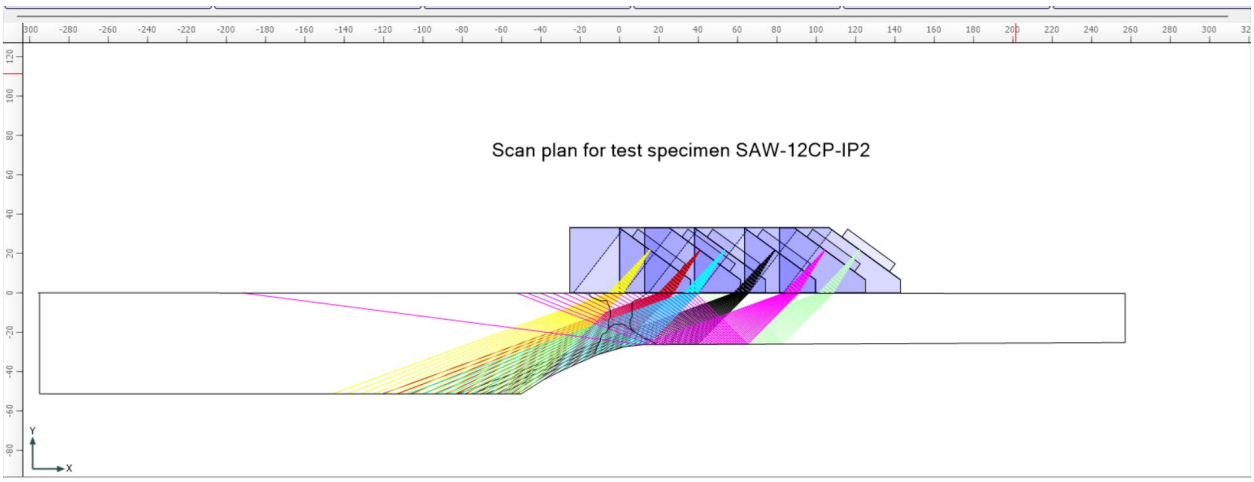

Source: FHWA.

B. Scan plan for test specimen SAW-12CP-IP2.

Figure 13. Schematics. SAW-12CP scan plans for test specimens.

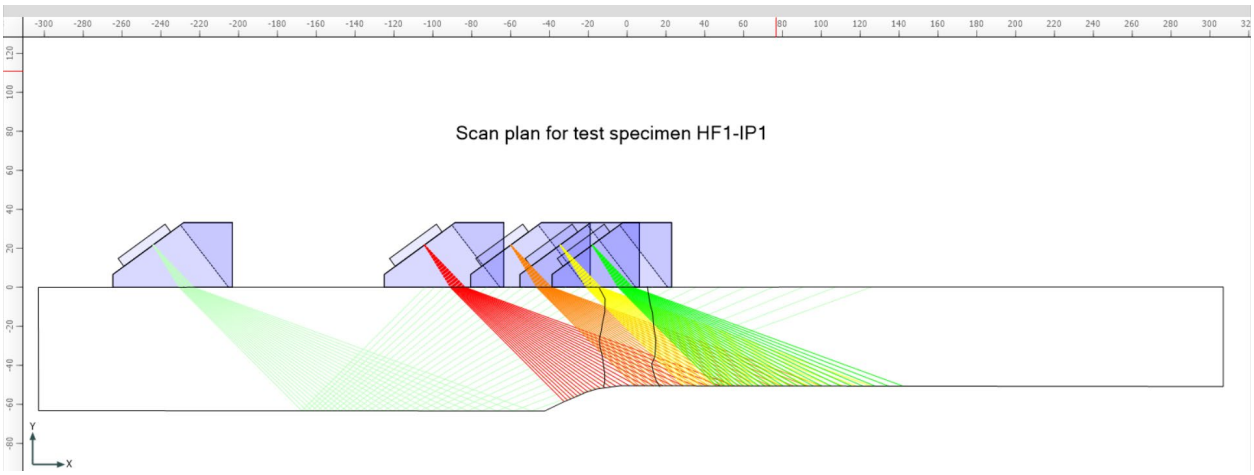

Source: FHWA.

A. Scan plan for test specimen Hirschfeld (HF)[8] 1-IP1.

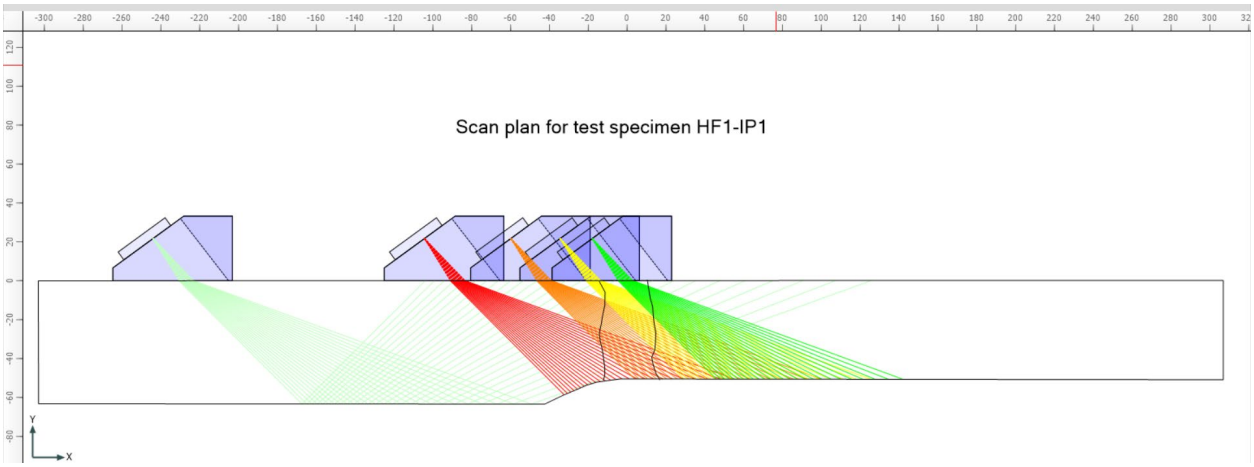

Source: FHWA.

B. Scan plan for test specimen HF1-IP2.

Figure 14. Schematics. HF1 scan plans for test specimens.

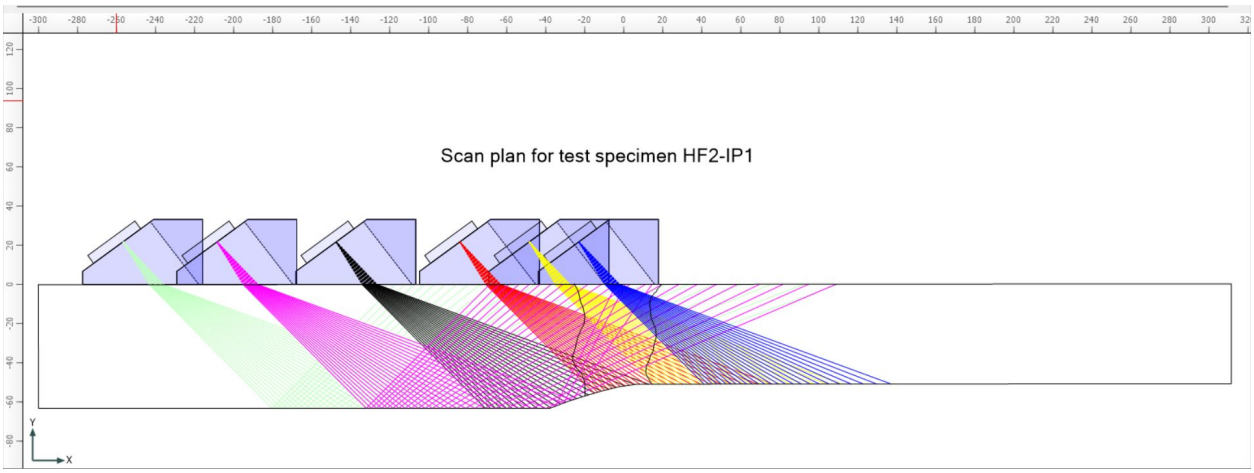

Source: FHWA.

A. Scan plan for test specimen HF2-IP1.

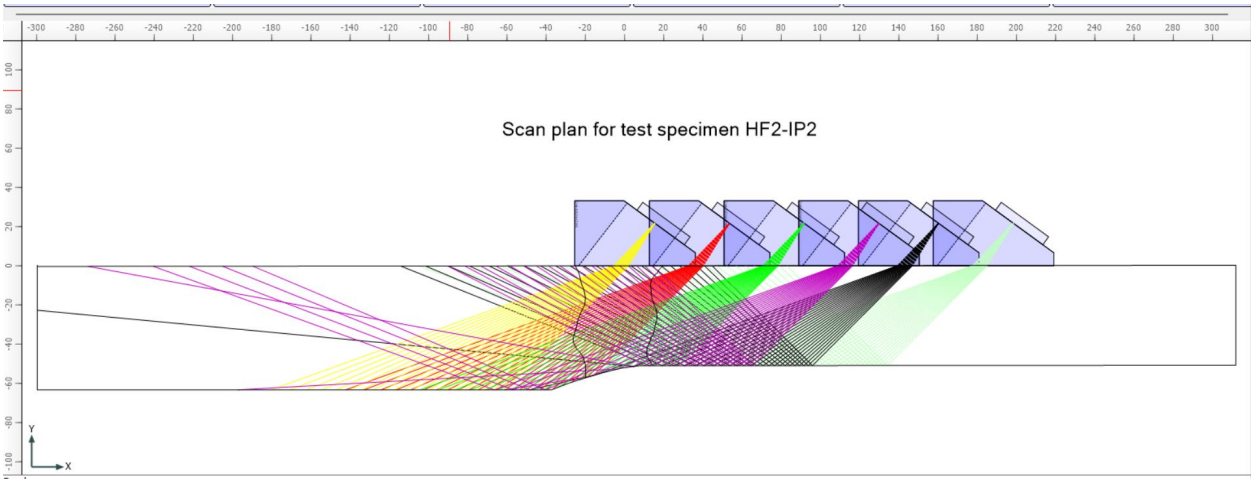

Source: FHWA.

B. Scan plan for test specimen HF2-IP2.

Figure 15. Schematics. HF2 scan plans for test specimens.

ACQUISITION AND ANALYSIS PROCEDURE

The data acquisition and analysis involved seven subtasks.

Subtask 1

The study team made detailed measurements of all the specimens involved in the testing, including specimen length, width, and height.

Subtask 2

The researchers labeled all the specimens (figure 16) with die stamps and photographed them to indicate the specimen's name, surface (top or bottom), and skew angles (90° or 270° side of weld).

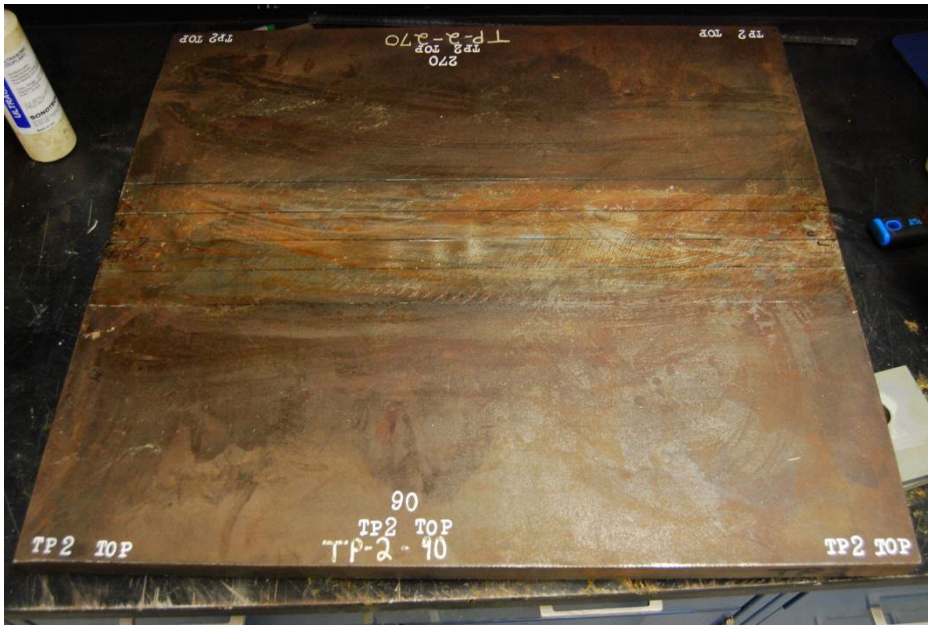

Source: FHWA.

Figure 16. Photo. Example of labeling of specimens.

Subtask 3

The team machined all the specimens to make the welds' cross sections visible. Next, they mechanically sanded and polished the weld surface and etching with nital etchant. Once the etching was completed, the researchers documented the results and took digital photographs of each etched surface, as illustrated in figure 17.

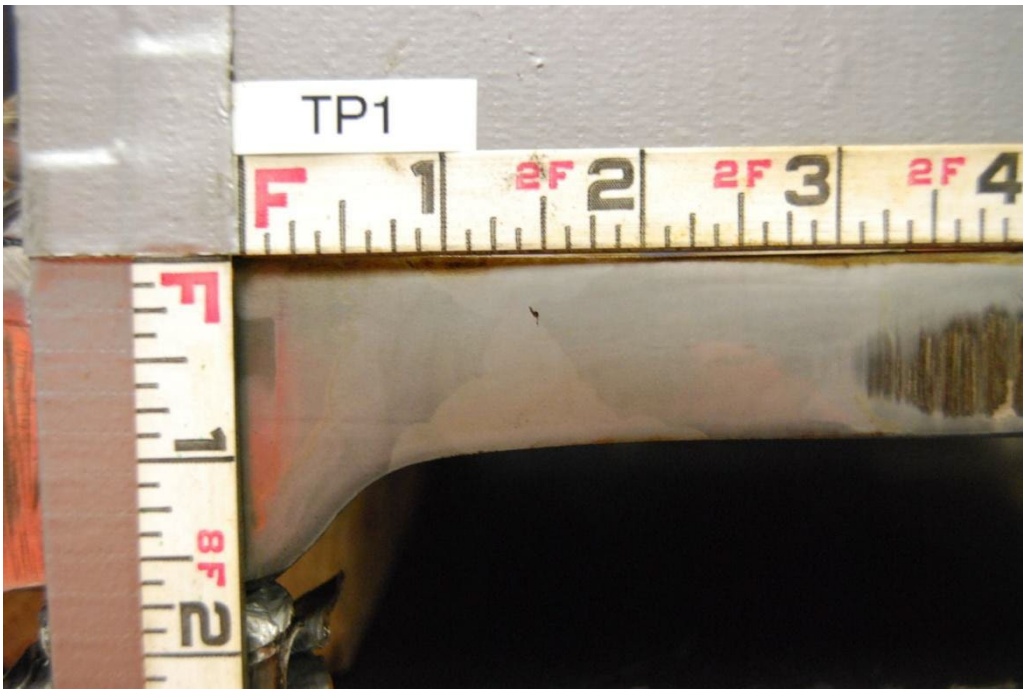

Source: FHWA.

Figure 17. Photo. Example of the etched specimen.

Subtask 4

The researchers developed computer-aided design (CAD) drawings using the etched surface details to show the specimen plan view and the weld profile dimension (figure 18).[(10)]

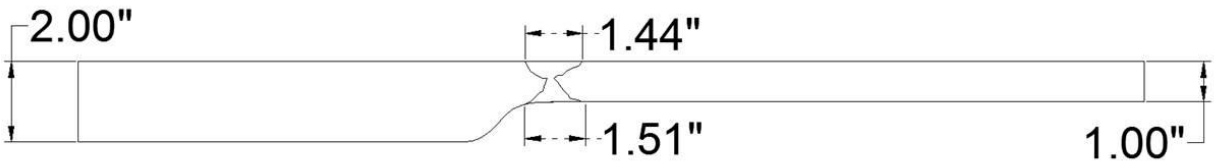

Source: FHWA.

Figure 18. Schematic. Example of CAD drawing based on the etched weld metal.

Subtask 5

For each test specimen, the study team developed scan plans using the information from etched surface details and the CAD drawings.

Subtask 6

The researchers completed the data acquisition using the scan plans developed in subtask 5.

Subtask 7

The research team analyzed the data from all the test specimens and performed a final analysis in accordance with 2020 AWS D1.5 Annex J on advanced ultrasonic examination[(2)] and in line with the approaches described earlier in this research effort.

DATA ANALYSIS

Using the 5 MHz probe, the team carried out the data acquisition with the PAUT system. The scan plans developed, as discussed in the previous section, were implemented in carrying out scans on each of the test specimens. They used a combination of A-, B-, C-, and S-scans[(6)] to interpret the data and determine the location and size of the discontinuities. The phased array equipment used in this research is capable of generating and displaying sectorial-scan (also called S-scan), B-scan, and C-scan images. The scan types are described in the following paragraph.

The researchers use "volume-corrected" C-scans as a first step to determine the approximate location of the discontinuities. The term "volume-corrected" refers to the corrections made to the image by the PAUT analysis software to properly scale the dimensions across the weld on the top C-scan view. Based on the locations of discontinuities inferred from the volume-corrected C-scans, the team further analyzed the data using a combination of S-scans and B-scans to accurately determine the location and size of each discontinuity. A combination of A-, B-, C-, and S-scan images was used to determine the length of the discontinuities (figure 19).

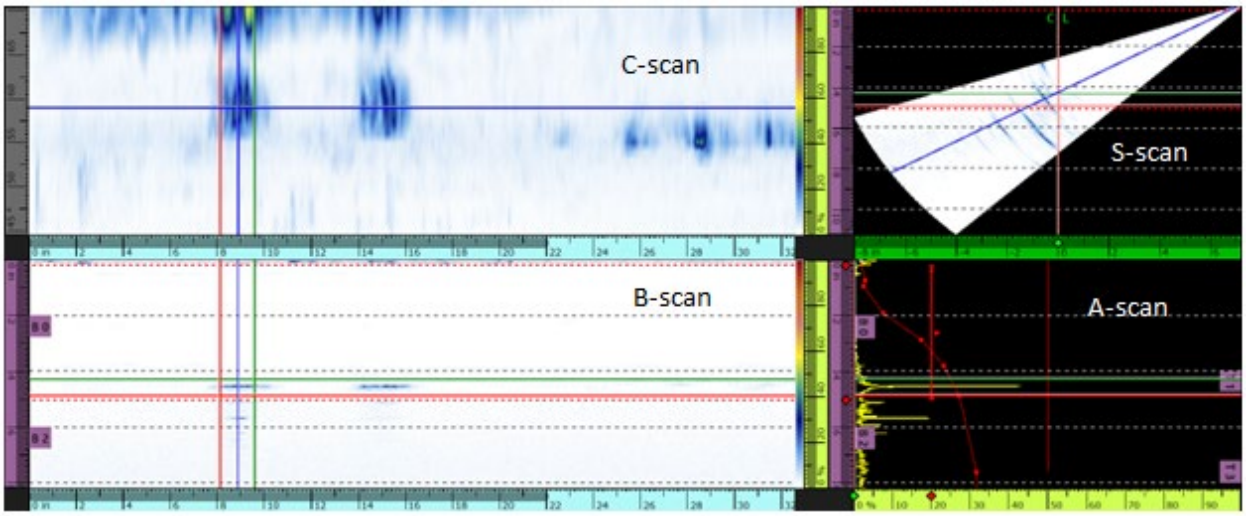

Source: FHWA.

Figure 19. Image. A-, B-, C-, and S-scan images.

The discontinuity length was determined using the 6-dB drop method in accordance with AWS D1.5.[(2)] Unlike conventional UT, in which the ultrasonic probe has to be physically moved, PAUT data can be analyzed as part of data postprocessing.[(5)] The data analysis software provides cursors that can be moved to determine the peak amplitude of the defect signal.[(11)] When the

peak defect signal is isolated, the flaw category can be defined in accordance with AWS D1.5, and the cursor is moved in both directions opposite the peak signal to determine flaw length.

CHAPTER 5. COMPARISON OF CONVENTIONAL UT, RT, AND PAUT

The research team inspected each test specimen by using the conventional single element UT system and then using the PAUT system. Based on the AWS D1.5 requirements for conventional UT, the discontinuities are classified as follows for a weld under tensile stress:[(2)]

- Class A (large discontinuity): Any indication in this category shall be rejected regardless of length.
- Class B (medium discontinuity): Any indication in this category having a length greater than 0.75 inch shall be rejected.
- Class C (small discontinuity): Any indication in this category having a length greater than 2 inches in the middle half, or 0.75-inch length in the top or bottom quarter of the weld thickness, shall be rejected.
- Class D (minor discontinuity): Any indication in this category shall be accepted regardless of length or location in the weld.

The requirements for welds under compressive stress are less stringent. Table 8.4 and table 8.5 in AWS D1.5 provide the acceptance-rejection criteria for tension and compression welds, respectively.[(2)] The team compared the results from conventional UT to the PAUT results (see table 4).

Figure 20 to figure 28 present comparisons of volume-corrected C-scan images to digital photographs from RT. The examples include both flat CJP butt welds and transition butt-weld specimens.

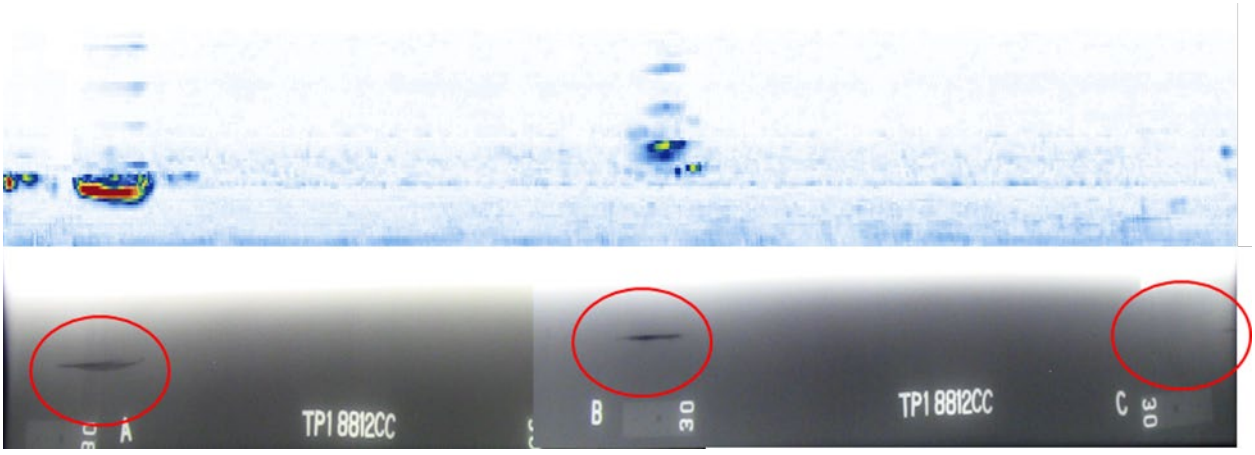

Source: FHWA.

Figure 20. Image. Comparison of volume-corrected C-scan image to RT digital photograph, specimen TP1 (butt-weld specimen).

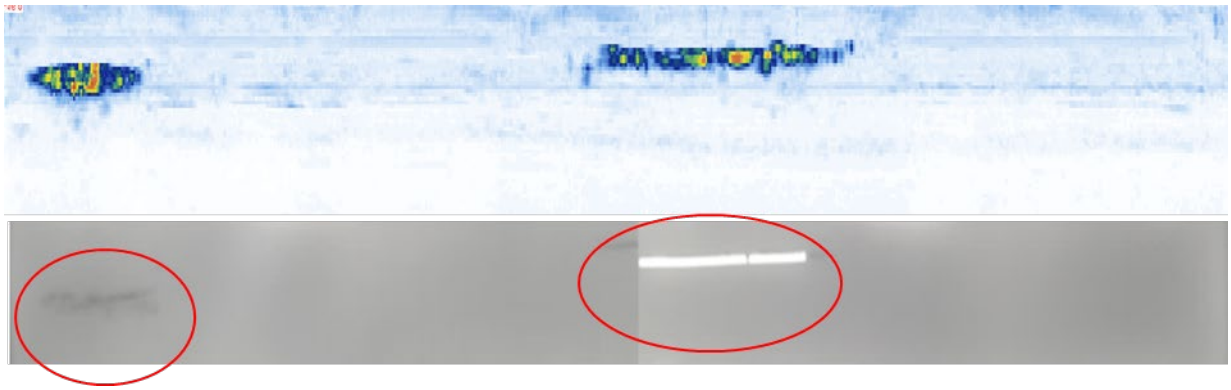

Source: FHWA.

Figure 21. Image. Comparison of volume-corrected C-scan image to RT digital photograph, specimen TP2 (butt-weld specimen).

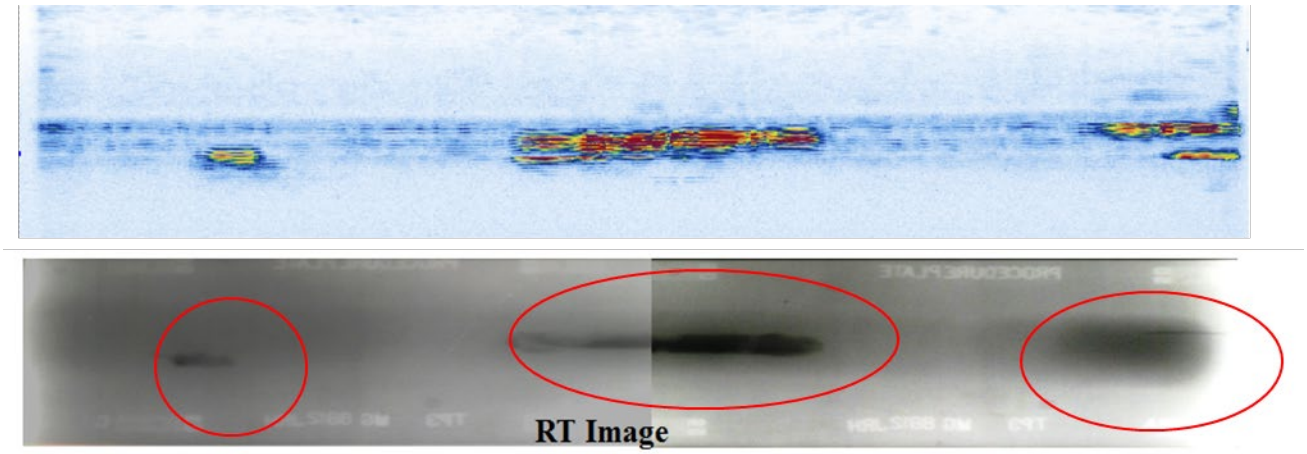

Source: FHWA.

Figure 22. Image. Comparison of volume-corrected C-scan image to RT digital photograph, specimen TP3 (butt-weld specimen).

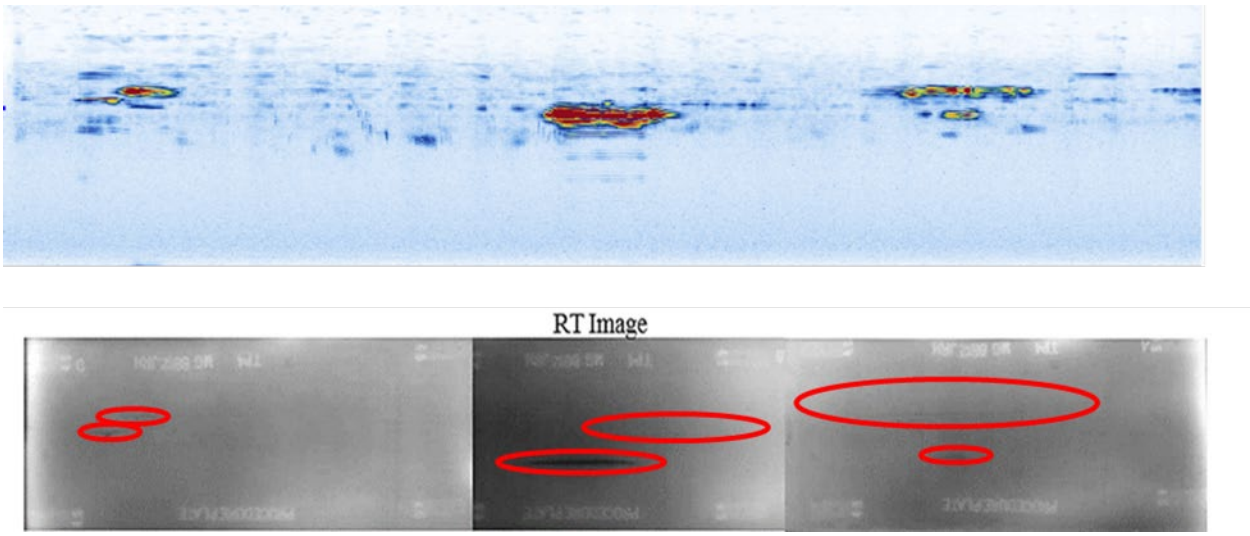

Source: FHWA.

Figure 23. Image. Comparison of volume-corrected C-scan image to RT digital photograph, specimen TP4 (butt-weld specimen).

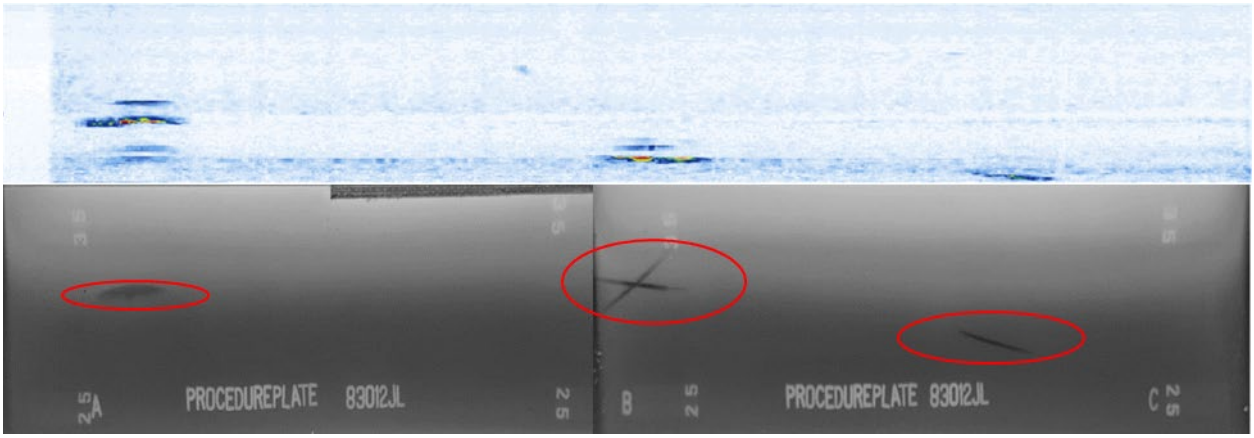

Source: FHWA.

Figure 24. Image. Comparison of volume-corrected C-scan image to RT digital photograph, specimen TP5 (butt-weld specimen).

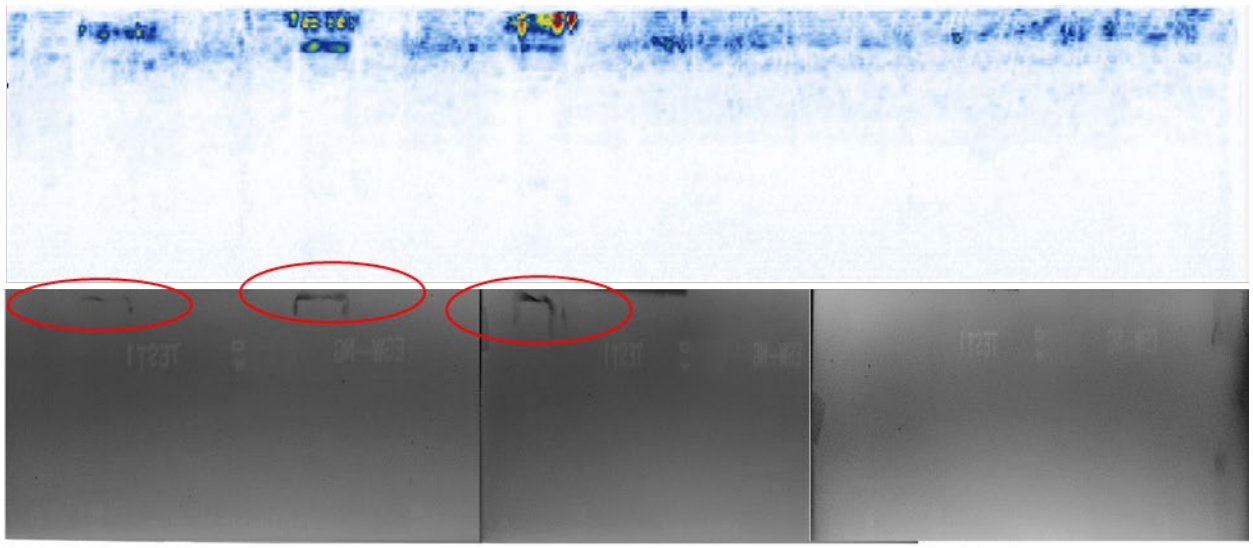

Source: FHWA.

Figure 25. Image. Comparison of volume-corrected C-scan image to RT digital photograph, specimen HF1 (butt-weld specimen).

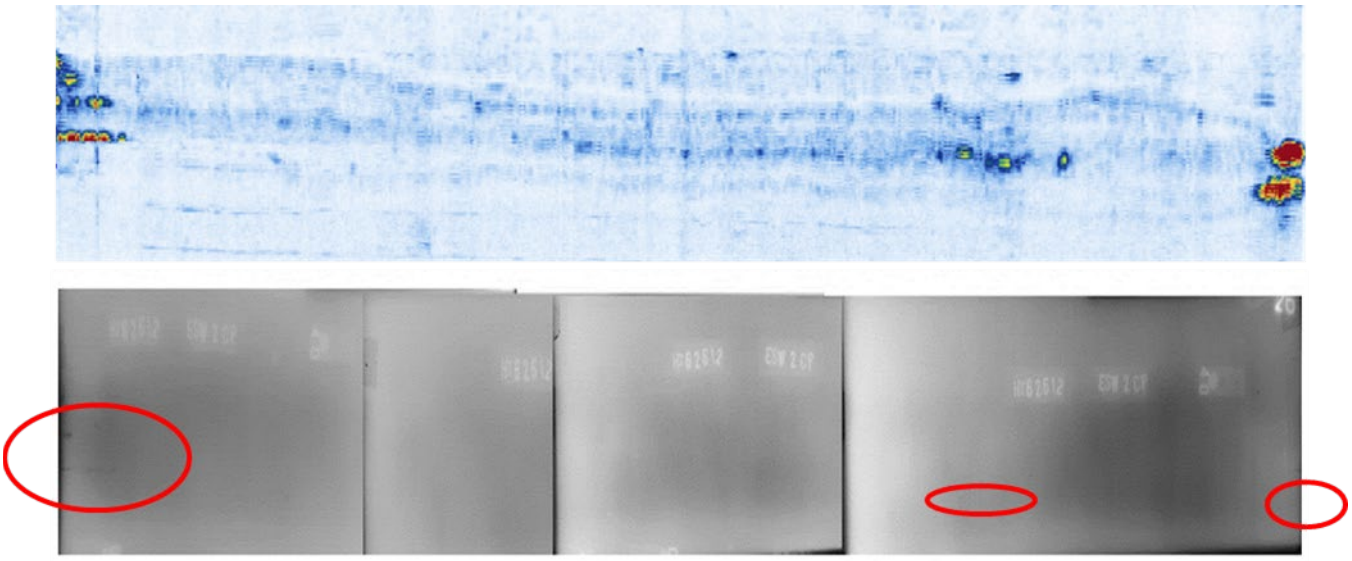

Source: FHWA.

Figure 26. Image. Comparison of volume-corrected C-scan image to RT digital photograph, specimen ESW-2CP (butt-weld specimen).

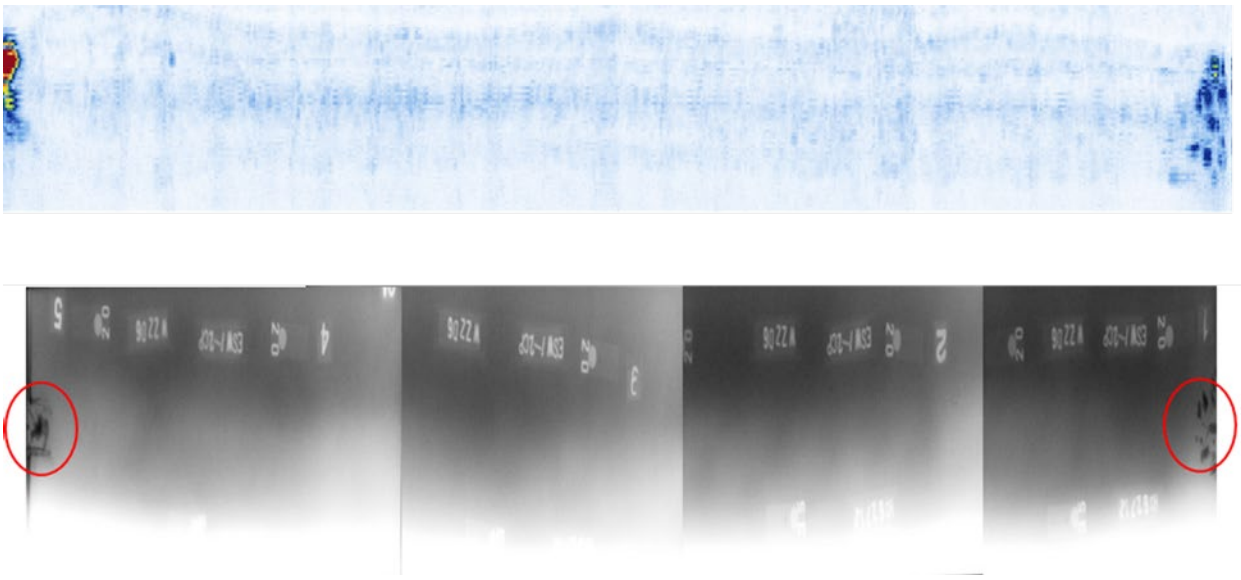

Source: FHWA.

Figure 27. Image. Comparison of volume-corrected C-scan image to RT digital photograph, specimen ESW-12CP (butt-weld specimen).

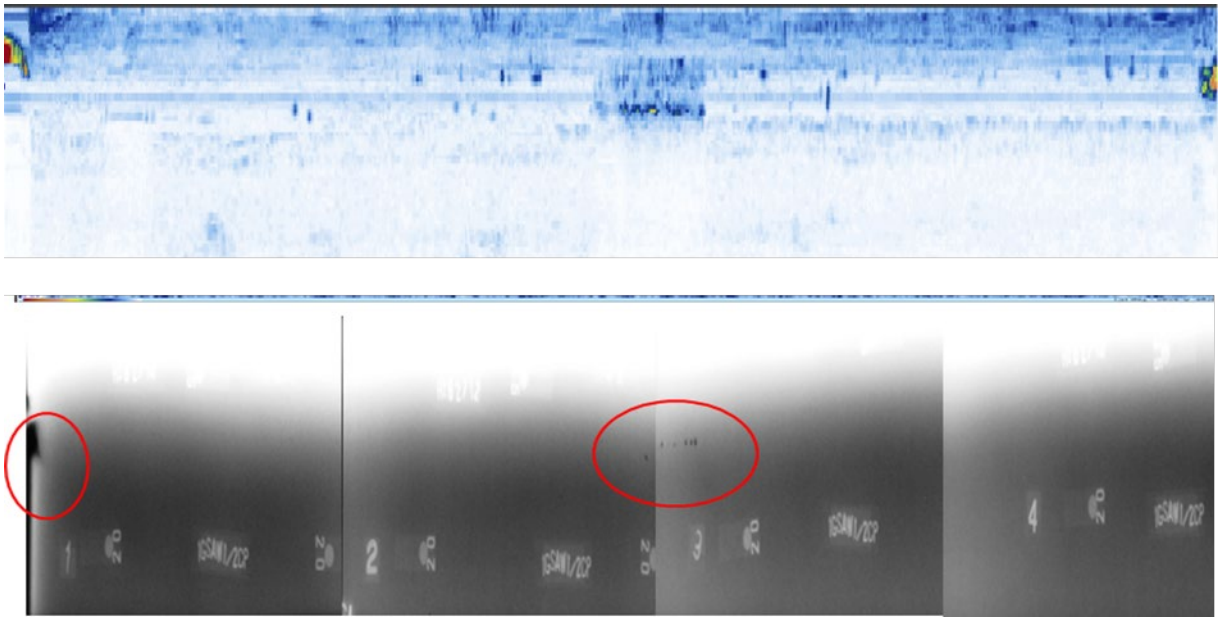

Source: FHWA.

Figure 28. Image. Comparison of volume-corrected C-scan image to RT digital photograph, specimen SAW-12CP (butt-weld specimen).

Figure 20 to figure 28 also present a subjective degree of correlation between discontinuity locations, as determined using volume-corrected C-scans and as revealed in the RT images. RT images are typically used only to locate discontinuities. The sizing of the images using RT can provide measurements of discontinuity length, but the depth at which the discontinuities occur cannot be inferred using RT. PAUT data, however, can be used to locate and size discontinuities.

This capability of PAUT to locate and size discontinuities provides an advantage of utilizing PAUT, particularly when repairs are required, and the repair depth needs to be determined. In addition, using RT in an industrial or laboratory setup gives rise to a variety of radiation regulatory and safety issues.

CHAPTER 6. FINAL COMPARATIVE PAUT, CONVENTIONAL UT, AND RT RESULTS

The results of the PAUT, conventional UT, and radiography are provided in table 4. The researchers collected and analyzed the PAUT data at the TFHRC NDE Laboratory. The radiography was performed by the specimen fabricators when they welded the TPs.

The discontinuity character column in table 4 is the best judged character for each discontinuity. Most of this information comes from the radiographs, where the image of the discontinuity provides the most useful characterization information. Planar discontinuities like lack of fusion, and most cracks are only detectable by RT when the discontinuity plane aligns with the radiation beam. The cracks can also be detected when the width of the lack of fusion is so wide that the volume of the discontinuity can be imaged by RT. Most of the lack of fusion in these plates was wide enough to be imaged by RT. Figure 29 presents the comparison of depth of the discontinuities between conventional UT and PAUT. Figure 30 presents a scatter plot for the depth of discontinuities in UT and PAUT. Figure 31 presents the comparison of the length of discontinuities between radiography and PAUT. Figure 32 presents a scatter plot for the length of discontinuities in RT and PAUT, and figure 33 presents the length comparison of PAUT and UT. Slight variations in the depth may arise as PAUT data are collected linearly. In a linear scan, the probe is not rastered to maximize the signal from discontinuities, and as a result, small depth positioning errors would occur in PAUT.[3]

Scatter plots are commonly used in the visualization of nondestructive testing measurements to determine the relationship between dimensions of discontinuities measured using different methods.. An identity line is drawn in each scatter plot, representing the measurements plotted on the x and y axes that are equal between inspection methods. Correlation factors (R) calculated for measurements using PAUT, UT, and RT indicate a strong correlation between them. Furthermore, a strong correspondence between the slope of the regression and identity lines and low y-intercept values of the regression lines, as shown in the scatter plots, indicate close similarities in the measurements.

From the scatter plot (figure 30) for the comparison between the depth measurements between the phased array and UT, a strong correlation (correlation factor = 0.953) can be assumed between the measured values and the slope of the regression line, which is 0.96. Additionally, the scatter plot comparing the length of discontinuities between PAUT and RT (figure 32) indicates a strong correlation (R = 0.89) with a regression line slope of 0.9.

A strong correlation of 0.91 is between the length measured by PAUT and UT, and the regression line slope is approximately 1, as observed in the scatter plot (figure 34).

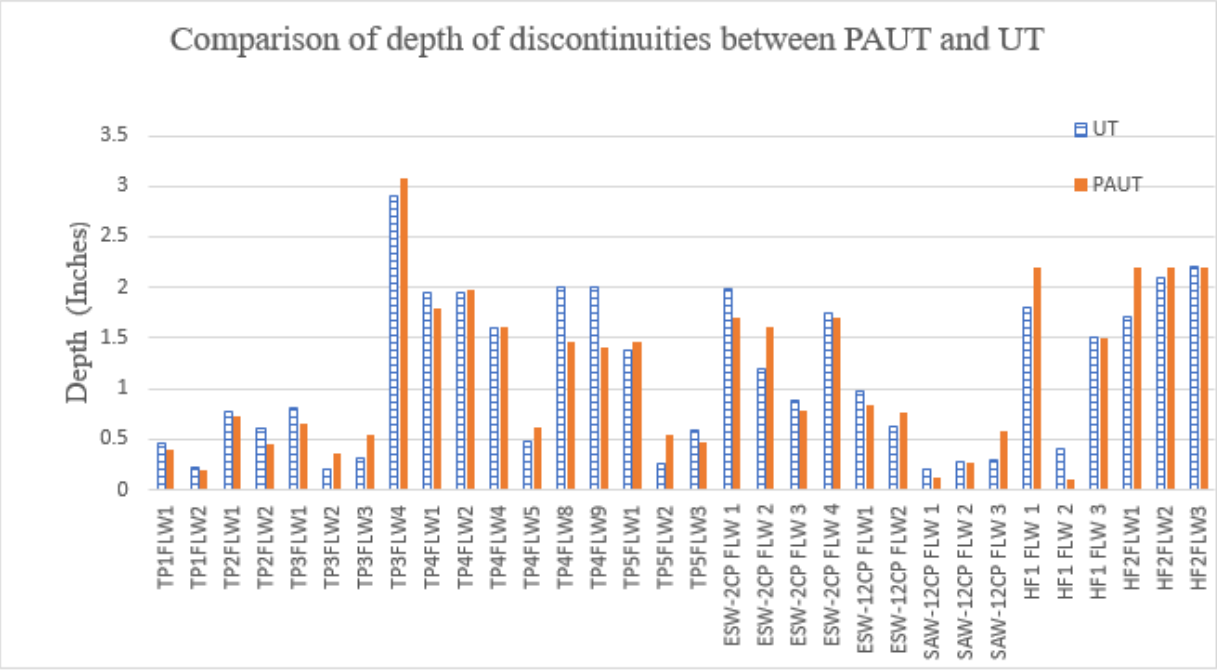

Source: FHWA.

Figure 29. Graph. Discontinuity depth comparison—UT and PAUT.

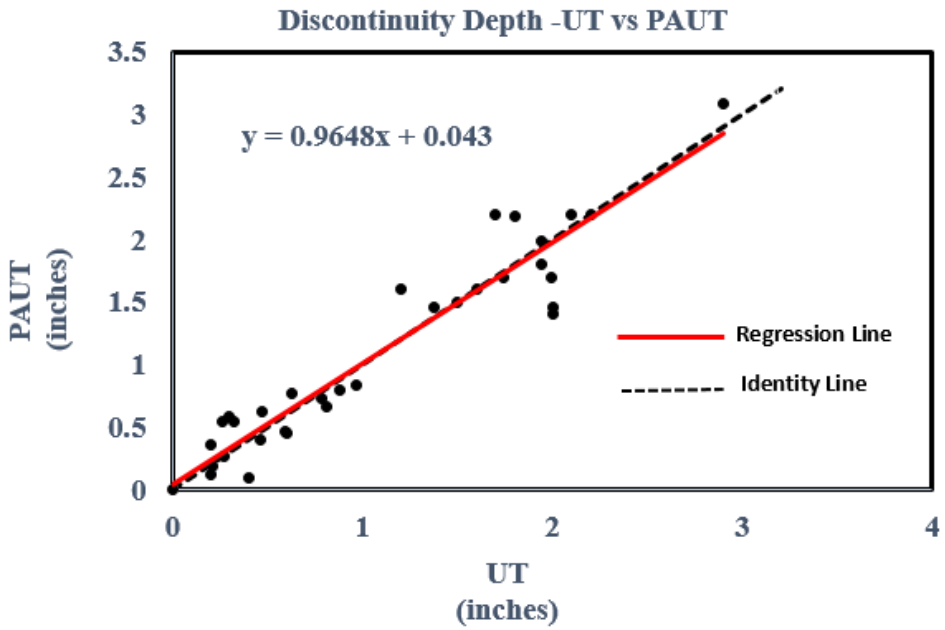

Source: FHWA.

Figure 30. Graph. Scatter plot for discontinuity depth—UT versus PAUT.

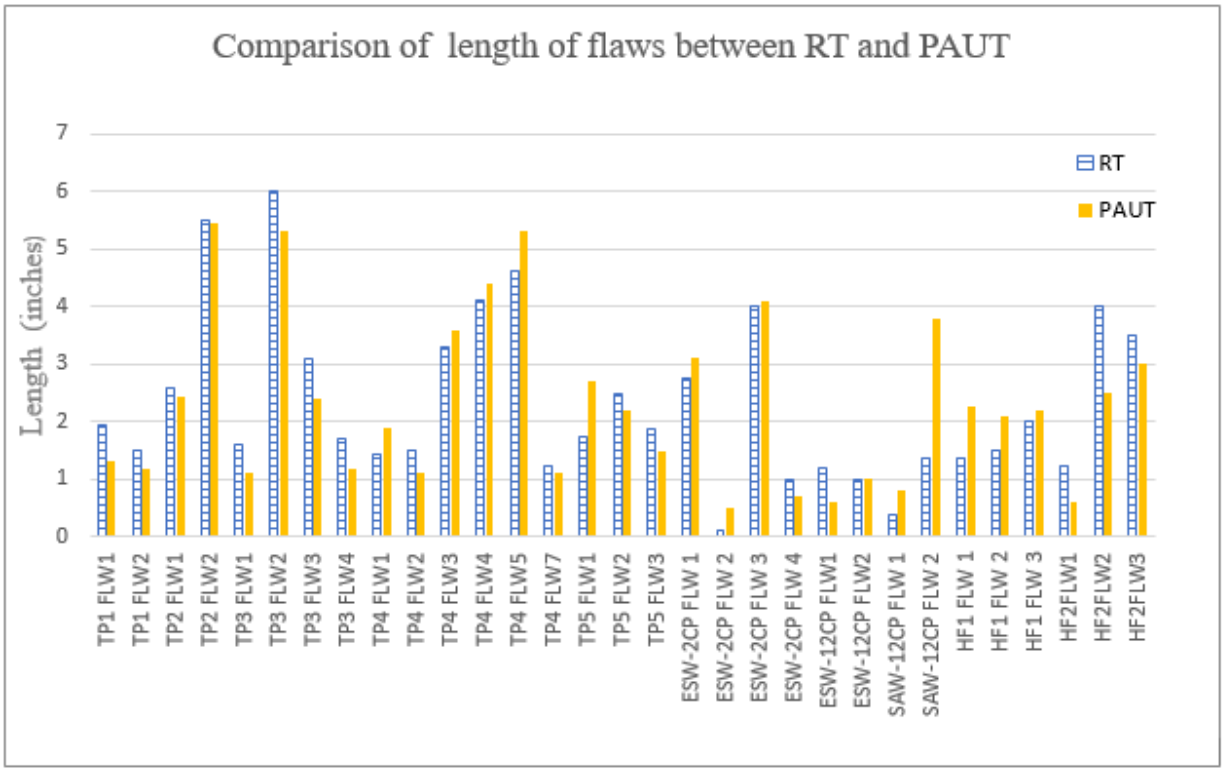

Source: FHWA.

Figure 31. Graph. Discontinuity length comparison—RT and PAUT

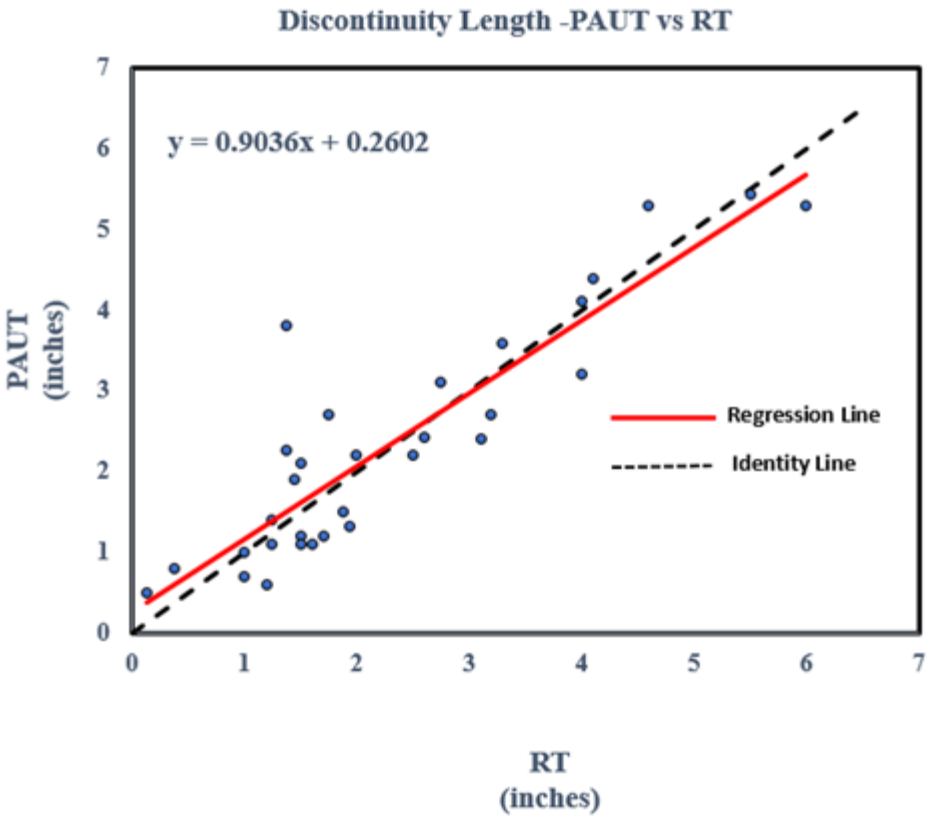

Source: FHWA.

Figure 32. Graph. Scatter plot for discontinuity length—PAUT versus RT.

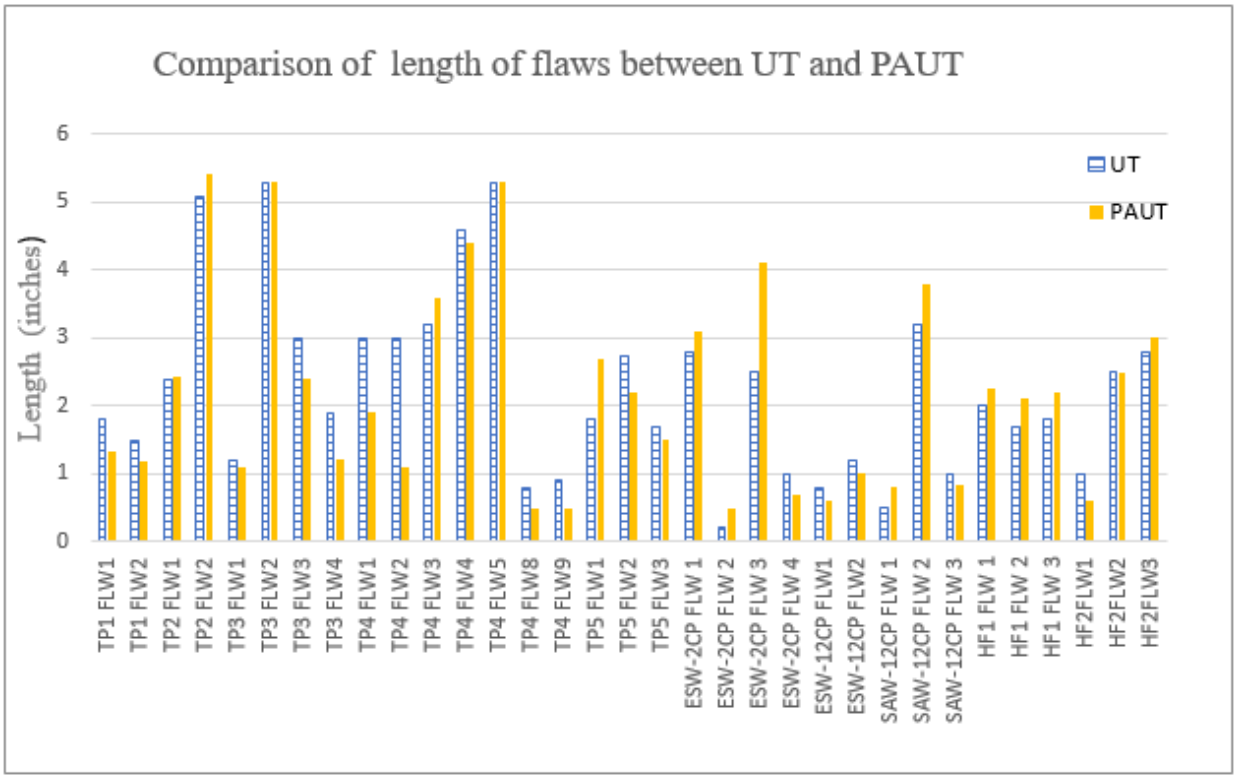

Source: FHWA.

Figure 33. Graph. Discontinuity length comparison—UT and PAUT.

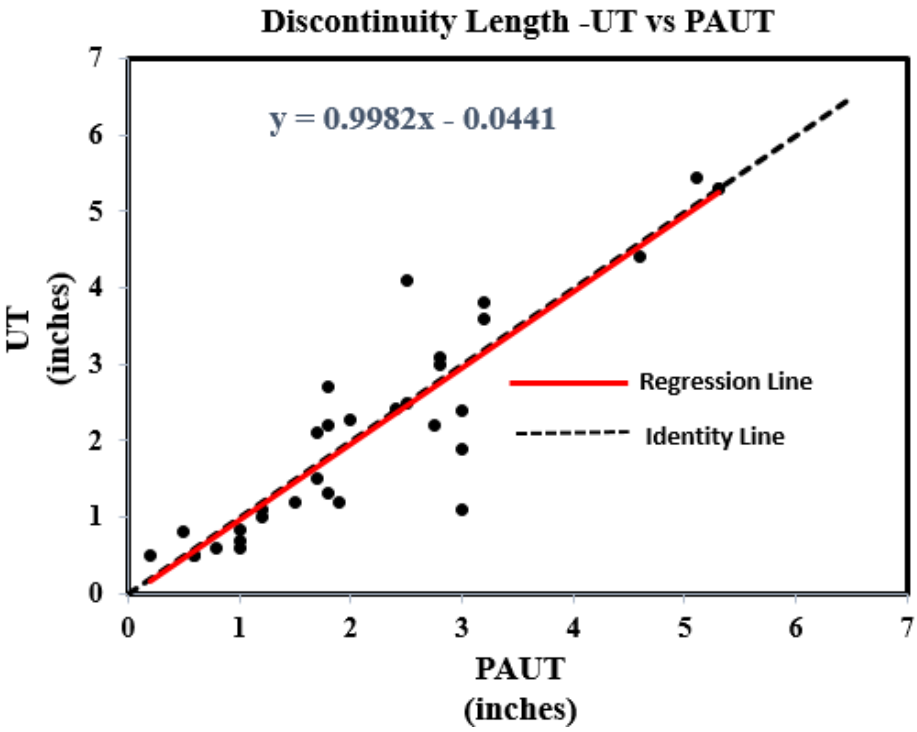

Source: FHWA.

Figure 34. Graph. Scatter plot for discontinuity length—UT versus PAUT.

Table 3 presents the variability in the measurement of depth between UT and PAUT and the length between PAUT and UT and between PAUT and RT. Considering the 95-percent limit of agreement, the team observed six outliers in the comparison results. The discontinuities identified as TP4-Flaw 8,9 and HF2-Flaw 1 indepth comparison; SAW12-CP Flaw 2 in RT and PAUT length comparison and TP4-Flaw 2; and ESW2-CP-Flaw 3 in UT and PAUT length comparison are the outliers observed. The term flaw is generally used to denote undesirable discontinuities in welds.

Table 3. Variance in the test results.

Variance	Depth (UT versus PAUT)	Length (RT versus PAUT)	Length (UT versus PAUT)
Maximum	0.5	0.8	1.9
Minimum	−0.6	−2.42	−1.6
Average	0.0042	−0.038	0.0481
Standard Deviation	0.239	0.658	0.596

Table 4 indicates that four discontinuities rejected in RT were either accepted or missed by PAUT. Such discrepancies in discontinuity acceptance between RT and PAUT are not uncommon.[(4)] Additionally, three discontinuities (lack of fusion) detected in PAUT were missed in radiography, and one rejected discontinuity in PAUT was accepted in RT.

Table 4. PAUT, conventional manual UT, and RT results.

Plate and Discontinuity ID	Joint Type	Welding Process	Nominal Plate Thickness(Inches)	Discontinuity Character	Technique (RT, Manual UT, PAUT)	UT Beam Direction	Start " Y" Along Weld (Inches)	Length (Inches)	Location " X" Across (Inches)	UT Depth (Inches)	Amplitude/Rating	D1.5 ACC/REJ (Tensile)[2]
TP1, FLAW 1	V2	SAW	1–2	LOF	RT	—	1	1.94	—	—	—	REJ
TP1, FLAW 1	V2	SAW	1–2	LOF	UT	270	1.2	1.8	0.1	0.465	−3 (A)	REJ
TP1, FLAW 1	V2	SAW	1–2	LOF	PAUT	270	1.68	1.32	0.2	0.402	74% (B)	REJ
TP1, FLAW 2	V2	SAW	1–2	LOF	RT	—	12.7	1.5	—	—	—	REJ
TP1, FLAW 2	V2	SAW	1–2	LOF	UT	90	12.6	1.5	−0.1	0.212	−5 (A)	REJ
TP1, FLAW 2	V2	SAW	1–2	LOF	PAUT	90	13.1	1.19	−0.1	0.19	30% (C)	REJ
TP1, FLAW 3	V2	SAW	1–2	LOF	RT	—	24.5	0.5	—	—	—	REJ
TP1, FLAW 3	V2	SAW	1–2	—	UT	—	—	—	—	—	—	MISS
TP1, FLAW 3	V2	SAW	1–2	—	PAUT	—	—	—	—	—	—	MISS
TP2, FLAW 1	SQ	ESW-NG	1.5	LOF	RT	—	0.75	2.6	—	—	—	REJ
TP2, FLAW 1	SQ	ESW-NG	1.5	LOF	UT	90	0.75	2.4	0.5	0.78	−6 (A)	REJ
TP2, FLAW 1	SQ	ESW-NG	1.5	LOF	PAUT	90	0.64	2.42	0.3	0.73	49% (C)	REJ
TP2, FLAW 2	SQ	ESW-NG	1.5	LOF/TUNG	RT	—	13.1	5.5	—	—	—	REJ
TP2, FLAW 2	SQ	ESW-NG	1.5	LOF/TUNG	UT	90	13.4	5.1	0.2	0.6	−2 (A)	REJ
TP2, FLAW 2	SQ	ESW-NG	1.5	LOF/TUNG	PAUT	90	13.3	5.43	0	0.45	40% (C)	REJ
TP3, FLAW 1	SQ	ESW-NG	3.3	LOF	RT	—	3.5	1.6	—	—	—	REJ
TP3, FLAW 1	SQ	ESW-NG	3.3	LOF	UT	270	3.5	1.2	−0.3	0.81	−2 (A)	REJ
TP3, FLAW 1	SQ	ESW-NG	3.3	LOF	PAUT	270	3.5	1.1	−0.5	0.66	44% (C)	REJ
TP3, FLAW 2	SQ	ESW-NG	3.3	Slag	RT	—	9.6	6.3	—	—	—	REJ
TP3, FLAW 2	SQ	ESW-NG	3.3	Slag	UT	90	9.9	5.3	0.1	0.2	−4 (A)	REJ
TP3, FLAW 2	SQ	ESW-NG	3.3	Slag	PAUT	90	10.1	5.3	0	0.36	90% (A)	REJ
TP3, FLAW 3	SQ	ESW-NG	3.3	Slag	RT	—	20.7	3.1	—	—	—	REJ
TP3, FLAW 3	SQ	ESW-NG	3.3	Slag	UT	90	20.7	3	0	0.32	−1 (A)	REJ

Plate and Discontinuity ID	Joint Type	Welding Process	Nominal Plate Thickness(Inches)	Discontinuity Character	Technique (RT, Manual UT, PAUT)	UT Beam Direction	Start " Y" Along Weld (Inches)	Length (Inches)	Location " X" Across (Inches)	UT Depth (Inches)	Amplitude/Rating	D1.5 ACC/REJ (Tensile)[2]
TP3, FLAW 3	SQ	ESW-NG	3.3	Slag	PAUT	90	21.2	2.4	0.1	0.55	31% (C)	REJ
TP3, FLAW 4	SQ	ESW-NG	3.3	LOF	RT	—	22.4	1.7	—	—	—	REJ
TP3, FLAW 4	SQ	ESW-NG	3.3	LOF	UT	270	21.8	1.9	−0.4–0.4	2.9	0 (A)	REJ
TP3, FLAW 4	SQ	ESW-NG	3.3	LOF	PAUT	270	22.4	1.2	−0.4–0.4	3.08	53% (B)	REJ
TP4, FLAW 1	V2	SAW	3	LOF	RT	—	1.75	1.45	—	—	—	REJ
TP4, FLAW 1	V2	SAW	3	LOF	UT	90	1.8	3	−0.2	1.94	−7 (A)	REJ
TP4, FLAW 1	V2	SAW	3	LOF	PAUT	90	2.38	1.94	−0.2	1.8	34% (C)	ACC
TP4, FLAW 2	V2	SAW	3	LOF	RT	—	2.7	1.5	—	—	—	REJ
TP4, FLAW 2	V2	SAW	3	LOF	UT	—	1.8	3	−0.7	1.94	−7 (A)	REJ
TP4, FLAW 2	V2	SAW	3	LOF	PAUT	270	3.7	1.1	−0.7	1.98	118% (A)	REJ
TP4, FLAW 3	V2	SAW	3	LOF	RT	—	15.3	3.3	—	—	—	REJ
TP4, FLAW 3	V2	SAW	3	LOF	UT	—	16	3.2	—	0	4 (C)	REJ
TP4, FLAW 3	V2	SAW	3	LOF	PAUT	90	16.34	3.59	0.4	0.1	101% (A)	REJ
TP4, FLAW 4	V2	SAW	3	LOF	RT	—	17	4.1	—	—	—	REJ
TP4, FLAW 4	V2	SAW	3	LOF	UT	—	17.5	4.6	—	1.6	0 (A)	REJ
TP4, FLAW 4	V2	SAW	3	LOF	PAUT	90	18.18	4.4	0	1.8	28% (C)	REJ
TP4, FLAW 5	V2	SAW	3	LOF	RT	—	25.5	4.6	—	—	—	REJ
TP4, FLAW 5	V2	SAW	3	LOF	UT	—	25.2	5.3	−0.2–0.2	0.472	0 (A)	REJ
TP4, FLAW 5	V2	SAW	3	LOF	PAUT	270	25.91	5.3	0.5	0.62	46% (C)	REJ
TP4, FLAW 6	V2	SAW	3	LOF	RT	—	26	0.5	—	—	—	REJ
TP4, FLAW 6	V2	SAW	3	—	UT	—	—	—	—	—	—	MISS
TP4, FLAW 6	V2	SAW	3	—	PAUT	—	—	—	—	—	—	MISS
TP4, FLAW 7	V2	SAW	3	Slag	RT	—	27.5	1.25	—	—	—	REJ
TP4, FLAW 7	V2	SAW	3	—	UT	—	—	—	—	—	—	MISS
TP4, FLAW 7	V2	SAW	3	Slag	PAUT	270	27.9	1.1	0.2	0.3	52% (B)	REJ
TP4, FLAW 8	V2	SAW	3	—	RT	—	—	—	—	—	—	MISS

Plate and Discontinuity ID	Joint Type	Welding Process	Nominal Plate Thickness(Inches)	Discontinuity Character	Technique (RT, Manual UT, PAUT)	UT Beam Direction	Start " Y" Along Weld (Inches)	Length (Inches)	Location " X" Across (Inches)	UT Depth (Inches)	Amplitude/Rating	D1.5 ACC/REJ (Tensile)[2]
TP4, FLAW 8	V2	SAW	3	LOF	UT	—	31.3	0.6	0	2	4(C)	ACC
TP4, FLAW 8	V2	SAW	3	LOF	PAUT	90	32.6	0.5	0	1.46	34% (C)	ACC
TP4, FLAW 9	V2	SAW	3	—	RT	—	—	—	—	—	—	MISS
TP4, FLAW 9	V2	SAW	3	LOF	UT	—	34.5	0.6	0	2	4 (C)	ACC
TP4, FLAW 9	V2	SAW	3	LOF	PAUT	90	35.2	0.5	0	1.46	34% (C)	ACC
TP5, FLAW 1	SQ	ESW-NG	1.5–2.7	LOF	RT	—	2	1.75	—	—	—	REJ
TP5, FLAW 1	SQ	ESW-NG	1.5–2.7	LOF	UT	—	2.3	1.8	—	1.38	3 (C)	REJ
TP5, FLAW 1	SQ	ESW-NG	1.5–2.7	LOF	PAUT	90	2.02	2.7	−0.4	1.46	35% (C)	REJ
TP5, FLAW 2	SQ	ESW-NG	1.5–2.7	LOF	RT	—	14.5	2.5	—	—	—	REJ
TP5, FLAW 2	SQ	ESW-NG	1.5–2.7	LOF	UT	—	13.5	2.75	—	0.265	−13 (A)	REJ
TP5, FLAW 2	SQ	ESW-NG	1.5–2.7	LOF	PAUT	270	14.7	2.2	—	0.54	28% (C)	REJ
TP5, FLAW 3	SQ	ESW-NG	1.5–2.7	LOF	RT	—	22.5	1.88	—	—	—	REJ
TP5, FLAW 3	SQ	ESW-NG	1.5–2.7	LOF	UT	—	23.5	1.7	—	0.593	−3 (A)	REJ
TP5, FLAW 3	SQ	ESW-NG	1.5–2.7	LOF	PAUT	270	23	1.5	—	0.47	36% (C)	ACC
ESW-2CP FLAW 1	SQ	ESW-NG	2	LOF/Slag	RT	—	0	2.75	—	—	—	REJ
ESW-2CP FLAW 1	SQ	ESW-NG	2	LOF/Slag	UT	—	0	2.8	0.2	1.99	−3 (A)	REJ
ESW-2CP FLAW 1	SQ	ESW-NG	2	LOF/Slag	PAUT	270	0	3.1	0.3	1.7	196% (A)	REJ
ESW-2CP FLAW 2	SQ	ESW-NG	2	Porosity	RT	—	8.25	0.13	—	—	—	ACC
ESW-2CP FLAW 2	SQ	ESW-NG	2	Porosity	UT	—	8.2	0.2	0	1.2	7 (C)	ACC
ESW-2CP FLAW 2	SQ	ESW-NG	2	Porosity	PAUT	90	7.9	0.51	−0.1	1.6	29% (C)	ACC
ESW-2CP FLAW 3	SQ	ESW-NG	2	Crack	RT	—	35.5	4	—	—	—	REJ
ESW-2CP FLAW 3	SQ	ESW-NG	2	Crack	UT	—	34.6	2.5	−0.1	0.88	7 (C)	REJ
ESW-2CP FLAW 3	SQ	ESW-NG	2	Crack	PAUT	90	33.56	4.1	−0.2	0.79	30% (C)	REJ
ESW-2CP FLAW 4	SQ	ESW-NG	2	LOF	RT	—	46	1	—	—	—	REJ
ESW-2CP FLAW 4	SQ	ESW-NG	2	LOF	UT	—	45.5	1	−0.3–0.3	1.74	−7 (A)	REJ
ESW-2CP FLAW 4	SQ	ESW-NG	2	LOF	PAUT	90	46.3	0.7	−0.3–0.3	1.7	190% (A)	REJ

Plate and Discontinuity ID	Joint Type	Welding Process	Nominal Plate Thickness(Inches)	Discontinuity Character	Technique (RT, Manual UT, PAUT)	UT Beam Direction	Start " Y" Along Weld (Inches)	Length (Inches)	Location " X" Across (Inches)	UT Depth (Inches)	Amplitude/Rating	D1.5 ACC/REJ (Tensile)[2]
ESW-12CP FLAW 1	SQ	ESW-NG	1–2	Slag	RT	—	0	1.2	—	—	—	REJ
ESW-12CP FLAW 1	SQ	ESW-NG	1–2	Slag	UT	—	0	0.8	0.3	0.97	7 (A)	REJ
ESW-12CP FLAW 1	SQ	ESW-NG	1–2	Slag	PAUT	270	0	0.6	0.4	0.83	101% (A)	REJ
ESW-12CP FLAW 2	SQ	ESW-NG	1–2	LOF	RT	—	46	1	—	—	—	REJ
ESW-12CP FLAW 2	SQ	ESW-NG	1–2	LOF	UT	—	45.5	1.2	—	0.63	0 (A)	REJ
ESW-12CP FLAW 2	SQ	ESW-NG	1–2	LOF	PAUT	270	45.5	1	0.4	0.77	51% (B)	REJ
SAW-12CP FLAW 1	SQ	SAW	1–2	LOF	RT	—	0	0.38	—	—	—	ACC
SAW-12CP FLAW 1	SQ	SAW	1–2	LOF	UT	—	0	0.5	0.1	0.2	−3 (A)	REJ
SAW-12CP FLAW 1	SQ	SAW	1–2	LOF	PAUT	90	0	0.8	0.3	0.12	180% (A)	REJ
SAW-12CP, FLAW 2	SQ	SAW	1–2	Porosity	RT	—	23.25	1.38	—	—	—	REJ
SAW-12CP, FLAW 2	SQ	SAW	1–2	Porosity	UT	—	24.1	3.2	0.2	0.27	5 (A)	REJ
SAW-12CP, FLAW 2	SQ	SAW	1–2	Porosity	PAUT	270	23.3	3.8	0.4	0.4	48% (C)	REJ
SAW-12CP, FLAW 3	SQ	SAW	1–2	LOF	RT	—	—	—	—	—	—	MISS
SAW-12CP, FLAW 3	SQ	SAW	1–2	LOF	UT	—	46.5	1	0.2	0.3	−2 (A)	REJ
SAW-12CP, FLAW 3	SQ	SAW	1–2	LOF	PAUT	90	46.6	0.84	0.3	0.58	42% (C)	ACC
SAW-12CP, FLAW 4	SQ	SAW	1–2	LOF	RT	—	4.5	0.3	—	—	—	ACC
SAW-12CP, FLAW 4	SQ	SAW	1–2	LOF	UT	—	—	—	—	—	—	MISS
SAW-12CP, FLAW 4	SQ	SAW	1–2	—	PAUT	—	—	—	—	—	—	MISS
HF1, FLAW 1	SQ	ESW-NG	2–2.5	LOF	RT	—	2.5	1.38	—	—	—	REJ
HF1, FLAW 1	SQ	ESW-NG	2–2.5	LOF	UT	—	2.25	2.3	−1	1.8	2 (A)	REJ
HF1, FLAW 1	SQ	ESW-NG	2–2.5	LOF	PAUT	90	1.98	2.27	−1	2.19	35% (C)	REJ
HF1, FLAW 2	SQ	ESW-NG	2–2.5	LOF	RT	—	8.5	1.5	−1	—	—	REJ
HF1, FLAW 2	SQ	ESW-NG	2–2.5	LOF	UT	—	8.2	1.7	−1	0.4	−22 (A)	REJ
HF1, FLAW 2	SQ	ESW-NG	2–2.5	LOF	PAUT	—	8	2.1	−1	0.1	56% (B)	REJ
HF1, FLAW 3	SQ	ESW-NG	2–2.5	LOF	RT	—	14	2	—	—	—	REJ
HF1, FLAW 3	SQ	ESW-NG	2–2.5	LOF	UT	—	14.1	1.8	−1	1.5	−12 (A)	REJ

Plate and Discontinuity ID	Joint Type	Welding Process	Nominal Plate Thickness(Inches)	Discontinuity Character	Technique (RT, Manual UT, PAUT)	UT Beam Direction	Start " Y" Along Weld (Inches)	Length (Inches)	Location " X" Across (Inches)	UT Depth (Inches)	Amplitude/Rating	D1.5 ACC/REJ (Tensile)[2]
HF1, FLAW 3	SQ	ESW-NG	2–2.5	LOF	PAUT	90	13.9	2.2	−1	1.5	69% (B)	REJ
HF2, FLAW 1	SQ	ESW-NG	2–2.5	LOF	RT	—	2.5	1.25	—	—	—	REJ
HF2, FLAW 1	SQ	ESW-NG	2–2.5	LOF	UT	—	3.5	1	−1.2	1.7	0 (A)	REJ
HF2, FLAW 1	SQ	ESW-NG	2–2.5	LOF	PAUT	270	3.3	1.4	−1.1	2.1	52% (B)	REJ
HF2, FLAW 2	SQ	ESW-NG	2–2.5	LOF	RT	—	9	3.2	—	—	—	REJ
HF2, FLAW 2	SQ	ESW-NG	2–2.5	LOF	UT	—	9	2.5	—	1.7	−8 (A)	REJ
HF2, FLAW 2	SQ	ESW-NG	2–2.5	LOF	PAUT	90	9.05	2.7	—	2.2	61% (B)	REJ
HF2, FLAW 3	SQ	ESW-NG	2–2.5	LOF	RT	—	18	4	—	—	—	REJ
HF2, FLAW 3	SQ	ESW-NG	2–2.5	LOF	UT	—	16.1	2.8	−1	1.8	−7 (A)	REJ
HF2, FLAW 3	SQ	ESW-NG	2–2.5	LOF	PAUT	90	15.5	3.2	−1.2	2.2	174% (A)	REJ

—No data.

ACC = accept; LOF = lack of fusion; MISS = missed discontinuity; REJ = reject; SQ = square; TUNG = tungsten; V2 = double vee.

CHAPTER 7. SUMMARY

The FHWA NDE Laboratory conducted a comprehensive study to assess the feasibility of using PAUT as an alternative to RT for inspecting complete joint penetration butt welds in bridge structures. The study aimed to understand the fundamental principles of PAUT and develop a preliminary technical approach, scan plans for 10 welded TPs, and test procedures based on AWS D1.5.[2] The research team inspected 10 weld specimens using PAUT and compared the results with RT and UT test results. The comparative results demonstrated a strong correlation between PAUT, UT, and RT, indicating the effectiveness of PAUT in accurately measuring discontinuity dimensions. This positive correlation provided compelling evidence of PAUT's capability as a viable alternative to RT for inspecting complete joint penetration butt welds in bridges.

However, the study team acknowledges the need for further data collection and evaluation of different defect types to confidently recommend the complete replacement of RT with PAUT. Additional efforts, such as expanded data collection, defect variation studies, and field applications are necessary to fully establish the reliability and applicability of PAUT in lieu of RT in bridge-weld inspections.

Figure 35 summarizes the PAUT, UT, and RT inspection results categorized by the type of discontinuities. As depicted in figure 35, the data analysis results from PAUT generally demonstrated consistency with those obtained from RT. The lack of agreement in the acceptance/rejection of the discontinuities observed is likely attributed to the differences in acceptance criteria utilized in RT and PAUT.[5]

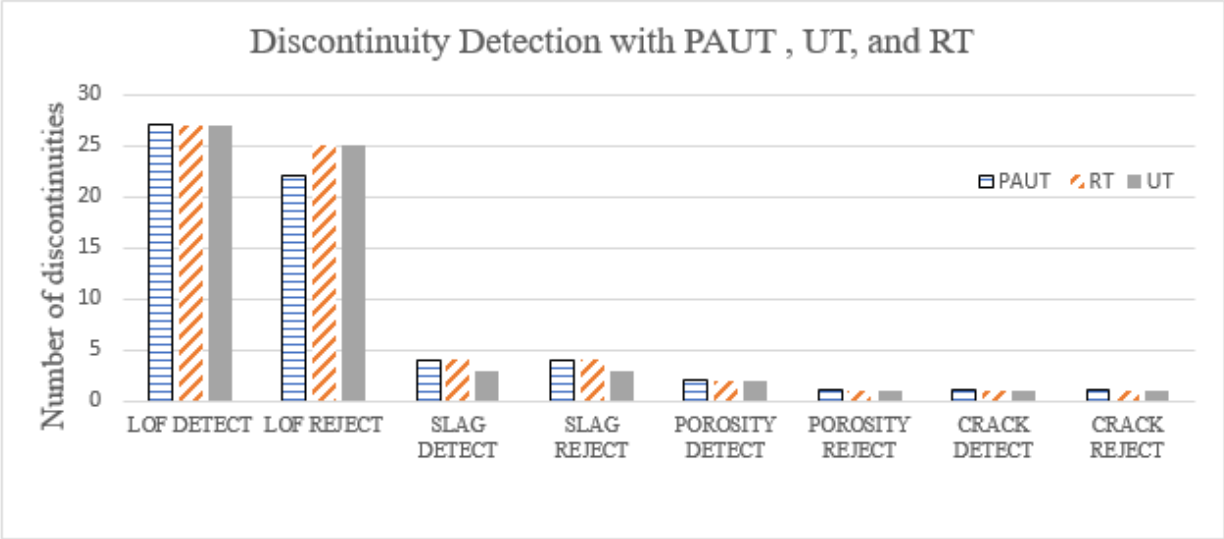

Source: FHWA.

Figure 35. Graph. PAUT, UT, and RT detection and rejection results.

CHAPTER 8. CONCLUSIONS

The comprehensive study highlighted good comparative results between PAUT, conventional UT, and RT measurements. While affirming PAUT's reliability, the research emphasizes the necessity for a more extensive evaluation encompassing diverse weld discontinuities and joint types for an inclusive assessment.

1. The results from PAUT, conventional UT, and RT had the following statistical correlations:

    a. Depth measurements made with UT and PAUT had a correlation factor of 0.95, with a maximum, minimum, and average variance of 0.5, −0.6, and .004, respectively, and a standard deviation of 0.239.

    b. Length measurements made with RT and PAUT had a correlation factor of 0.89, with a maximum, minimum, and average variance of 0.8, −2.42, and −0.038, respectively, and a standard deviation of 0.658.

    c. Length measurements made with UT and PAUT had a correlation factor of 0.91, with a maximum, minimum, and average variance of 1.9, −1.6, and 0.0481, respectively, and a standard deviation of 0.596.

2. The ultrasonic sound-beam, ray-path analysis carried out to develop the PAUT scan plans indicates a need to carry multiple scans along each side of the weld at different probe index point offsets from the weld centerline to ensure complete volumetric coverage of these relatively thick welds. This scanning approach is applicable to both equal thickness butt welds and transition thickness butt welds.

3. The large-grain microstructure observed in electroslag welds did not influence the propagation of ultrasonic waves to a point where the detectability of the implanted flaws using 5 MHz shear wave transducer was affected.

4. The primary objective of this research initiative was to establish PAUT as a viable and reliable alternative to radiography. The study results provide substantial support for achieving this objective. However, further enhancing the research by developing a more comprehensive set of weld discontinuities is essential. This expanded set should encompass various discontinuity types, additional welding processes, thicker and thinner joints, and tee and corner joints to ensure a fully representative discontinuity evaluation.

CHAPTER 9. RECOMMENDATIONS

The study entailed inspecting 10 specimens that are representative of the weld joints commonly used in real-world bridge fabrication. Using the results obtained from this study as a foundation, further expansion, incorporating the provided recommendations, can be considered for future investigations in bridge weld quality assurance.

1. Fabricate additional weld specimens to ensure a more complete matrix of representative discontinuity types, joint configurations, and plate thicknesses are addressed (including transverse discontinuities). The specific new specimen discontinuity types should be established after getting additional input from subject matter experts. The expected weld discontinuities include longitudinal cracks, transverse hydrogen-related cracks, incomplete fusion, incomplete penetration, slag, and piping porosity.

2. Evaluate the feasibility of using advanced ultrasonic discontinuity modeling software to supplement the ultrasonic validation data. Through modeling, the ultrasonic response from discontinuities with a different type, size, length, and orientation can be predicted and evaluated in accordance with the AWS D1.5 criteria.[2] This modeling should limit the number of additional specimens to be fabricated and inspected. The small set of actual implanted discontinuities should also be modeled and used to physically validate the modeling and provide additional confidence in all the modeling results.

3. Evaluate time of flight diffraction (TOFD)[12] and other advanced UT techniques like two-dimensional PAUT arrays,[13] total focus method/full matrix capture,[14] pitch-catch PAUT,[13] and intermodal total focus method[15] to evaluate potential discontinuity detection and discontinuity sizing improvements. The use of TOFD techniques should support adding an accurate quantifiable acceptance criterion for this condition. AWS is considering adopting new acceptance criteria that utilize the discontinuity through wall height because of a general industry trend toward more of a fitness-for-service approach to ultrasonic acceptance criteria in lieu of the historic workmanship discontinuity signal amplitude-based criteria.[3] TOFD techniques would also support the implementation of any type of a fitness-for-service approach.

APPENDIX A. PROCEDURE

ULTRASONIC PHASED ARRAY EXAMINATION EQUIPMENT AND ACCESSORIES

The phased array equipment used in this research is capable of generating and displaying sectorial-scan (also called S-scan), B-scan, and C-scan images, which can be stored and recalled for subsequent review.

The same couplant material, including batch number, where applicable, used for standardization shall be used for examinations. Transducer and wedge shall be, as per table 5, for PAUT. The range of angles for the wedge used for inspection is 45°–70°. The scan shall be performed using a robotic arm (figure 36) that is programmed to maintain a fixed index offset from the weld center line.

An encoder interfaced with the phased array instrument shall be used to track the probe movement. The encoder shall be calibrated to coordinate its movement with the PAUT equipment.

Table 5. Probe and wedge.

Phased Array Transducers and Wedges			
Probe Description	**Frequency (MHz)**	**Number of Elements**	**Element Pitch (inch**
Linear array	5	64	0.019
Wedge—55° refracted shear wave wedge			

Source: FHWA.

Figure 36. Photo. Robotic arm.

STANDARDIZATION

The equipment standardization was conducted in accordance with AWS D1.5.[2]

Horizontal Sweep

The horizontal sweep shall be adjusted to represent the actual material path distance throughout all the configured angles using an IIW block. If the joint configuration or thickness prevents full examination of the weld at these settings, the distance standardization shall be made at increased screen ranges as depicted in the scan plan.

TCG

The TCG shall be established throughout all configured angles at a minimum of three points throughout the material range to be tested in the TCG standardization block (figure 5). The TCG shall balance all standardization points within ±5 percent amplitude of each other.

Encoder Standardization

The encoder shall be calibrated at least weekly and verified through daily in-process checks to be within 1 percent of measured length for a minimum of half the total scan length. Encoder resolution shall be configured so that data are taken at 1 mm (0.04 inch) increments.

ACCEPTANCE CRITERIA

The standard sensitivity level (SSL), which determines the test sensitivity of the inspection, shall be established at 50 percent ±5 percent of full-screen height of the 1.5 mm (0.06 inch) reflector. This decibel level shall be noted as the primary reference level decibel. The automatic reject level (ARL) shall be defined as 5 dB over SSL above which all discontinuities are rejected irrespective of position and size, which equals 89 percent FSH level The discontinuities with amplitude less than or equal to disregard level (DRL) shall be defined as 6 dB under SSL, which equals 25 percent FSH (figure 37), are always acceptable. The classification of discontinuities based on the amplitude level is provided in table 6. The length and amplitude-based acceptance criteria is presented in table 7.

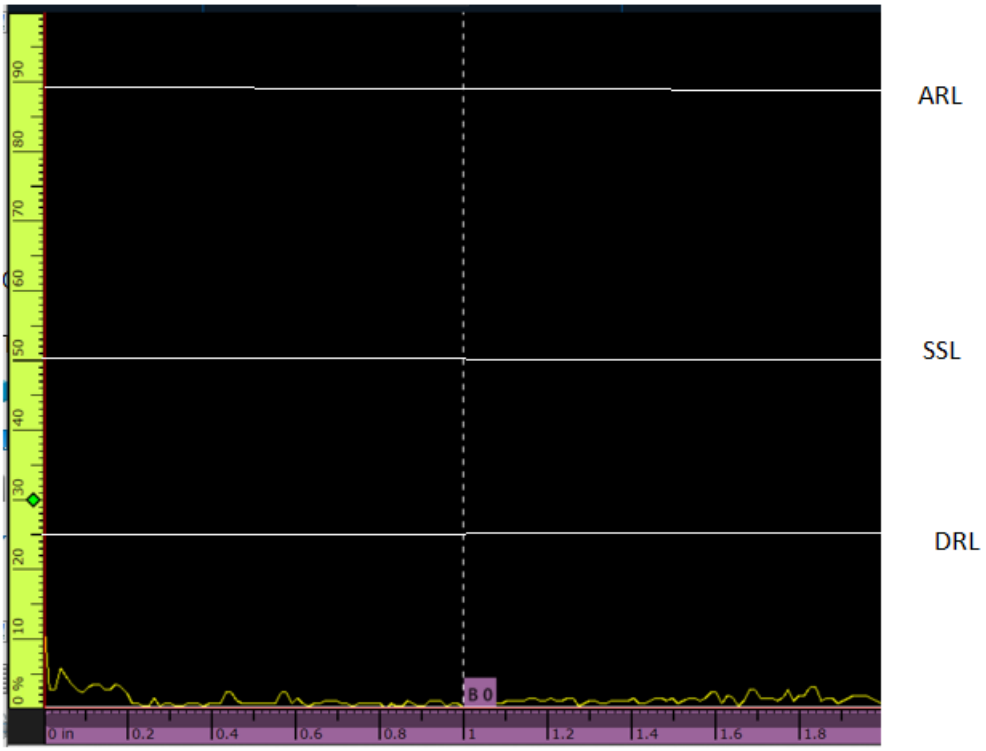

Source: FHWA.

Figure 37. Image. Sensitivity level.[2]

Table 6. Discontinuity classification.

Discontinuity Classification	Description
A	>ARL
B	>SLL, ≤ARL
C	>DRL, ≤SLL
D	≤DRL

Table 7. PAUT acceptance criteria.

Maximum Discontinuity Amplitude Level Obtained	Maximum Discontinuity Lengths by the Type of Loading	
	Compression	Tension
Class A	None allowed	None allowed
Class B	0.78 inch	0.47 inch
Class C	1.96 inches	Middle half of weld: 1.96 inches Top or bottom quarter of weld: 0.78 inch
Class D	Disregard	Disregard

EXAMINATION

The encoded line scanning at fixed offsets, as defined by the scan plan, will be performed during the data acquisition. The data will be collected at the primary reference level. The robotic arm scanner shall be used at a scan speed whereby data dropout shall not exceed 1 percent of the recorded data, and no two adjacent data lines shall be missed. The data collected shall be complete A-scans with no exclusionary gating and filtering other than the receiver band pass filter.

EVALUATION

During data evaluation, the gain shall be increased by 6 dB using the soft gain function in the evaluation software.[11] The length of discontinuities shall be determined by measuring the distance between the transducer centerline locations where the indication rating drops 50 percent (6 dB) below the rating for the applicable discontinuity classification. The depth of the discontinuity is measured as the location of the peak amplitude at the angle producing the maximum signal amplitude.

APPENDIX B. TEST RESULTS

Typical results of the PAUT data acquisition and analysis steps of the test specimens are provided in this appendix.

SPECIMEN TP1

Figure 38 through figure 42 cover specimen TP1. The specimen had the following characteristics:

- Weld type: SAW.
- Length: 25.0 inches.
- Width: 26.5 inches.
- Height: 1–2 inches.

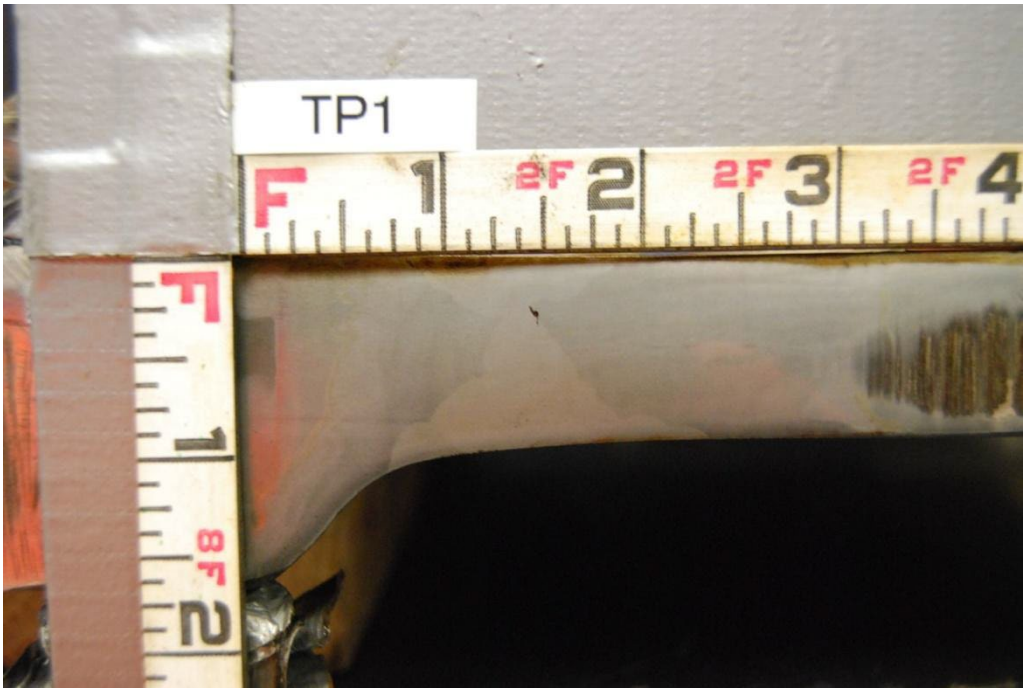

Source: FHWA.

Figure 38. Photo. TP1 unprocessed etched.

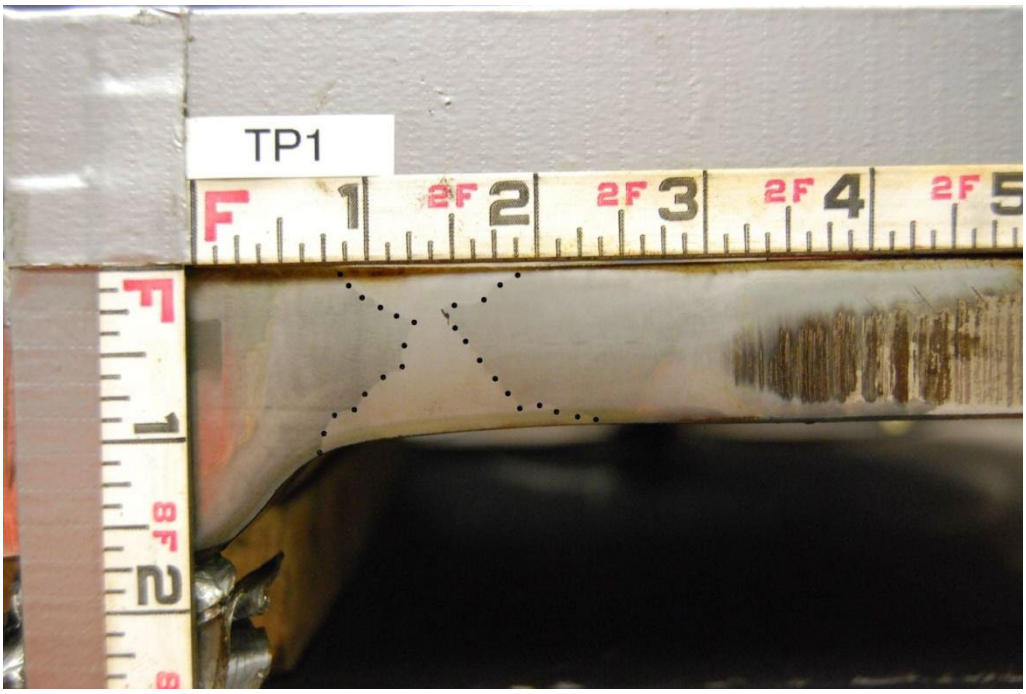

Source: FHWA.

Figure 39. Photo. TP1 etched image with weld edge traced.

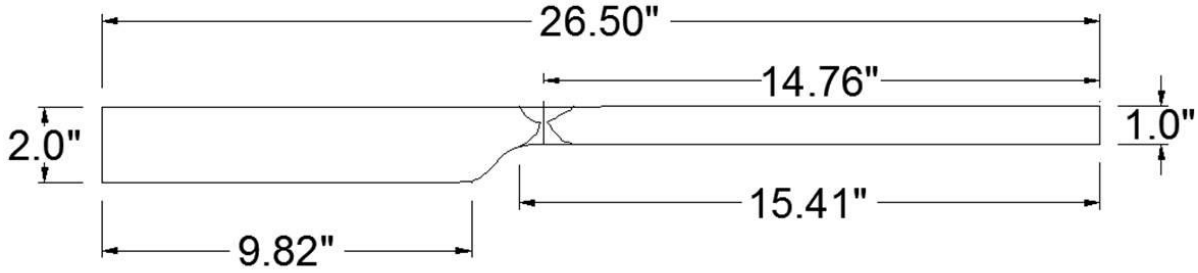

Source: FHWA.
" = inches.

Figure 40. Schematic. TP1 dimensions.

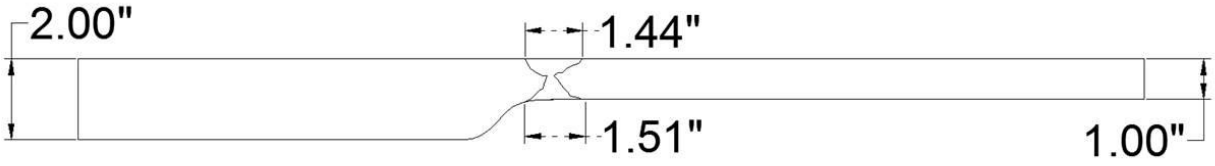

Source: FHWA.

Figure 41. Schematic. TP1 CAD image with traced HAZ dimensions.

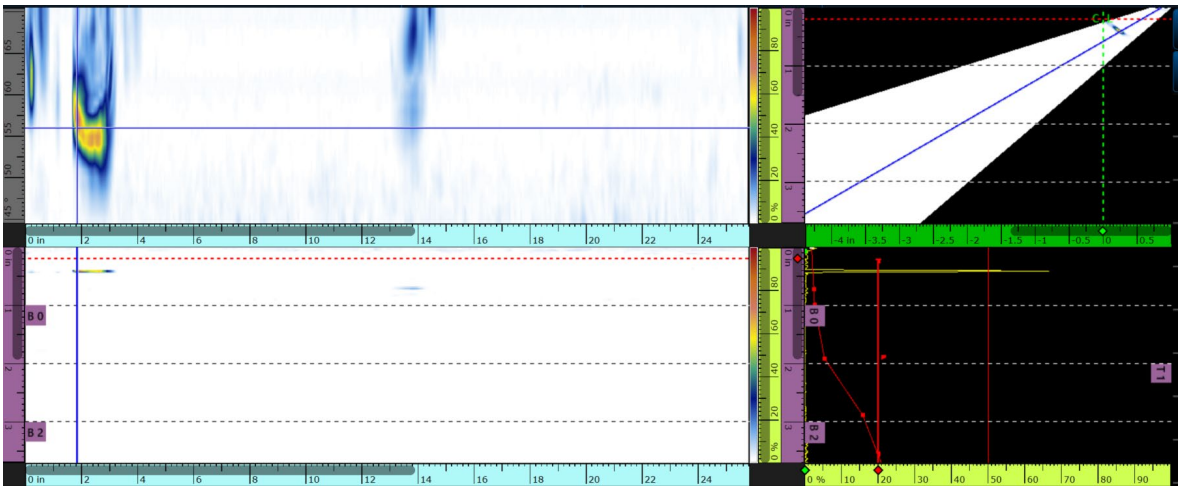

Source: FHWA.

Figure 42. Images. Composite scan view for test specimen TP1.

Even though the researchers detected the same discontinuity at different IPs, they reported the discontinuity sizing from the data corresponding to the IP that had the discontinuity indication with the maximum length. In the test specimen TP1, for IP2 and offset 0, the first discontinuity was located at 1.68 inches from the start at a depth of 0.40 inch and was 1.32 inches in length. The second discontinuity indication was observed in IP1 at a 6.0-inch offset, which was located at 13.10 inches from the start at a depth of 0.19 inch and was 1.19 inches in length.

SPECIMEN TP2

Figure 43 to figure 47 cover specimen TP2. The specimen had the following characteristics:

- Weld type: ESW-NG.
- Length: 28.0 inches.
- Width: 24.5 inches.
- Height: 1.5 inches.

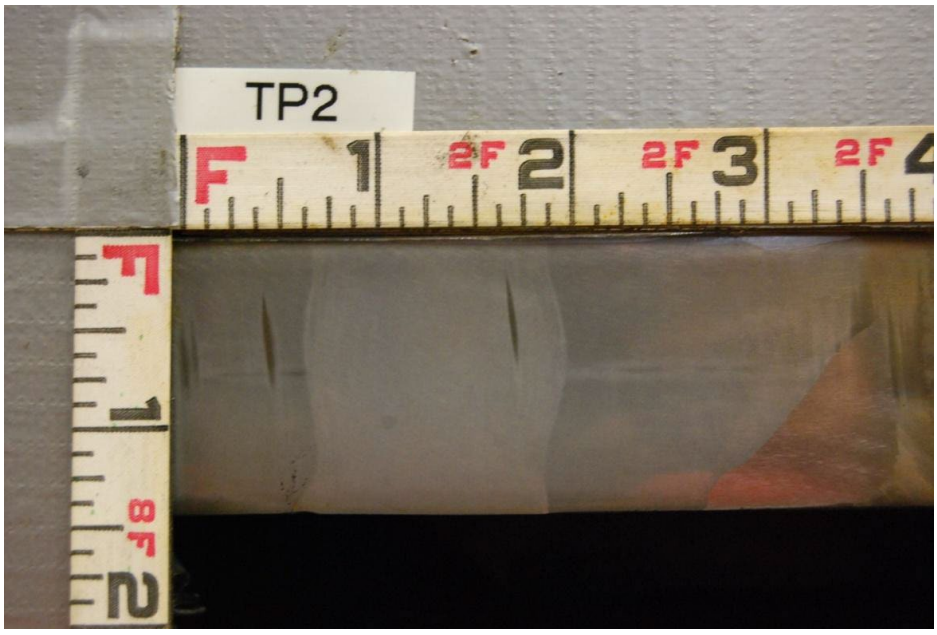

Source: FHWA.

Figure 43. Photo. TP2 unprocessed etched image.

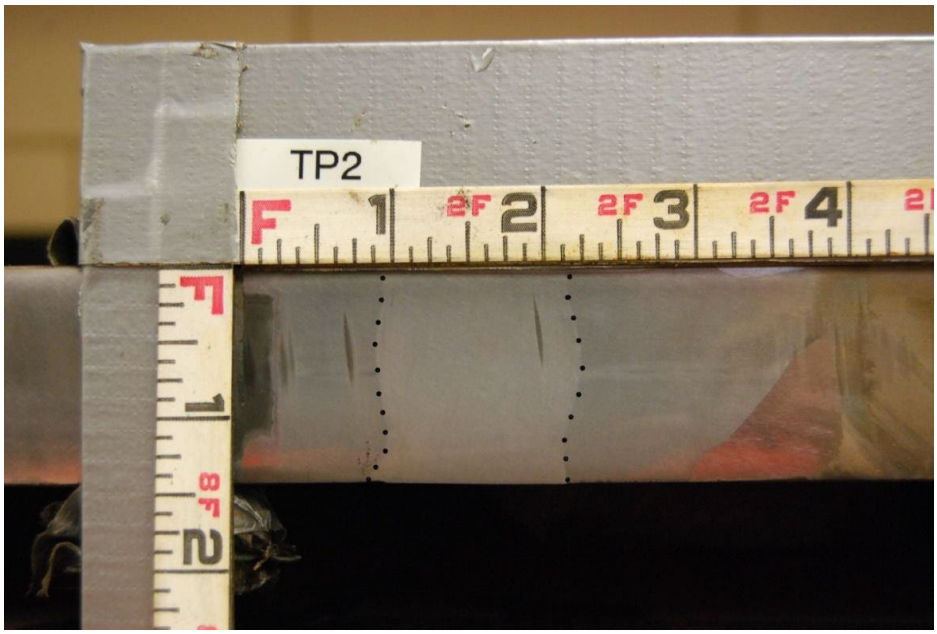

Source: FHWA.

Figure 44. Photo. TP2 etched image with weld edge traced.

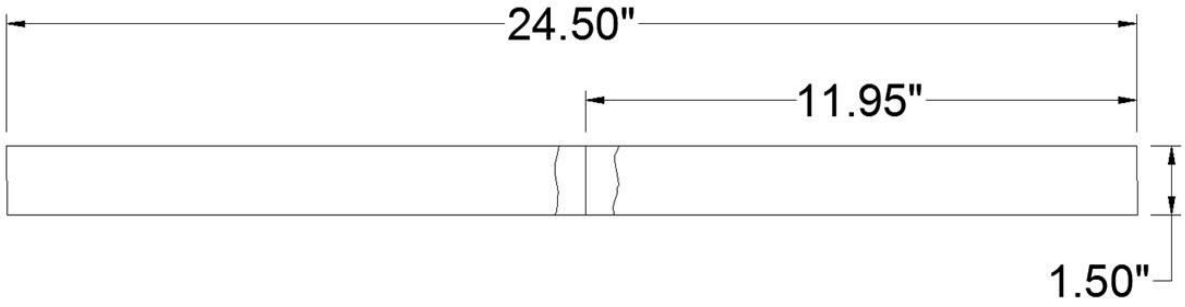

Source: FHWA.

Figure 45. Schematic. TP2 dimensions.

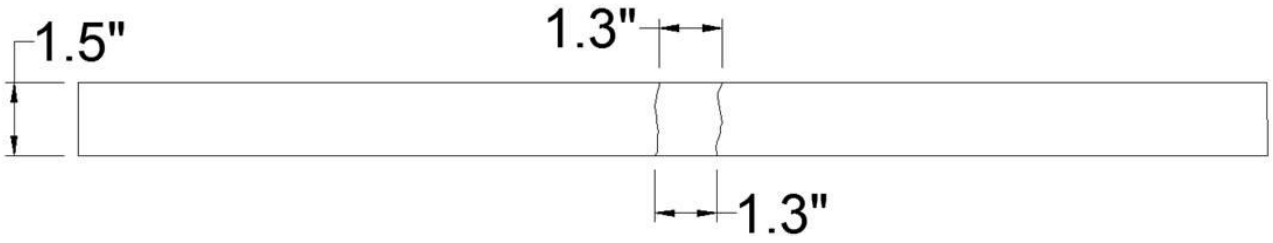

Source: FHWA.

Figure 46. Schematic. TP2 CAD image with traced HAZ with dimensions.

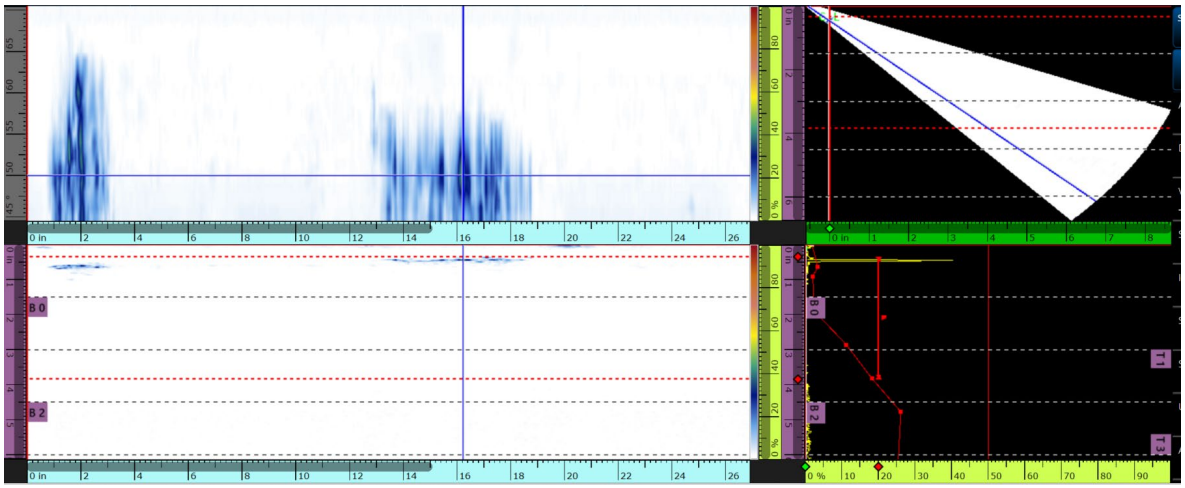

Source: FHWA.

Figure 47. Image. Composite scan view for test specimen.

For test specimen TP2, two discontinuity indications at position 0.64 and 13.30 inches from the start were reported at IP1. The lengths of these discontinuities were 2.42 and 5.43 inches, respectively, and the depth from the top surface was 0.73 and 0.45 inch, respectively.

SPECIMEN TP3

Figure 48 through figure 52 cover specimen TP3. The specimen had the following characteristics:

- Weld type: ESW-NG.
- Length: 22.0 inches.
- Width: 23.5 inches.
- Height: 3.3 inches.

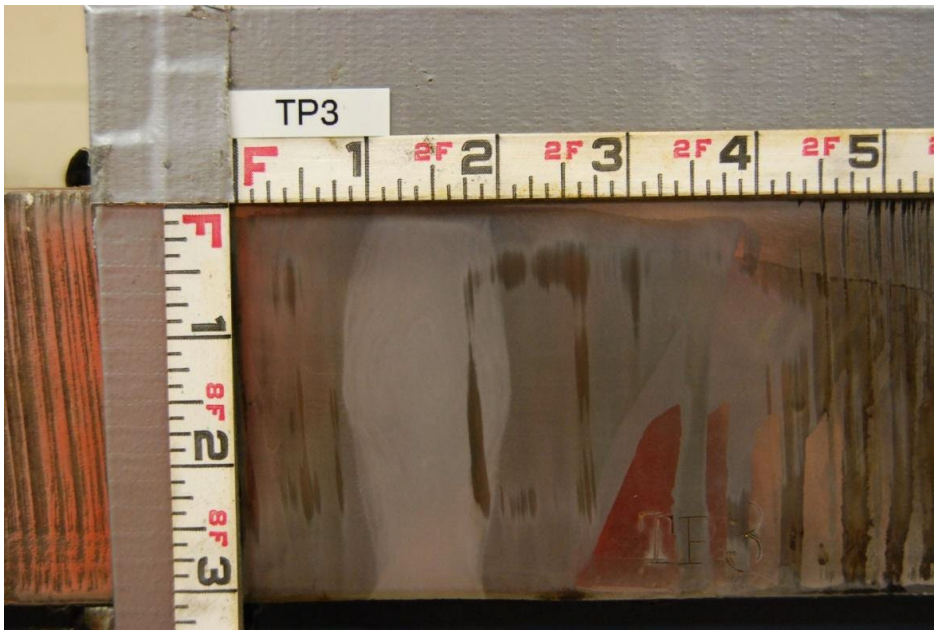

Source: FHWA.

Figure 48. Photo. TP3 unprocessed etched image.

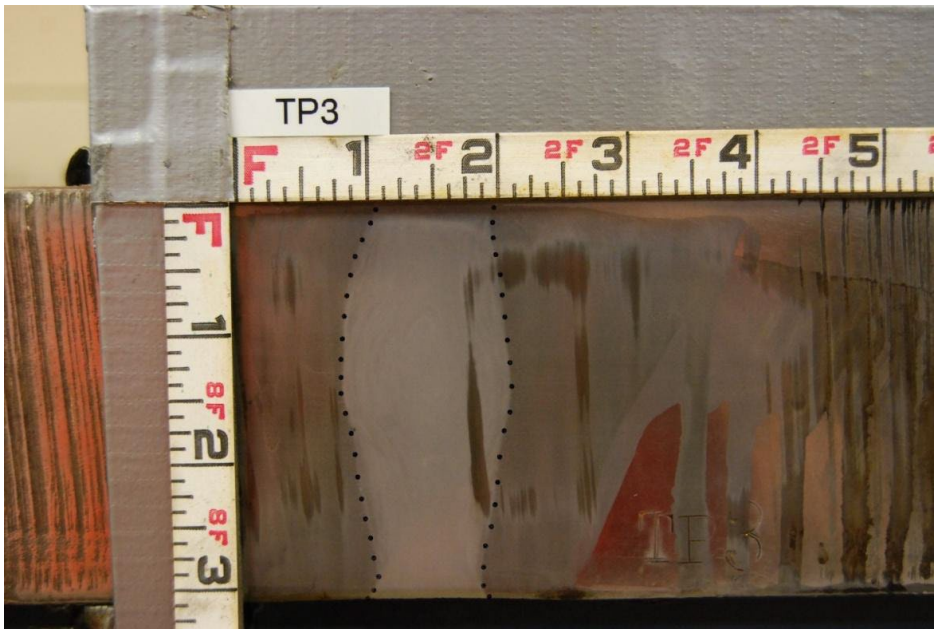

Source: FHWA.

Figure 49. Photo. TP3 etched image with weld edge traced.

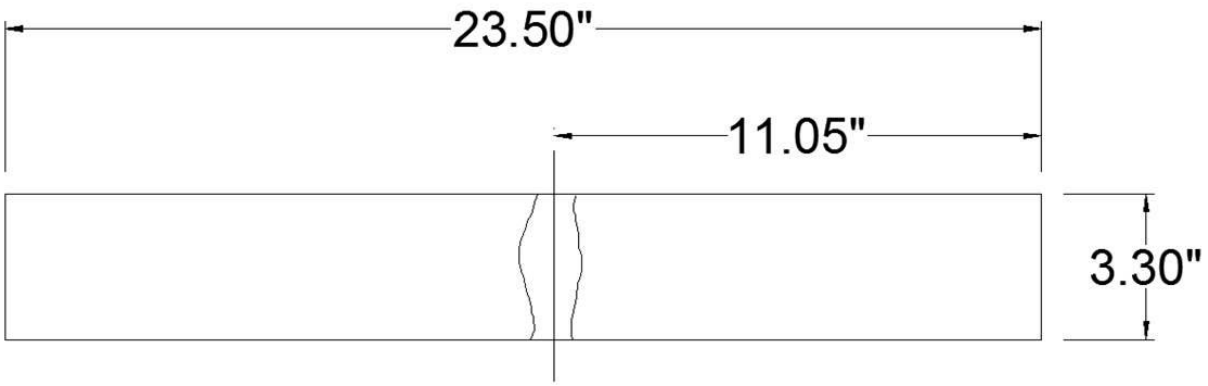

Source: FHWA.

Figure 50. Schematic. TP3 dimensions.

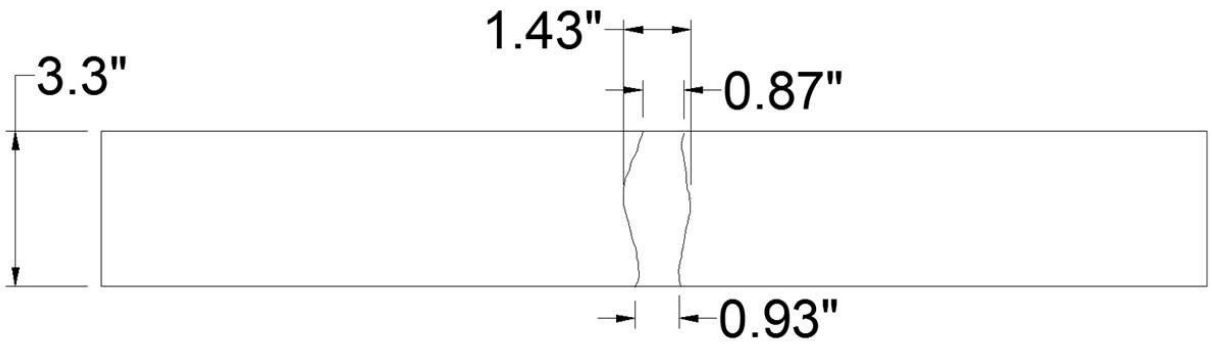

Source: FHWA.

Figure 51. Schematic. TP3 CAD image with traced HAZ with dimensions.

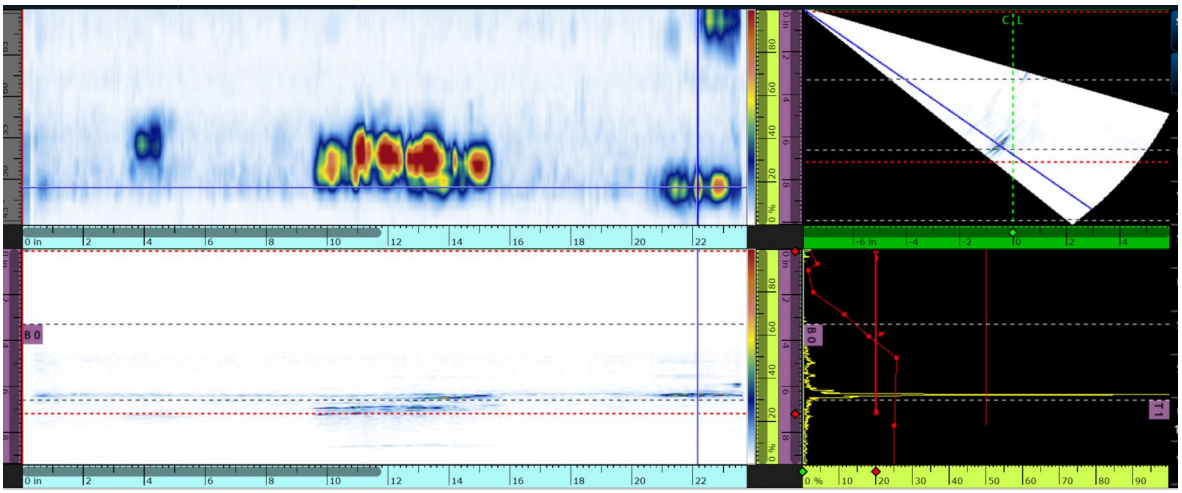

Source: FHWA.

Figure 52. Images. Composite scan view for test specimen TP3.

For test specimen TP3, the team detected four indications in PAUT. They observed the first discontinuity in IP2 at an offset of 7.25 inches, located at 3.5 inches from the start at a depth of 0.66 inch and a length of 1.1 inches. The second discontinuity indication was detected at IP1 at an offset of 0.35 inch, and the discontinuity was located at 10.1 inches from the start position at a depth of 0.36 inch from the top surface and length of this discontinuity was 5.3 inches. The third discontinuity indication was observed at IP1 at an offset of −7.25 inches and was located at 21.2 inches from the start position, at a depth of 0.55 inch from the surface, and the length of this indication was measured as 2.4 inches. The fourth discontinuity indication was observed at the IP2 at an offset of 7.25 inches, the discontinuity was located at 22.4 inches from the start position at a depth of 3.0 inches, and the length of this discontinuity was measured as 1.2 inches.

SPECIMEN TP4

Figure 53 through figure 57 cover specimen TP4. The specimen had the following characteristics:

- Weld type: SAW.
- Length: 36.5 inches.
- Width: 18.0 inches.
- Height: 3.0 inches.

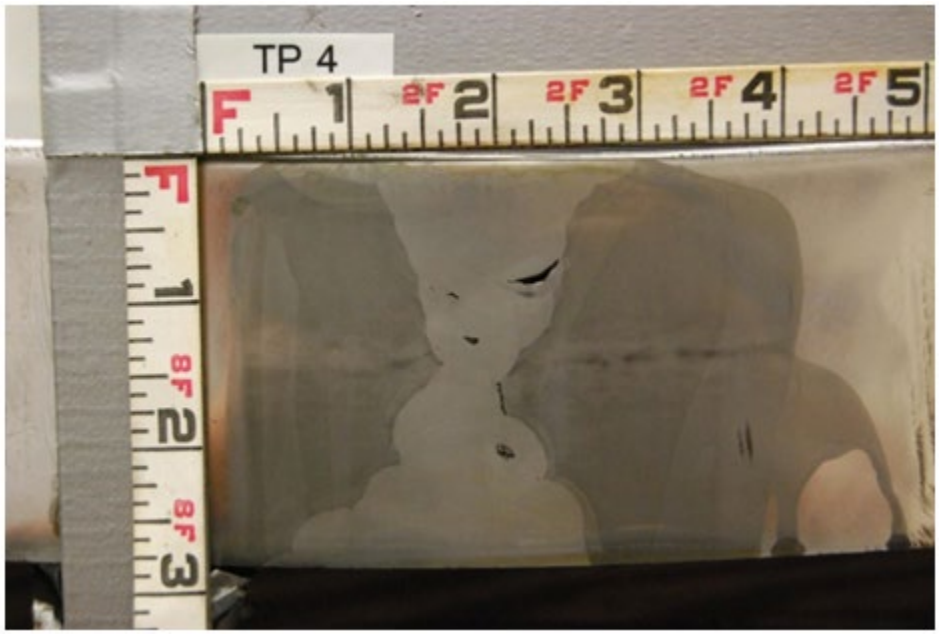

Source: FHWA.

Figure 53. Photo. TP4 unprocessed etched image.[8]

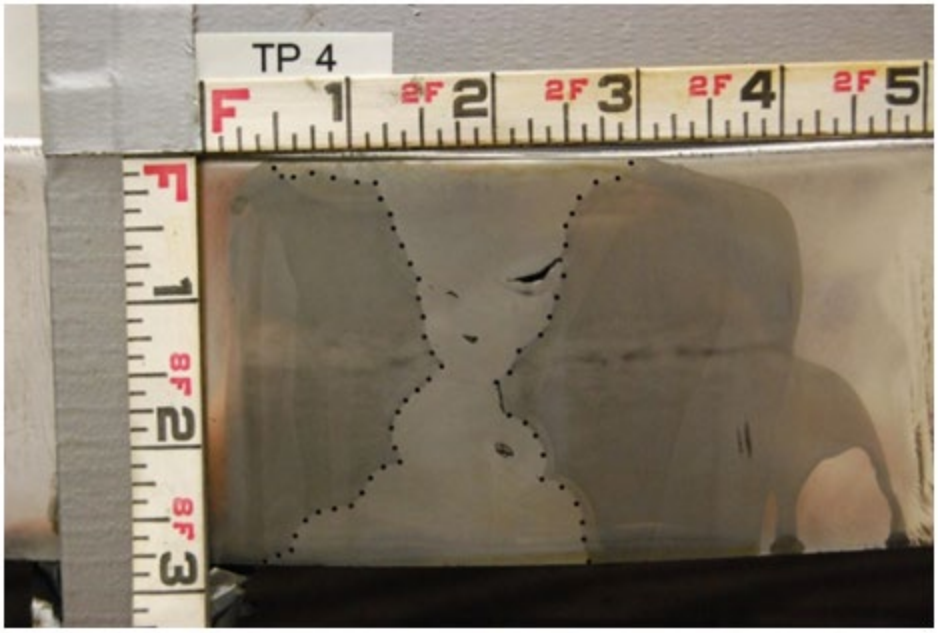

Source: FHWA.

Figure 54. Photo. TP4 etched image with weld edge traced.[8]

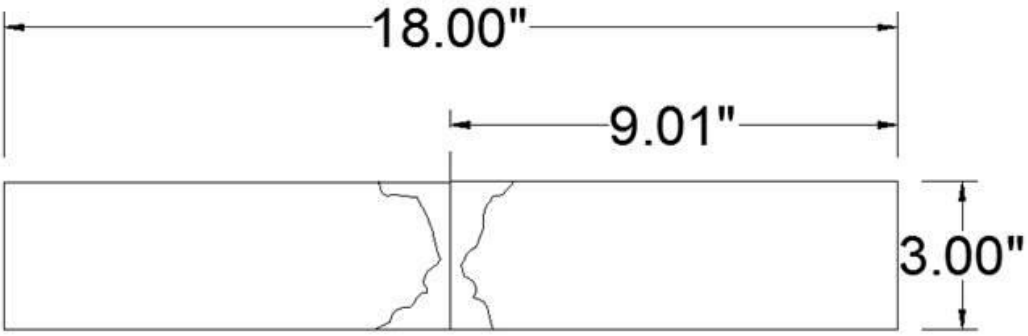

Source: FHWA.

Figure 55. Schematic. TP4 dimensions.

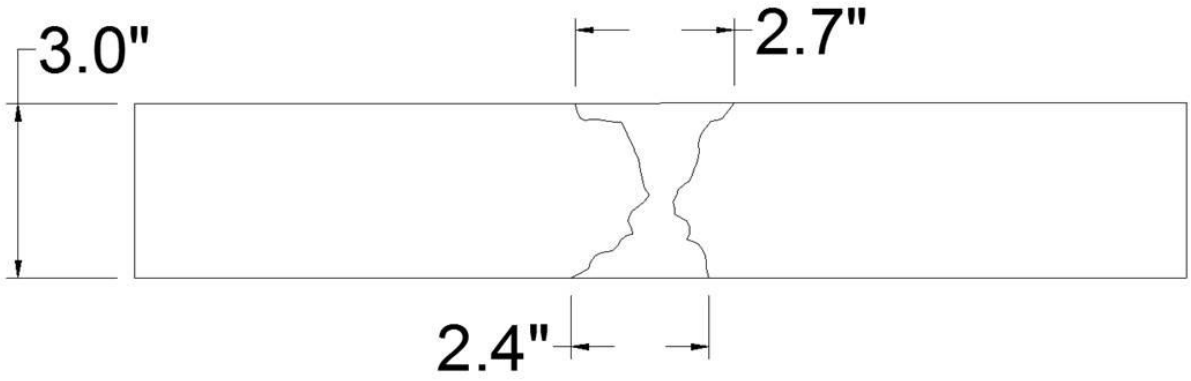

Source: FHWA.

Figure 56. Schematic. TP4 CAD image with traced HAZ with dimensions.

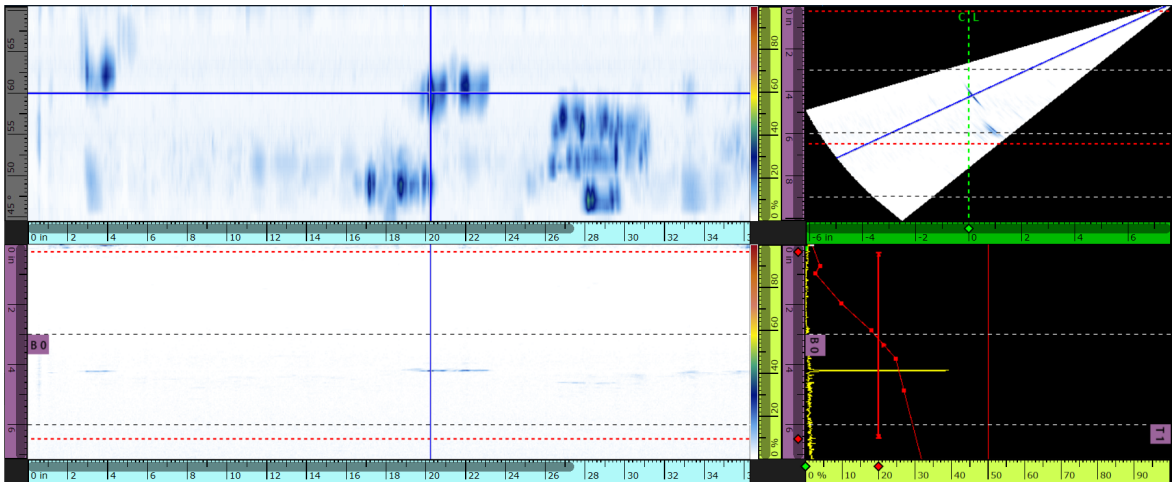

Source: FHWA.

Figure 57. Images. Composite scan view for test specimen TP4.

The study team detected nine discontinuities in test specimen TP4. The discontinuities designated with numbers 3 and 4 were detected at IP1 at an index offset position of −5.7 inches (table 4). Discontinuity 1 was detected at IP1 and an index offset position of −3.2 inches. Discontinuity 2 was detected at an offset of −0.5 inch in IP2 position. Discontinuity 5 was observed at IP2, with an index offset position of 5.7 inches, and discontinuity 7 was detected at IP2, with an index offset position of 6.6 inches. Discontinuities 8 and 9 were detected at IP1 at an index offset of −0.5 inch. Although the discontinuities were observed in different offset scans, the amplitude and length vary in each scan position.

SPECIMEN TP5

Figure 58 through figure 62 cover specimen TP5. The specimen had the following characteristics:

- Weld type: ESW-NG.
- Length: 30.0 inches.
- Width: 24.5 inches.
- Height: 1.5–2.7 inches.

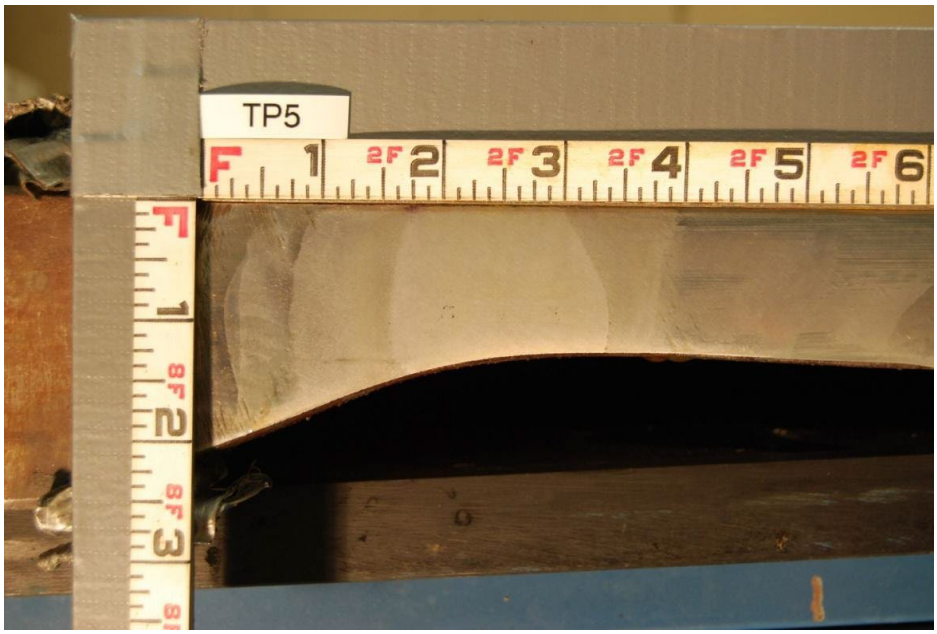

Source: FHWA.

Figure 58. Photo. TP5 unprocessed etched image.

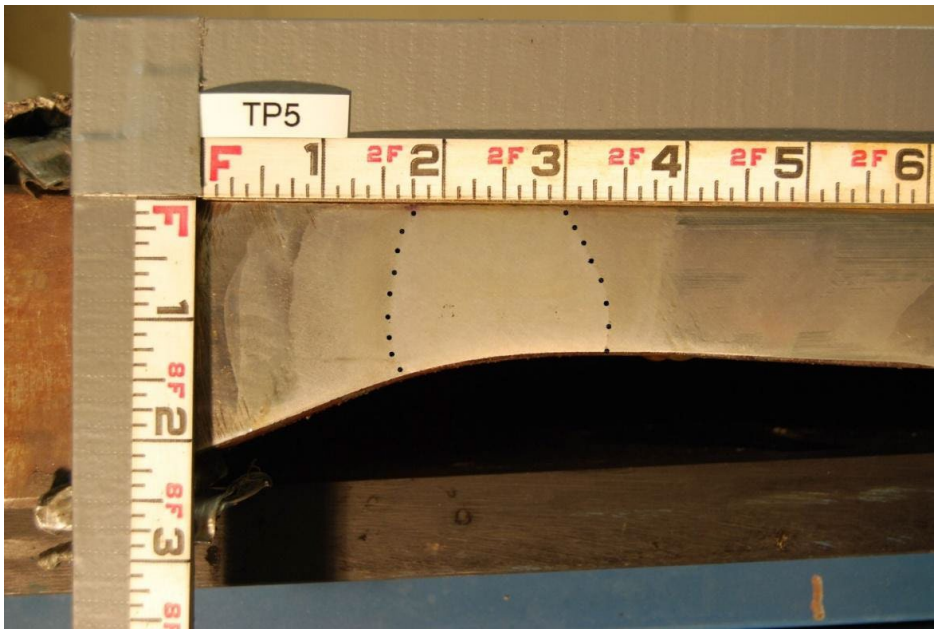

Source: FHWA.

Figure 59. Photo. TP5 etched image with weld edge traced.

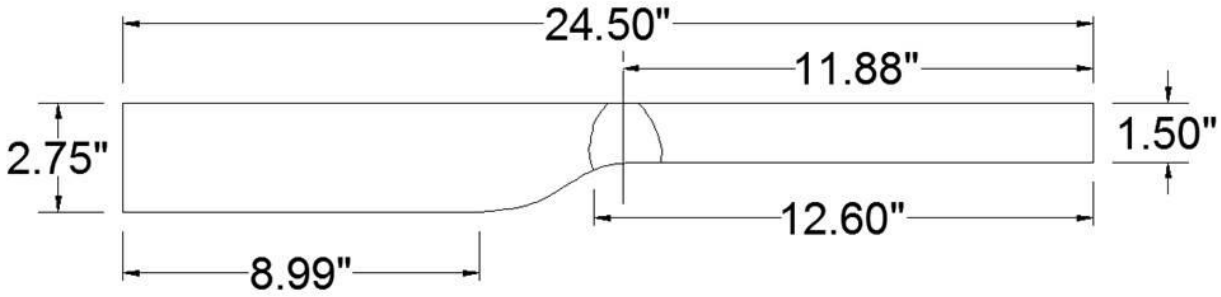

Source: FHWA.

Figure 60. Schematic. TP5 dimensions.

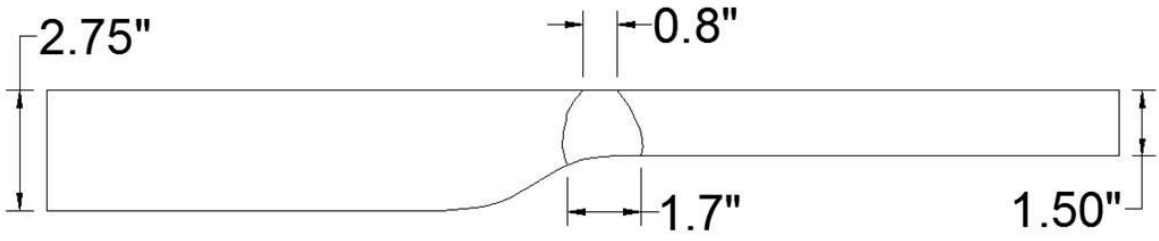

Source: FHWA.

Figure 61. Schematic. TP5 CAD image with traced HAZ with dimensions.

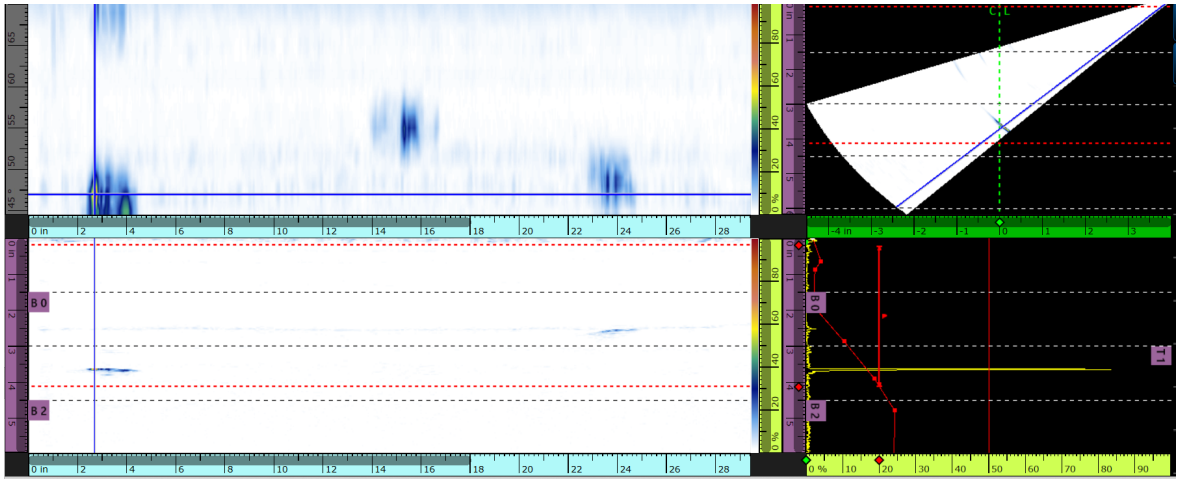

Source: FHWA.

Figure 62. Images. Composite scan view for test specimen TP5.

In the test specimen TP5, the team observed the first discontinuity indication at 2.02 inches from the starting position at a depth of 1.46 inches at the index position of −9.5, IP1.The second discontinuity indication was at 14.7 inches from the datum at a depth of 0.54 inch from the surface; the length of the indication was 2.2 inches, and it was detected in the IP2, 6.6-inch offset position. The third indication was observed at an offset of 3 inches at IP2, located at 23 inches from the start position at a depth of 0.47 inch and a length of 1.5 inches.

SPECIMEN ESW-2CP

Figure 63 through figure 67 cover specimen ESW-2CP. The specimen had the following characteristics:

- Weld type: ESW-NG.
- Length: 48.0 inches.
- Width: 48.0 inches.
- Height: 2.0 inches.

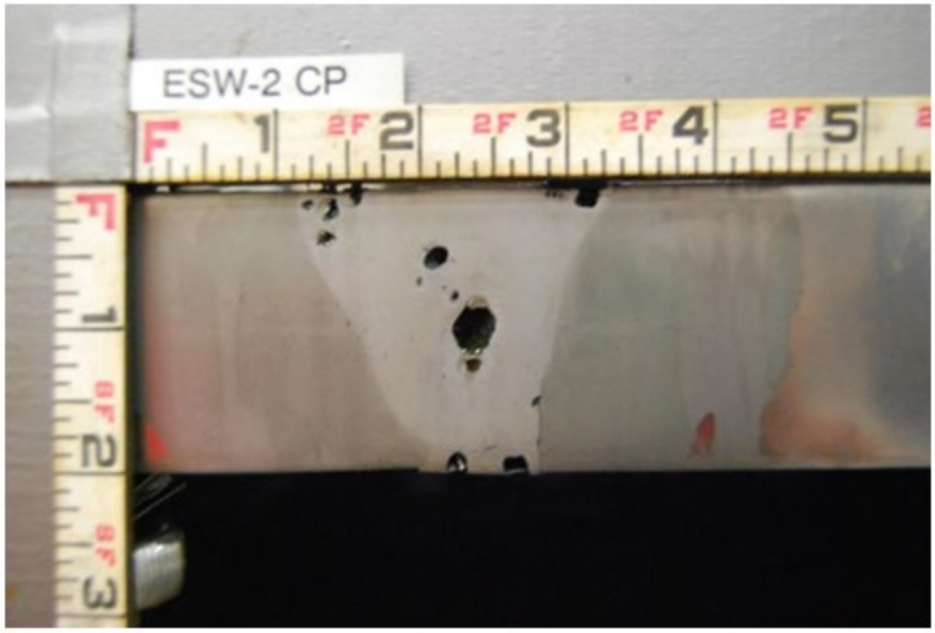

Source: FHWA.

Figure 63. Photo. ESW-2CP unprocessed etched image.

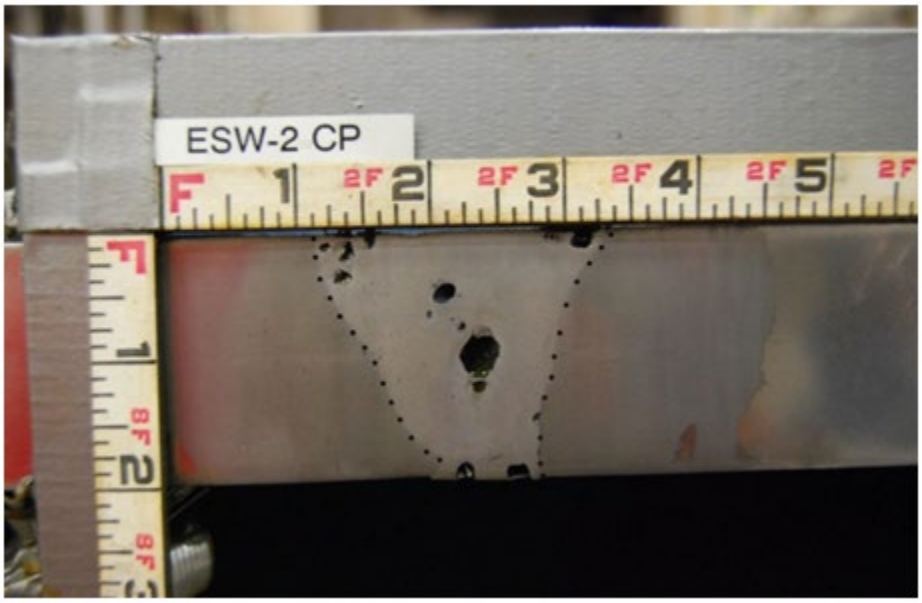

Source: FHWA.

Figure 64. Photo. ESW-2-CP etched image with weld edge traced.

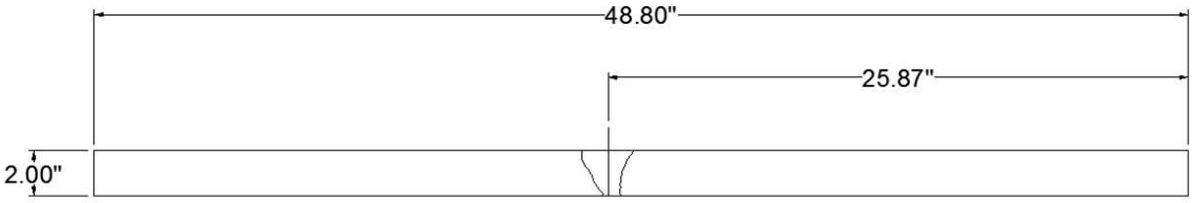

Source: FHWA.

Figure 65. Schematic. ESW-2CP dimensions.

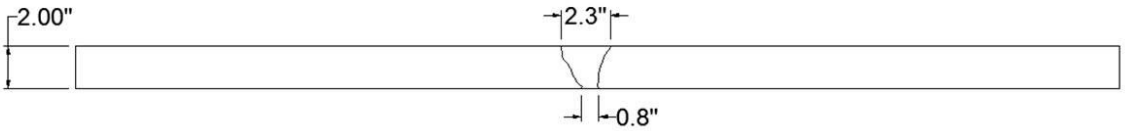

Source: FHWA.

Figure 66. Schematic. ESW-2CP CAD image with traced HAZ with dimensions.

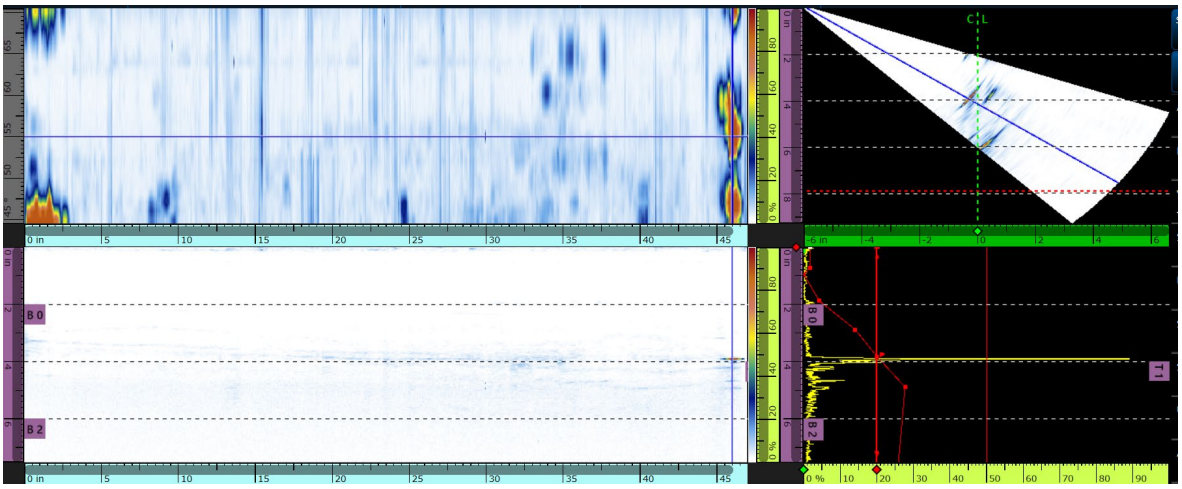

Source: FHWA.

Figure 67. Images. Composite scan view for test specimen ESW-2CP.

At IP1 and an offset of 5 inches, the researchers noted three discontinuities at 7.9, 33.56, and 45.2 inches from the start at depths of 1.6, 0.79, and 1.7 inches, respectively. The lengths of the discontinuities were 0.51, 4.1, and 0.7 inches. Another discontinuity was located at datum with a length of 3.1 inches at a depth of 1.7 inches, and it was detected at an offset position of 5 inches, IP2.

SPECIMEN ESW-12CP

Figure 68 through figure 72 cover specimen ESW-12CP. The specimen had the following characteristics:

- Weld type: ESW-NG.
- Length: 48.0 inches.
- Width: 48.0 inches.
- Height: 1.0–2.0 inches.

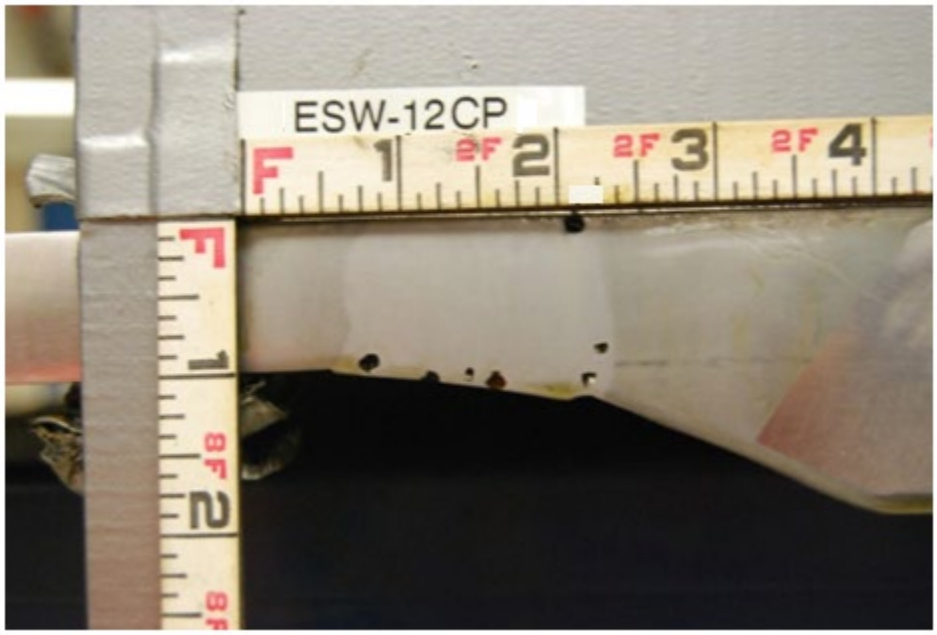

Source: FHWA.

Figure 68. Photo. ESW-12CP unprocessed etched image.

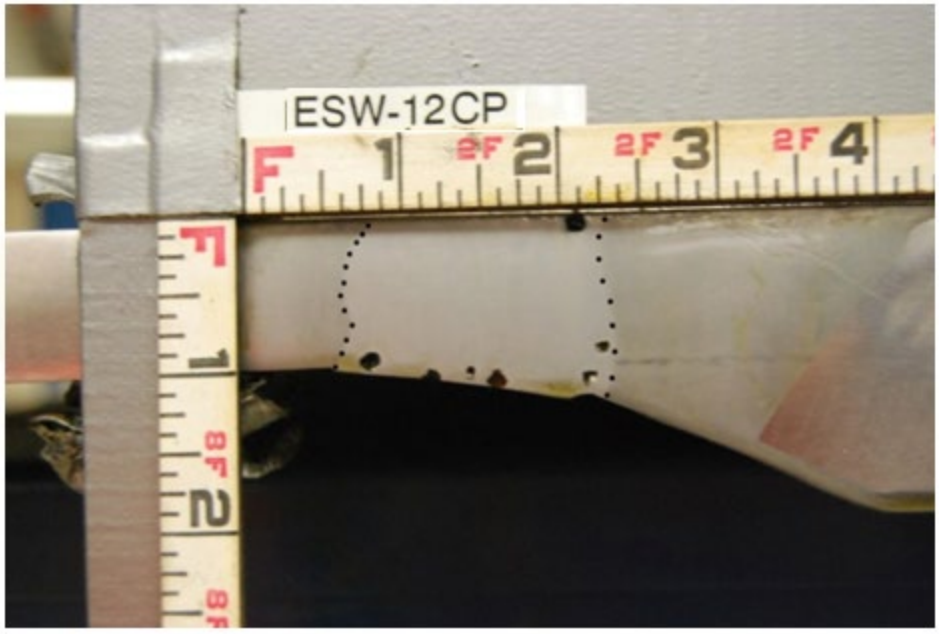

Source: FHWA.

Figure 69. Photo. ESW-12CP etched image with weld edge traced.

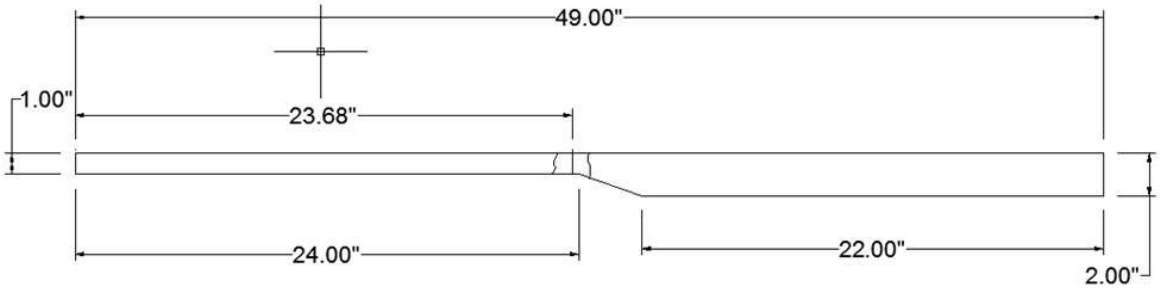

Source: FHWA.

Figure 70. Schematic. ESW-12CP dimensions.

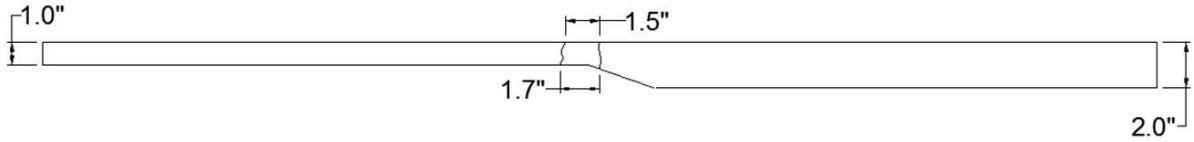

Source: FHWA.

Figure 71. Schematic. ESW-12CP CAD image with traced HAZ with dimensions.

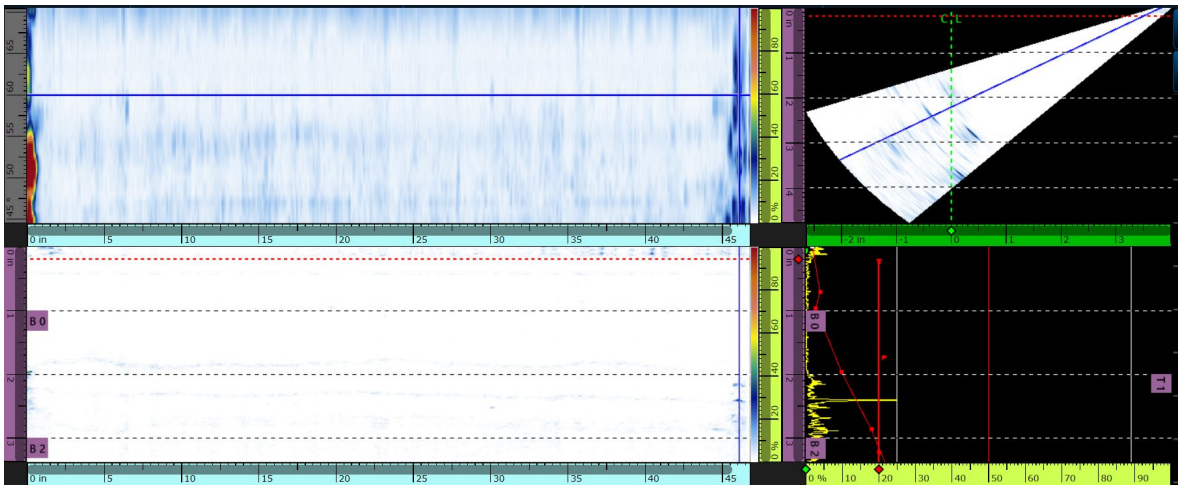

Source: FHWA.

Figure 72. Images. Composite scan view for test specimen ESW-12CP at IP1.

The research team detected two indications observed in PAUT analysis of the test specimen ESW 12-CP at an offset of 3 inches, IP2, and located at 0 and 45.5 inches from the datum, respectively. The indications were located at depths of 0.83 and 0.77 inch, respectively.

SPECIMEN SAW-12CP

Figure 73 through figure 77 cover specimen SAW-12CP. The specimen had the following characteristics:

- Weld type: SAW.
- Length: 48.0 inches.
- Width: 48.0 inches.
- Height: 1.0–2.0 inches.

Source: FHWA.

Figure 73. Photo. SAW-12CP unprocessed etched image.

Source: FHWA.

Figure 74. Photo. SAW-12CP etched image with weld edge traced.

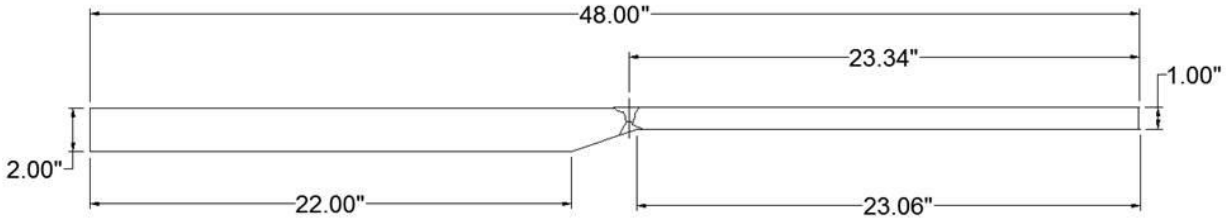

Source: FHWA.

Figure 75. Schematic. SAW-12CP dimensions.

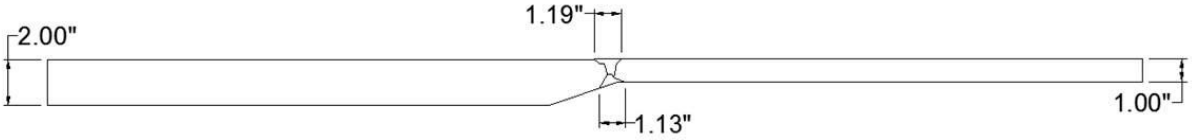

Source: FHWA.

Figure 76. Schematic. SAW-12CP CAD image with traced HAZ with dimensions.

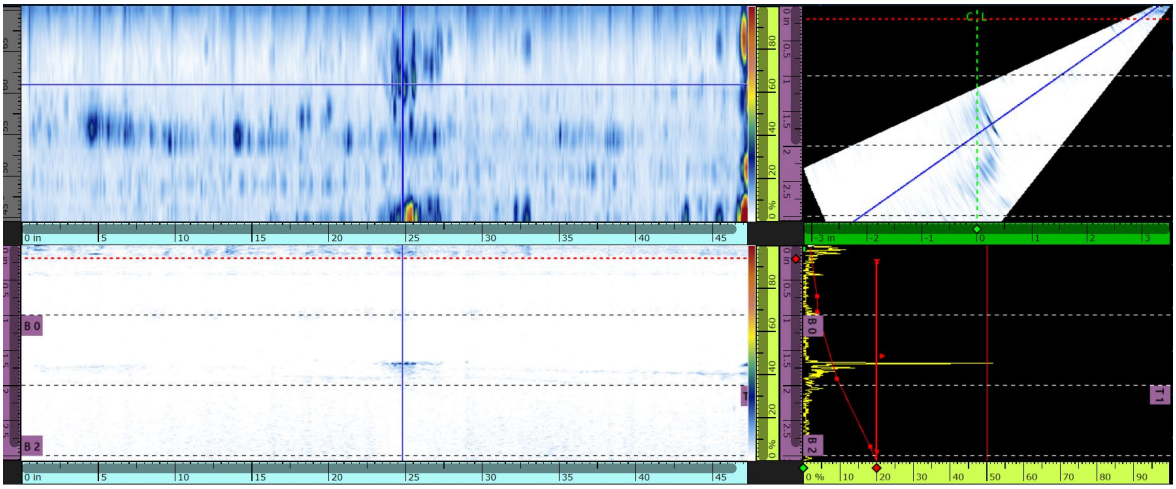

Source: FHWA.

Figure 77. Images. Composite scan view for test specimen SAW-12CP at IP1.

At the IP1, 0.25 offset, the team noted two discontinuities at 0 and 46.6 inches from the start at a depth of 0.12 and 0.58 inch, respectively. The lengths of the discontinuities were 0.8 and 0.84 inch, respectively. Another discontinuity indication was observed at index offset 0.5, IP2, located at 23.3 inches from the datum and at a depth of 0.4 inch, and the length of this indication was measured as 3.8 inches.

SPECIMEN HF1

Figure 78 through figure 82 cover specimen HF1. The specimen had the following characteristics:

- Weld type: ESW-NG.
- Length: 36.0 inches.
- Width: 49.0 inches.
- Height: 2.0–2.5 inches.

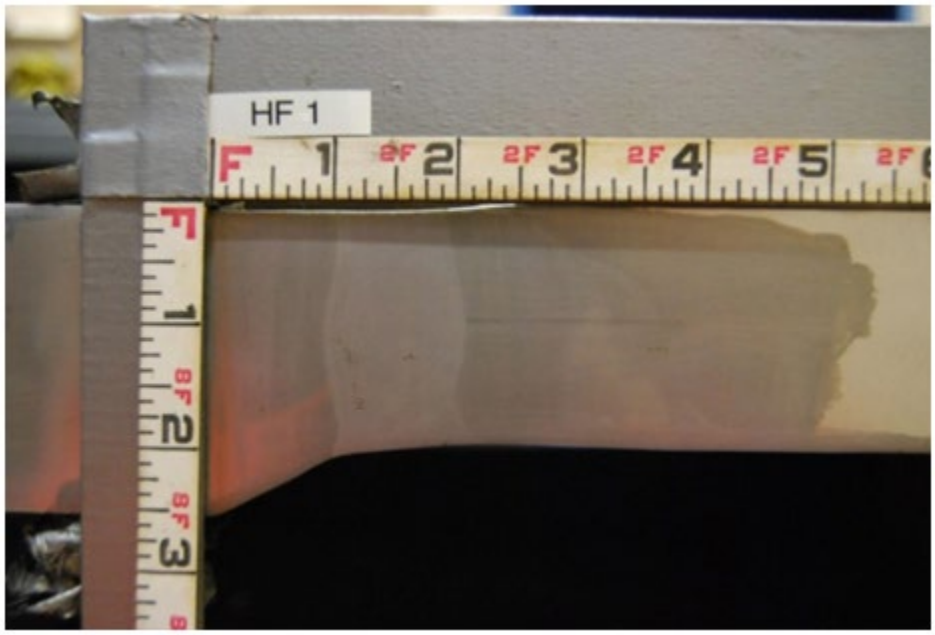

Source: FHWA.

Figure 78. Photo. HF1 unprocessed etched image.

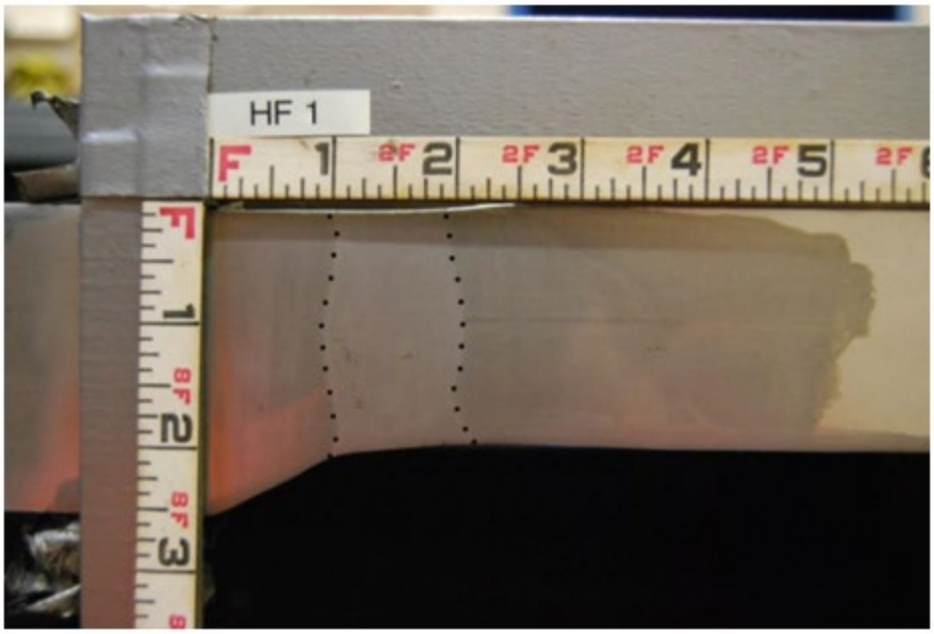

Source: FHWA.

Figure 79. Photo. HF1 Etched image with weld edge traced.

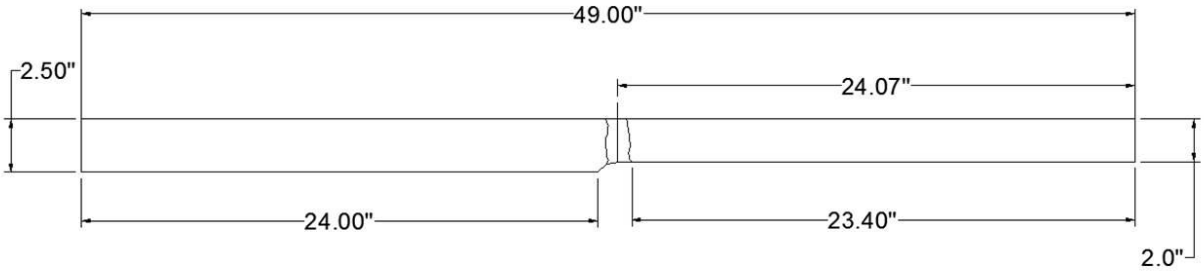

Source: FHWA.

Figure 80. Schematic. HF1 dimensions.

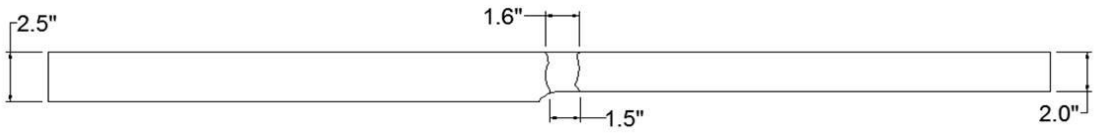

Source: FHWA.

Figure 81. Schematic. HF1 CAD image with traced HAZ with dimensions.

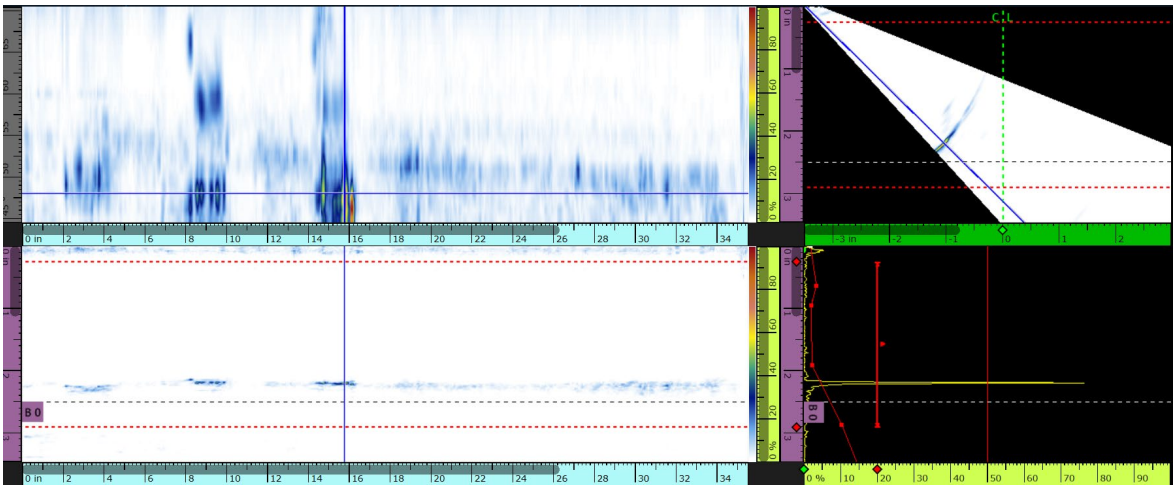

Source: FHWA.

Figure 82. Images. Composite scan view for test specimen HF1 at IP1.

The researchers observed the first discontinuity indication at an index offset of −2.5 inches, IP1, located at 1.98 inches from the datum position and at a depth of 2.19 inches. The length of this indication was measured as 2.27 inches. The second discontinuity was located at 8.06 inches from the datum point at a depth of 0.1 inch and a length of 2.1 inches. The team observed this indication at an offset position of −8 inches, IP1. The third discontinuity position was at 13.92 inches from the datum, and the length and depth are 2.2 inches and 1.5 inches, respectively. The offset position for this indication was 4.5 inches, IP2.

SPECIMEN HF2

Figure 83 through figure 87 cover specimen HF2. The specimen had the following characteristics:

- Weld type: ESW-NG.
- Length: 36.0 inches.
- Width: 49.0 inches.
- Height: 2.0–2.5 inches.

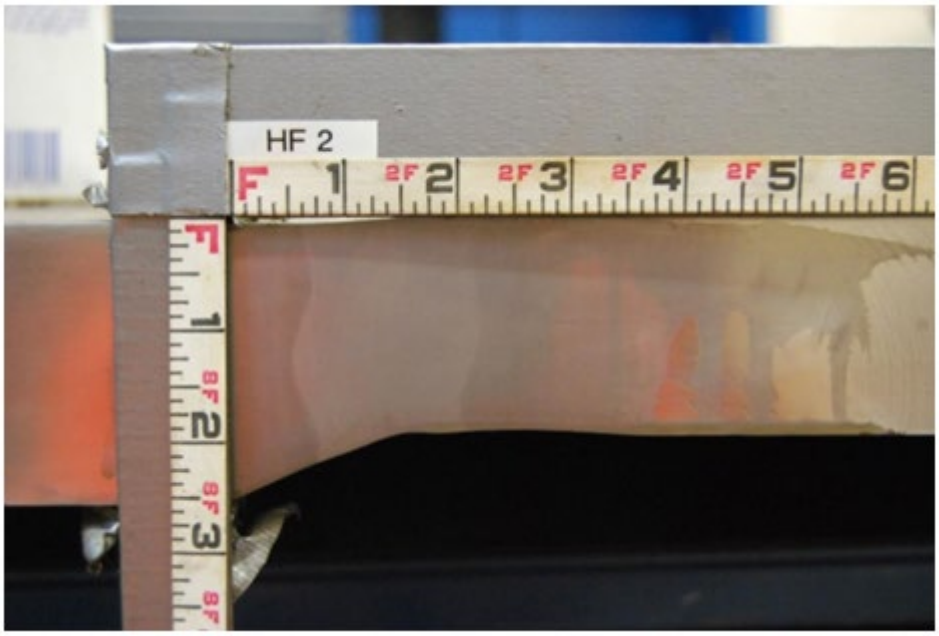

Source: FHWA.

Figure 83. Photo. HF2 unprocessed etched image.

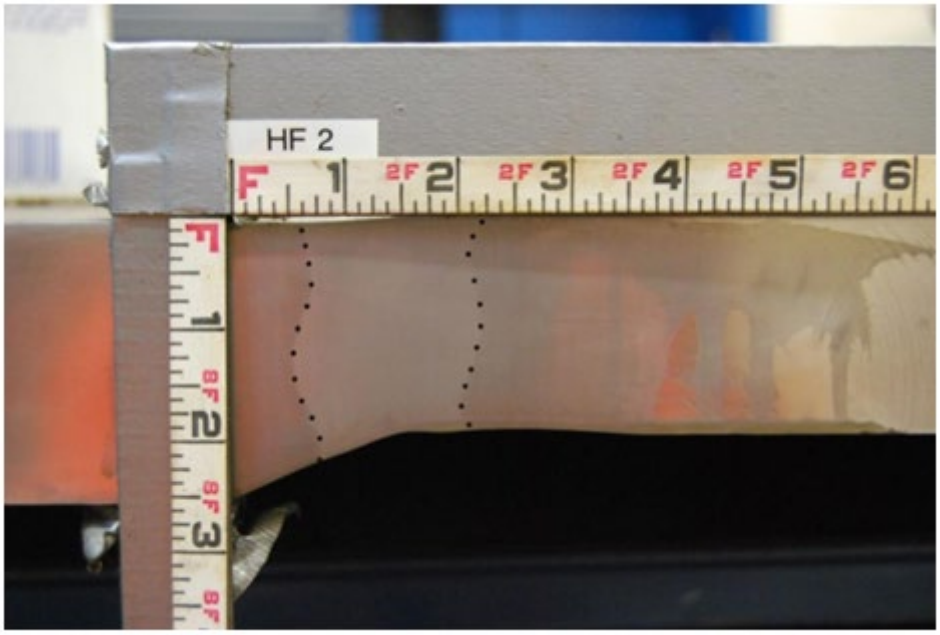

Source: FHWA.

Figure 84. Photo. HF2 etched image with weld edge traced.

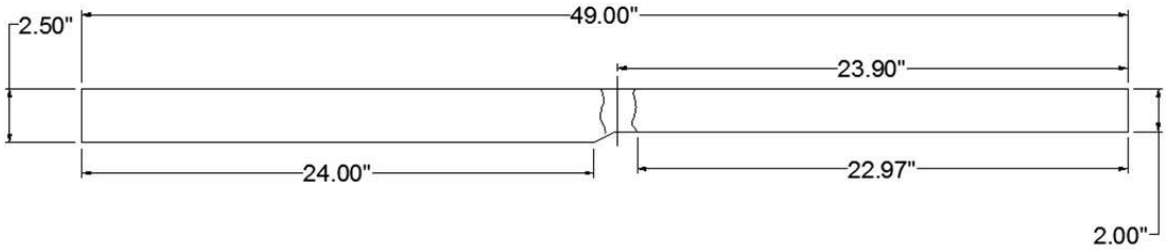

Source: FHWA.

Figure 85. Schematic. HF2 dimensions.

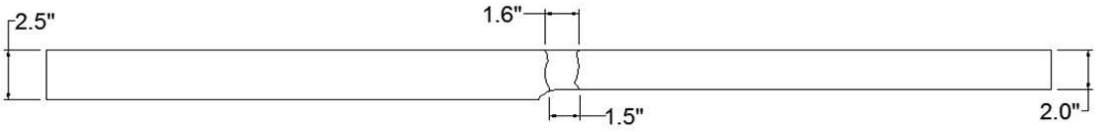

Source: FHWA.

Figure 86. Schematic. HF2 CAD image with traced HAZ with dimensions.

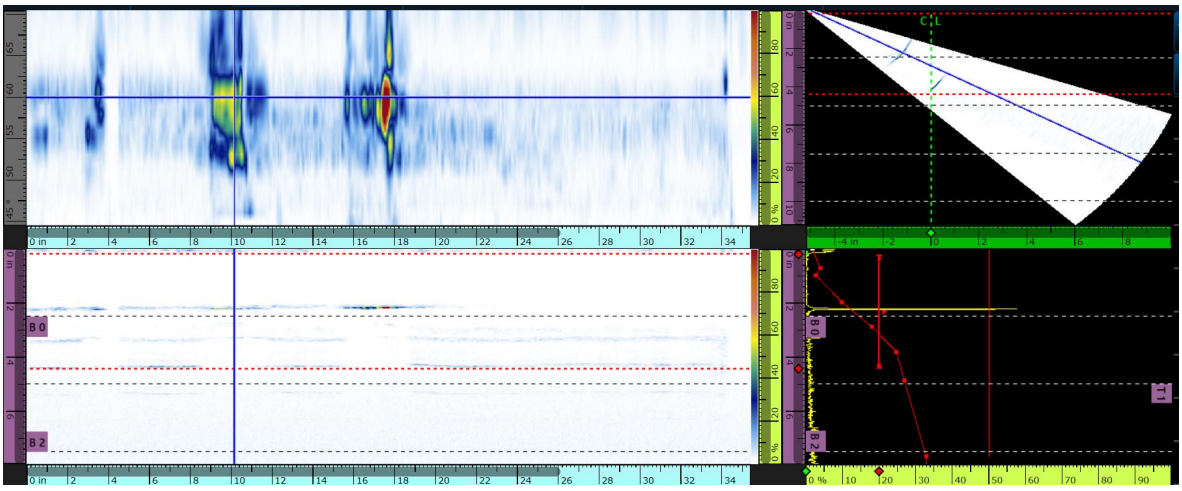

Source: FHWA.

Figure 87. Images. Composite scan view for test specimen HF2 at IP1.

The research team observed three indications in the test specimen HF2 at the index offset of −4.2 inches, IP1. They located the first discontinuity at 3.3 inches from the datum at a depth of 2.1 inches, and the second discontinuity at 9.05 inches from the datum at a depth of 2.2 inches. The team detected the third discontinuity at 15.5 inches from the datum at 2.2 inches from the surface.

REFERENCES

1. Ghasemi, H. 2014. *Development of Phased Array Ultrasonic Testing Acceptability Criteria (Phase I)*. Report No. FHWA-HRT-14-074. McLean, VA: Federal Highway Administration.

2. AASHTO/AWS. 2020. *Bridge Welding Code*, AASHTO/AWS D1.5M/D1.5, 8th ed. Washington, DC/Miami, FL: American Association of State Highway and Transportation Officials/American Welding Society.

3. Connor, J., C. J. Schroeder, B. M. Crowley, G. A. Washer, and P. E. Fish. 2019. *Acceptance Criteria of Complete Joint Penetration Steel Bridge Welds Evaluated Using Enhanced Ultrasonic Methods*. NCHRP Research Report 908. Washington, DC: National Academies of Sciences, Engineering, and Medicine.

4. P. G. Holloway. 2016. "Improving on the 6 dB Drop Technique for Determination of Flaw Length." *Materials Evaluation* 74: 1224–1233.

5. Schroeder, C. J., W. Hardy, P. Fish, and P. W. Sauser. 2017. "Comparison of Phased Array Ultrasound to Conventional Ultrasound and Radiographic Testing for Bridge Welds." *Materials Evaluation* 75, no. 1: 94–100.

6. Akundi, A., T-L. Tseng, Md. F. Rahman, and E. D. Smith. 2018. "Non-Destructive Testing (NDT) and Evaluation Using Ultrasonic Testing Equipment to Enhance Workforce Skillset for Modern Manufacturing." Presented at the *2018 American Society for Engineering Education (ASEE) Annual Conference and Exposition,* Salt Lake City, UT, June 23, 2018. https://monolith.asee.org/public/conferences/106/papers/21499/download, last accessed September 12, 2023.

7. Ronnie, M. 2014. *Bridge Welding Reference Manual.* Report No. FHWA-HIF-19-088. McLean, VA: Federal Highway Administration.

8. Azari, H., and R. Kok. 2022. "Implementation of American Association of State Highway and Transportation Officials/American Welding Society D1.5 Phased Array Ultrasonic Weld Inspection Programs." *Transportation Research Record* 2676, 10: 486–494. https://doi.org/10.1177/03611981221090240, last accessed November 16, 2023.

9. Eclipse Scientific. n.d. *BeamTool10* (software). Version 10.

10. Autodesk, Inc. 2023. *Autodesk AI* (software). AutoCAD Version 1.

11. Evident Scientific, Inc. n.d. *OmniPC 5* (software). Version 5.9.0

12. Silk, M. G., and B. H. Lidington. 1975. “The Potential of Scattered or Diffracted Ultrasound in the Determination of Crack Depth.” *Non-Destructive Testing* 8, no. 3: 146–151.

13. Evident Scientific, Inc. 2007. *Introduction To Phased Array Ultrasonic Technology Applications: R/D Tech Guideline [J]*. Waltham, MA: Evident Scientific, Inc.

14. Sumana, S., and A. Kumar. 2021. “Total Focusing Method-Based Ultrasonic Phased Array Imaging in Thick Structures.” *Journal of Nondestructive Evaluation, Diagnostics and Prognostics of Engineering Systems* 4, no. 4:041005.

15. Holloway, P., and E. Ginzel. 2021. “TFMi™: Using Intermodal Analysis to Improve TFM Imaging.” *The e-Journal of Nondestructive Testing*. https://ndt.nu/data/mediablocks/TFMi_-_Using_Intermodal_Analysis_to_Improve_TFM_Imaging.pdf, last accessed November 16, 2023.

Recommended citation: Federal Highway Administration,
Implementation of Phased Array Ultrasonic Testing (PAUT) For Bridge Welds
(Washington, DC: 2024) https://doi.org/10.21949/1521788

HRDI-20/02-24(WEB)E